UNIVERSIDAD AUTÓNOMA DE SAN LUIS POTOSÍ

FACULTAD DE CIENCIAS QUÍMICAS

Posgrado en Ciencias en Ingeniería Química

DESARROLLO DE MATERIALES MULTIFUNCIONALES CON ACTIVIDAD ADSORBENTE, FOTOCATALÍTICA Y ELECTROCATALÍTICA PARA EL TRATAMIENTO DE CONTAMINANTES EMERGENTES Y APLICACIONES SUSTENTABLES

Tesis que para obtener el grado de:

DOCTORADO EN CIENCIAS EN INGENIERÍA QUÍMICA

Presenta:

AGUILAR MARURI SAUL ALEJANDRO

Director de Tesis:

Dr. RAÚL OCAMPO PÉREZ

Codirector de Tesis:

Dra. ALMA GABRIELA PALESTINO ESCOBEDO

SAN LUIS POTOSÍ, S. L. P. FECHA: ENERO 2026

Este proyecto se realizó en el Laboratorio de Procesos Avanzados de Oxidación adscrito a la Facultad de Ciencias Químicas de la Universidad Autónoma de San Luis Potosí, en el periodo comprendido entre Enero de 2022 a Marzo de 2025, bajo la dirección del Dr. Raúl Ocampo Pérez y co-dirección de la Dra. Alma Gabriela Palestino Esobedo.

El programa de Doctorado en Ciencia en Ingeniería Química de la Universidad Autónoma de San Luis Potosí pertenece al Sistema Nacional de Posgrados de Calidad (SNP) del CONAHCYT, registro 000897. Número de la beca otorgada por CONAHCYT: 955004.

Los datos del trabajo titulado *DESARROLLO DE MATERIALES MULTIFUNCIONALES CON ACTIVIDAD ADSORBENTE, FOTOCATALÍTICA Y ELECTROCATALÍTICA PARA EL TRATAMIENTO DE CONTAMINANTES EMERGENTES Y APLICACIONES SUSTENTABLES* se encuentran bajo el resguardo de la Facultad de Ciencias Químicas y pertenecen a la Universidad Autónoma de SanLuis Potosí.

Solicitud de Registro de Tesis Doctorado

San Luis Potosí SLP a 01/ 20 /2026

Comité Académico
En atención a: Coordinador/a del Posgrado

Por este conducto solicito a Usted se lleve a cabo el registro de título de tesis de Doctorado, el cual quedo definido de la siguiente manera: DESARROLLO DE MATERIALES MULTIFUNCIONALES CON ACTIVIDAD ADSORBENTE, FOTOCATALÍTICA Y ELECTROCATALÍTICA PARA EL TRATAMIENTO DE CONTAMINANTES EMERGENTES Y APLICACIONES SUSTENTABLES que desarrollará el/la estudiante: Saul Alejandro Aguilar Maruri bajo la dirección y/o Co-dirección de: Dr. Raúl Ocampo Pérez y Dra. Alma Gabriela Palestino Escobedo
Asimismo, le comunico que el proyecto en el cual trabajará el alumno involucrará el manejo de animales de experimentación, estudios con seres humanos o muestras derivadas de los mismos, el manejo y/o generación de organismos genéticamente modificados y requiere de aval de Comité de Ética e investigación de la FCQ.

(Complete la opción que aplique en su caso):

( ) Sí debido a que:____________________________________

( ) No

(x) No Aplica

Sin otro particular, quedo de Usted.

A T E N T A M E N T E

Saul Alejandro Aguilar Maruri
Nombre y firma del estudiante

Dr. Raúl Ocampo Pérez
Nombre y firma del/la Director/a de Trabajo terminal

Dra. Alma Gabriela Palestino Escobedo
Nombre y firma del/la Director/a de Trabajo terminal

UNIVERSIDAD AUTÓNOMA DE SAN LUIS POTOSÍ

FACULTAD DE CIENCIAS QUÍMICAS

Posgrado en Ciencias en Ingeniería Química

DESARROLLO DE MATERIALES MULTIFUNCIONALES CON ACTIVIDAD ADSORBENTE, FOTOCATALÍTICA Y ELECTROCATALÍTICA PARA EL TRATAMIENTO DE CONTAMINANTES EMERGENTES Y APLICACIONES SUSTENTABLES

Tesis que para obtener el grado de:

DOCTORADO EN CIENCIAS EN INGENIERÍA QUÍMICA

Presenta:

AGUILAR MARURI SAUL ALEJANDRO

SINODALES:

Presidente: ____________________

Dra. Erika Padilla Ortega

Secretario: ____________________

Dr. César Fernando AzaelGómez Durán

Vocal: ____________________

Dr. Raúl Ocampo Pérez

Vocal: ____________________

Dra. Alma Gabriela Palestino Escobedo

Vocal: ____________________

Dr. Nahúm Andrés Medellín Castillo

SAN LUIS POTOSÍ, S. L. P. FECHA: ENERO 2026

INTEGRANTES DEL COMITÉ TUTORIAL ACADÉMICO

Dr. Raúl Ocampo Pérez: Director de tesis. Adscrito al Posgrado en Ciencias en Ingeniería Química de la Universidad Autónoma de San Luis Potosí, San Luis Potosí, S.L.P.

Dra. Alma Gabriela Palestino Escobedo: Co-directora de tesis. Adscrita al Posgrado en Ciencias en Ingeniería Química de la Universidad Autónoma de San Luis Potosí, San Luis Potosí, S.L.P.

Dra. Erika Padilla Ortega: Sinodal de tesis. Adscrito al Posgrado en Ciencias en Ingeniería Química de la Universidad Autónoma de San Luis Potosí, San Luis Potosí, S.L.P.

Dr. César Fernando Azael Gómez Durán: Sinodal de tesis. Adscrito al Posgrado en Ciencias en Ingeniería Química de la Universidad Autónoma de San Luis Potosí, San Luis Potosí, S.L.P.

Dr. Nahúm Andrés Medellín Castillo: Sinodal de tesis. Adscrito a la Maestría en Tecnología y Gestión del Agua y Posgrado en Ciencias Ambientales de la Universidad Autónoma de San Luis Potosí, San Luis Potosí, S.L.P.

UNIVERSIDAD AUTÓNOMA DE SAN LUIS POTOSÍ
Facultad de Ciencias Químicas
Centro de Investigación y Estudios de Posgrado
Posgrado en Ciencias en Ingeniería Química
Programa de Doctorado

Formato D5

Carta Cesión de Derechos

San Luis Potosí SLP a 01/ 20 / 2026

En la ciudad de *San Luis Potosí* el día *20* del mes de *Enero* del año *2026.* El que suscribe *Saul Alejandro Aguilar Maruri* Alumno(a) del programa de posgrado *Doctorado en Ciencias en Ingeniería Química* adscrito a *Facultad de Ciencias Químicas* manifiesta que es autor(a) intelectual del presente trabajo terminal, realizado bajo la dirección de: *Dr. Raúl Ocmapo Pérez y Dra. Alma Gabriela Palestino Escobedo* y cede los derechos del trabajo titulado *DESARROLLO DE MATERIALES MULTIFUNCIONALES CON ACTIVIDAD ADSORBENTE, FOTOCATALÍTICA Y ELECTROCATALÍTICA PARA EL TRATAMIENTO DE CONTAMINANTES EMERGENTES Y APLICACIONES SUSTENTABLES* a la **Universidad Autónoma de San Luis Potosí**, para su difusión con fines académicos y de investigación.

Los usuarios de la información no deben reproducir de forma total o parcial texto, gráficas, imágenes o cualquier contenido del trabajo si el permiso expreso del o los autores. Éste, puede ser obtenido directamente con el autor o autores escribiendo a la siguiente dirección *A348454@alumnos.uaslp.mx o raul.ocampo@uaslp.mx*. Si el permiso se otorga, el usuario deberá dar el agradecimiento correspondiente y citar la fuente del mismo.

_____Saul Alejandro Aguilar Maruri___
Nombre y firma del alumno

UNIVERSIDAD AUTÓNOMA DE SAN LUIS POTOSÍ
Facultad de Ciencias Químicas
Centro de Investigación y Estudios de Posgrado
Posgrado en Ciencias en Ingeniería Química
Programa de Doctorado

Formato D28

Carta de Análisis de Similitud

San Luis Potosí SLP a 01/ 22 /2026

L.B. Nayeli Ortiz
Biblioteca de Posgrado FCQ

Asunto: Reporte de porcentaje de similitud de tesis de grado

Por este medio me permito informarle el porcentaje de similitud obtenido mediante Ithenticate para la tesis titulada Desarrollo de materiales multifuncionales con actividad adsorbente, fotocatalítica y electrocatalítica para el tratamiento de contaminantes emergentes y aplicaciones sustentables presentada por el autor M.C. Saúl Alejandro Aguilar Maruri. La tesis es requisito para obtener el grado de Doctorado en el Posgrado en Ciencias en Ingeniería Química. El análisis reveló un porcentaje de similitud de 49% excluyendo referencias y metodología. Es importante mencionar que este porcentaje es aceptado ya que presenta una tesis como Trabajo terminal derivado de productos como artículos.

Agradezco sinceramente su valioso tiempo y dedicación para llevar a cabo una exhaustiva revisión de la tesis. Quedo a su disposición para cualquier consulta o inquietud que pueda surgir en el proceso.

Sin más por el momento, le envío un cordial saludo.

A T E N T A M E N T E

POSGRADO EN CIENCIAS
EN INGENIERIA QUIMICA

____

Coordinador Académico del Posgrado
en Ciencias en Ingeniería Química

AGRADECIMIENTOS INSTITUCIONALES

Centro de Investigación y Estudios de Posgrado
Facultad de Ciencias Químicas
Universidad Autónoma de San Luis Potosí

Consejo Nacional de Ciencia y Tecnología
(CONACYT)
CVU No. 955004

Acknowledgments

First and foremost, I thank God for accompanying me every step of the way, which I hope conveys a sense of spiritual support and reassurance to the audience. Thank you for giving me the strength, courage, and wisdom to overcome each obstacle and for illuminating my path in moments of uncertainty. This achievement would not have been possible without your constant guidance and infinite grace.

To my family, my deepest gratitude for your unconditional love, tireless sacrifice, and constant support, which provided me with the emotional stability to focus on my research. You have been the cornerstone of my life and the foundation upon which I have built this academic achievement. Thank you for believing in me even when I doubted myself, for encouraging me to persevere, and for lovingly and patiently supporting me at every stage of this journey.

My sincerest appreciation to Dr. Raúl Ocampo, thesis advisor, for his invaluable guidance, patience, and commitment throughout this process, which I hope makes the audience feel valued. His experience and support have been key to the development and completion of this work. I also extend my deepest gratitude to my co-advisor, Dr. Gabriela Palestino, and to the examiners for their time spent reviewing this project and for their comments, suggestions, and constructive contributions. Thanks also to my friends and colleagues in the lab. Sharing this process with you made it more bearable, and your support and camaraderie were fundamental in maintaining my motivation. Your humor, encouragement, and constant company were a firm anchor on this challenging but enriching academic journey.

Finally, I express my gratitude to the Secretariat of Science, Humanities, Technology, and Innovation (SECIHTI) for the scholarship awarded (registration 955004), which provided essential financial support that enabled me to focus entirely on my research and academic development.

Resumen

Este trabajo aborda el desarrollo de **materiales multifuncionales con propiedades adsorbentes, fotocatalíticas y electrocatalíticas** para la remediación ambiental y aplicaciones energéticas sustentables, priorizando el uso de materiales de bajo costo y derivados de biomasa. Se sintetizaron xerogeles de resorcinol–formaldehído con una alta capacidad de adsorción de metformina (hasta **325 mg g^{-1}**), gobernada por interacciones electrostáticas y enlaces de hidrógeno, con marcada dependencia del pH y la temperatura. Estos materiales mostraron buena selectividad y estabilidad tras varios ciclos de reutilización.

Asimismo, residuos agroindustriales fueron valorizados como soportes fotocatalíticos eficientes. Los carbones derivados de bagazo de agave dopados con óxido de cerio alcanzaron **más del 99.5% de degradación de azul de metileno bajo irradiación UV**, manteniendo su eficiencia en ciclos sucesivos. De manera similar, hidrocarbones obtenidos de residuos de café y dopados con BiOCl, $BiOCl/CeO_2$ y $BiOCl/Fe_2O_3$ exhibieron eficiencias fotocatalíticas de hasta **100%** en la degradación de colorantes, mediante mecanismos dependientes del dopante que involucran especies reactivas de oxígeno y reacciones foto-Fenton.

Finalmente, la funcionalización solvotérmica alcalina de nanotubos de carbono de paredes múltiples, seguida del dopaje con Pt–Pd, mejoró notablemente su desempeño electrocatalítico para la reacción de evolución de hidrógeno, logrando bajos sobrepotenciales, cinéticas favorables y alta estabilidad. En conjunto, los resultados demuestran que el diseño racional de materiales y la valorización de biomasa permiten desarrollar soluciones eficientes, reutilizables y sustentables para el tratamiento de contaminantes emergentes y la generación de energía limpia.

Palabras clave:

Materiales multifuncionales, contaminantes emergentes, catalizadores derivados de biomasa, degradación fotocatalítica, reacción de evolución de hidrógeno

Summary

This work presents the development of **multifunctional materials with adsorptive, photocatalytic, and electrocatalytic activity** for environmental remediation and sustainable energy applications, emphasizing the valorization of low-cost and biomass-derived resources. Resorcinol–formaldehyde xerogels were synthesized and evaluated as adsorbents for metformin, a persistent pharmaceutical contaminant. The xerogels exhibited a high adsorption capacity of up to **325 mg g^{-1}**, governed primarily by electrostatic interactions and hydrogen bonding, with strong dependence on pH and temperature. Competitive adsorption and reuse studies demonstrated good selectivity and stability over multiple cycles.

In parallel, agroindustrial wastes were transformed into efficient photocatalytic supports. Cerium oxide–doped carbons derived from agave bagasse achieved **over 99.5% degradation of methylene blue under UV irradiation**, maintaining high performance during reuse cycles. Similarly, hydrochars synthesized from coffee grounds and doped with BiOCl, BiOCl/CeO_2, and BiOCl/Fe_2O_3 showed excellent photocatalytic activity toward indigo blue degradation, with efficiencies up to **100%**, driven by dopant-dependent mechanisms involving reactive oxygen species, photo-Fenton reactions, and enhanced charge separation.

Finally, alkaline solvothermal functionalization of multi-walled carbon nanotubes, followed by Pt–Pd decoration, significantly improved their electrocatalytic performance for the hydrogen evolution reaction, achieving a low overpotential (−0.20 V at 10 mA cm^{-2}), favorable kinetics, and long-term stability.

Overall, this study demonstrates that rational material design combined with biomass revalorization enables high-performance, reusable multifunctional materials for contaminant removal and clean energy generation.

Keywords:

Multifunctional materials, emerging contaminants, biomass-derived catalysts, photocatalytic degradation, hydrogen evolution reaction

General index

Index of figures

Index of tables

1. Introduction

In recent decades, rapid industrial, agricultural, pharmaceutical, and urban growth has led to the continuous release of a wide variety of chemical compounds into bodies of water (Nishmitha et al., 2025).Many of these compounds, known as emerging contaminants, are not efficiently removed by conventional wastewater treatment systems, which highlights the importance of understanding their impact. Even at extremely low concentrations, on the order of µg/L, these contaminants can cause significant disruptions to aquatic ecosystems, affect human health, and compromise the quality of drinking water sources (Balakrishnan et al., 2022a).

Emerging contaminants, such as pharmaceutical compounds, personal care products, pesticides, herbicides, aromatic hydrocarbons, and synthetic dyes, have physicochemical properties that hinder their natural degradation (X. Li et al., 2024). Many of these pollutants possess high molecular stability, high water solubility, and complex structures that confer resistance to biological and chemical degradation, thereby favoring their persistence and bioaccumulation in the environment (Nishmitha et al., 2025). It is estimated that more than 350,000 synthetic compounds are in circulation worldwide, and the processes for eliminating, degrading, and controlling them are not clearly established, which increases the urgency of developing new, more efficient, and sustainable removal technologies (Balakrishnan et al., 2022a).

Among the most relevant emerging contaminants are pharmaceuticals and synthetic dyes. Metformin, for example, is one of the most prescribed antidiabetic drugs worldwide due to its low cost and high effectiveness. However, its high consumption has led to its presence in groundwater, hospital wastewater, and surface water bodies. Due to its high solubility, chemical stability, and low biodegradation rate, metformin can persist in the environment for extended periods, potentially causing adverse effects on aquatic organisms and on human health, including reproductive disturbances and possible carcinogenic effects (Balakrishnan et al., 2022a).

On the other hand, industrial dyes such as methylene blue and indigo blue are widely used in the textile, paper, pharmaceutical, and cosmetic industries (Groeneveld et al., 2023). These compounds not only alter the appearance of water by increasing its turbidity and reducing sunlight penetration, but also interfere with natural processes such as photosynthesis, oxygenation of the aquatic environment, and ecosystem dynamics (Chiu et al., 2019). Furthermore, many of these dyes exhibit toxicity, mutagenic potential, and the ability to generate even more dangerous byproducts through chemical transformations in the environment (Awad et al., 2023).

In response to this problem, multiple technologies have been proposed for removing emerging contaminants, including physical processes (filtration, sedimentation), chemical processes (coagulation, oxidation, ozonation), and biological processes (biodegradation) (Reza et al., 2017). However, these methodologies often have limitations, including high operating costs, low selectivity, the production of toxic secondary byproducts, and reduced efficiency when dealing with complex matrices (Asefa et al., 2024). For this reason, alternative technologies such as adsorption, photocatalysis, and electrocatalysis have gained increasing interest in the scientific community due to their high efficiency, simplicity, versatility, and compatibility with green chemistry approaches (Reza et al., 2017).

Adsorption has become established as one of the most effective techniques for removing contaminants from aqueous solutions. However, many commercial adsorbents, such as traditional activated carbons, have limited removal capacities, necessitating the use of large volumes of material or its frequent replacement (McMichael et al., 2021). In this scenario, new highly porous polymeric materials have emerged, such as xerogels derived from the resorcinol-formaldehyde reaction, which have a high density of surface functional groups and can interact efficiently with contaminant molecules through hydrogen bonds and electrostatic interactions (Balakrishnan et al., 2022a).

In parallel, heterogeneous photocatalysis has emerged as one of the most promising technologies for the advanced degradation of organic pollutants

(Nasrollahpour & Moradi, 2016). This process involves activating semiconductor materials under UV or visible irradiation, generating electron-hole pairs that react with water and oxygen to form highly oxidizing reactive species, such as hydroxyl radicals (•OH) and superoxide ($O_2•^-$) (Chiu et al., 2019). These species can break covalent bonds and mineralize complex pollutants, transforming them into less toxic products or even CO_2 and H_2O (Low et al., 2017).

Within this family of photocatalytic materials, semiconductor oxides such as BiOCl, CeO_2, and Fe_2O_3 stand out for their favorable crystalline structure, good chemical stability, and appropriate band energy levels (Low et al., 2017). Bismuth oxychloride (BiOCl) has been reported as a highly efficient material for the degradation of dyes under UV and visible radiation (Vinoth et al., 2021), while cerium oxide (CeO_2) provides redox properties and oxygen vacancies that improve charge separation and the formation of reactive species (Bakry et al., 2022). The incorporation of iron oxides, through Fenton and photo-Fenton mechanisms, further increases the degradation efficiency, especially under acidic conditions (Yu et al., 2022).

A key advance in this field has been the use of carbonaceous materials derived from residual biomass as catalytic supports (Nasrollahpour & Moradi, 2016). Agro-industrial waste, such as agave bagasse and coffee waste, has been transformed through pyrolysis and hydrothermalization into highly porous biochars and hydrochars (Huo et al., 2023; Mota-Resendiz et al., 2025). These materials not only contribute to a circular economy but also serve as ideal supports for the dispersion of catalytic nanoparticles, increasing the specific surface area, improving light absorption, acting as electron reservoirs, reducing electron-hole pair recombination, and significantly improving photocatalytic efficiency (Dujearic-Stephane et al., 2021).

Additionally, the field of electrocatalysis has gained significant importance due to its strategic role in the production of green hydrogen and in advanced electrochemical degradation processes of pollutants (Qadeer et al., 2024; M. Zhao et al., 2014). The hydrogen evolution reaction (HER) represents a fundamental step toward sustainable energy systems. However, this reaction has slow kinetics, which necessitates the development of highly efficient, stable, and low-cost catalysts (S. Wang et al., 2021).

In this context, multi-walled carbon nanotubes (MWCNTs) have proven to be excellent electrocatalytic supports thanks to their high surface area, high electrical conductivity, and chemical stability (M. Zhao et al., 2014). When these materials are functionalized by solvothermal treatments in an alkaline medium, controlled defects and oxygenated functional groups are generated that facilitate the anchoring of metallic nanoparticles such as Pt and Pd (S. Li et al., 2020). This synergy between the carbonaceous support and the metallic nanoparticles results in highly active materials for HER, reducing overpotential, increasing the exchange current density, and improving the durability of the electrocatalytic system (Trivedi & Chakraborty, 2025). The simultaneous presence of platinum and palladium nanoparticles generates metal-oxygen-carbon interfaces that act as active sites for the Volmer-Heyrovsky/Tafel steps of hydrogen evolution, promoting more efficient electron transfer (Quinson et al., 2018). These materials also have high potential for use in the electrodegradation of organic pollutants, especially in complex aqueous systems, thereby expanding their applicability beyond the energy sector towards comprehensive environmental treatment (Qadeer et al., 2024).

2. Background

The increased presence of emerging pharmaceutical contaminants, such as metformin, in water bodies has generated an urgent need to develop advanced materials and technologies capable of efficiently, selectively, and sustainably removing and degrading them (X. Li et al., 2024). Several studies have demonstrated high efficiency in removing this type of contaminant (Nishmitha et al., 2025). Carbonaceous adsorbents have been extensively tested for metformin adsorption and typically exhibit high capacities and good regenerability (Balakrishnan et al., 2022a). Examples include conventional activated carbons, biocarbons/nanobiocarbons, and magnetically modified carbon compounds, which have been tested in batch and column modes

(Sanchez-Silva et al., 2022a). Water hyacinth activated carbon produced by activation with H_3PO_3 achieved a Langmuir q_{max} of 122.47 mg/g and behaved as a spontaneous endothermic adsorbent. Ninety-two percent of the metformin was desorbed using 0.1 M HCl/ethanol, and the carbon retained approximately 84% recovery after five cycles (Huang et al., 2016). Magnetic carbon compounds (Fe_3O_3 grafted onto PAC, graphene nanoplatelets, and MWCNT) were also used as regenerable adsorbents. Reported q_m values were 8.83 mg/g for the magnetic graphene nanoplatelet (M-GNP) composite under standard conditions and 26.17 mg/g for magnetic MWCNT (M-MWCNT) at 318 K, with a magnetic fraction of approximately 70% Fe3O4 and measurable desorption using a phosphate buffer (M-GNP desorption approximately 66%) (Cusioli et al., 2023). The silica-alumina (SA) composite exhibited a high BET surface area (~470 m²/g) and removed high concentrations of metformin, with a maximum reported uptake of 46 mg/L at an optimum pH of 9.0; thermal regeneration at 673 K resulted in complete regeneration and removal of ~95% after three cycles (Mohammad et al., 2022). The Leucaena leucocephala pod biosorbent (chemically/thermally modified) reached a maximum adsorption capacity of 56.18 mg/g at 313 K, achieved a removal of ~53.24% at 300 min in kinetic tests, and showed a decrease in absorption in the presence of Na^+, Ca^{2+}, and Mg^{2+} salts (Hethnawi et al., 2020). The persistence and high solubility of metformin in aquatic environments make it essential to continue research and development of new, increasingly efficient, selective, and sustainable adsorbent and catalytic materials for its removal and degradation.

Furthermore, the persistent presence of synthetic dyes such as methylene blue and indigo in bodies of water has driven the development of advanced materials and technologies capable of removing and degrading them efficiently, sustainably, and safely. Materials such as carbonized Citrullus Colocynthis have shown near-100% removal under UV irradiation, but their long-term stability and reusability are critical factors for practical deployment. Various materials for the photodegradation of methylene blue have been investigated, demonstrating effective removal capabilities (Bhatti et al., 2024). The chitosan-Al_2O_3 compounds synthesized using the sol-gel method showed promising results, with the 1:1 ratio compound achieving a degradation efficiency of 79.35% at pH 10 after 200 minutes of contact time (Desnelli et al., 2023). Metal-modified TiO_2 photocatalysts have also proven effective, with Au-TiO_2 and Pt-TiO_2 materials showing improved performance because the metal nanoparticles act as electron sinks during photocatalytic reactions (Murcia Mesa et al., 2017). For the photodegradation of indigo blue, TiO_2-based photocatalysts have been used, demonstrating significant efficiency; a combination of TiO_2 and natural zeolite achieved 58.7% degradation under UV radiation at optimal conditions (Ulya et al., 2022). Advanced electrode materials have shown great effectiveness, with Ti/RuO_2-TiO_2 electrodes modified with tin and tantalum oxides achieving complete degradation of indigo blue by photoelectrocatalysis in 60 minutes (Tomaz et al., 2022). Furthermore, calcium oxide nanoparticles (30-36 nm) have been successfully used as photocatalysts for the degradation of indigo carmine under various radiation conditions, showing optimal performance at pH 9 (Devarahosahalli Veeranna et al., 2014). The persistence, toxicity, and resistance to degradation of dyes in bodies of water make it essential to continue research and development of new, more efficient, selective, and sustainable materials for their removal and disposal.

The increasing presence of pollutants in aqueous environments has driven the development of electrochemical processes using advanced catalysts that are highly effective at degrading pollutants and enabling sustainable hydrogen production. Various electrode and photocatalyst materials have been investigated for the electrochemical degradation of pollutants and the simultaneous production of hydrogen. Composite electrodes incorporating N, C-doped TiO_2/ITO structures demonstrate effective photoelectrocatalytic performance, achieving hydrogen production rates of 12.0 $\mu mol\ cm^{-2}\ h^{-1}$ while degrading organic pollutants under sunlight (K.-R. Wu et al., 2012). Traditional metal electrodes, such as aluminum, titanium, iron, and magnesium, have been evaluated for wastewater electrolysis, producing hydrogen with purities ranging from 87.9% to 96.1% while removing ammonia and phosphate contaminants (Antonini et al., 2025). Advanced photocatalytic materials encompass heterojunction systems, metal oxides, g-C_3N_4, CeO_2, metal-organic frameworks, and carbon quantum dots, with multicomponent catalysts showing superior performance compared to single-component systems (Balu et al., 2024). Pt/CdS/TiO_2 photocatalysts achieve a quantum efficiency of 20% at 470 nm for hydrogen production while degrading both inorganic and organic pollutants; CdS-rich materials favor inorganic degradation, and TiO_2-rich systems are more effective for organic pollutants (Daskalaki et al., 2010).

Recognizing the critical role of innovative materials, this work aims to inspire researchers by emphasizing the importance of designing multifunctional materials that integrate adsorbent, photocatalytic, and electrocatalytic properties within a single platform. The combination of porous polymer matrices (xerogels), carbonaceous materials derived from agro-industrial waste (biochar/hydrochar), and nanoparticles of metal oxides and noble metals represents a highly innovative strategy, aligned with the principles of green chemistry, the circular economy, and sustainable development.

This approach not only enhances the efficiency of removing and degrading emerging contaminants in water but also offers promising opportunities for integrating these technologies into hybrid systems for clean energy production, resource recovery, and the development of advanced materials for environmental, industrial, and energy applications, inspiring confidence in sustainable solutions.

3. Justification

The increasing presence of emerging contaminants in water bodies, such as pharmaceuticals and synthetic dyes, should concern environmental scientists because of their persistence, toxicity, and resistance to conventional degradation. Compounds such as metformin, methylene blue, and indigo blue have been detected in wastewater, groundwater, and industrial water, affecting water quality, aquatic ecosystems, and potentially human health. This problem underscores the importance of developing new, highly efficient materials that allow for their removal and degradation, such as highly porous polymeric xerogels for metformin adsorption and carbonaceous materials derived from agro-industrial waste doped with metal oxides (BiOCl, CeO_2, Fe_2O_3) for the photodegradation of dyes such as indigo blue and methylene blue.

Additionally, the transition to sustainable, energy-efficient processes is inspiring for researchers, as it drives the development of multifunctional materials capable not only of treating aqueous pollutants through adsorption and photocatalysis, but also of actively participating in hydrogen production via electrocatalysis. In this regard, the solvothermal alkaline functionalization of carbon nanotubes doped with Pt-Pd nanoparticles increases the active surface area, improves electron transfer, and reduces the overpotential of the hydrogen evolution reaction, thereby consolidating an integrated strategy that connects environmental remediation with the generation of clean, sustainable energy.

4. Hypothesis

The integration of porous polymer matrices and biomass-derived carbonaceous and nanostructured carbon materials, both functionalized with specific chemical groups, with the carbon materials additionally doped with metal oxides and noble metal nanoparticles, will enable the development of multifunctional materials capable of efficiently removing and degrading emerging contaminants in water and enhancing electrocatalytic performance for hydrogen production.

5. Objectives

5.1 General objective

To develop multifunctional materials with adsorbent, photocatalytic, and electrocatalytic properties, based on polymeric matrices and carbonaceous supports doped with oxides and metallic nanoparticles, for the efficient removal of emerging contaminants in aqueous media and their application in sustainable processes, including hydrogen production.

5.2 Specific objectives

- To synthesize polymeric xerogels from resorcinol-formaldehyde with different molar ratios to maximize their metformin adsorption capacity in aqueous solution.
- To physically and chemically characterize the obtained xerogels using techniques such as FT-IR, SEM, XRD, BET, and TGA, and to relate their structure to their adsorption performance, ensuring a thorough understanding and reliable results.
- To evaluate the influence of pH, temperature, and initial contaminant concentration on the metformin adsorption efficiency of the synthesized xerogels, addressing key environmental variables that affect real-world applications.
- To determine the adsorption isotherms and kinetic parameters associated with the removal of metformin.
- To investigate the reusability and regeneration capacity of the xerogels without significant loss of efficiency.
- Synthesize carbonaceous materials (biochar and hydrochar) from agro-industrial waste such as coffee grounds and agave bagasse using pyrolysis and hydrothermalion processes.
- Dope the carbonaceous supports with semiconducting metal oxides such as BiOCl, CeO_2, and Fe_2O_3 to enhance their photocatalytic activity.
- To characterize the optical, structural, and surface properties of the photocatalytic materials using techniques such as Raman spectroscopy, XPS, UV-Vis DRS, SEM-EDS, and TEM, with the goal of correlating these properties to photocatalytic efficiency in pollutant degradation.
- Assess the photodegradation efficiency of dyes like methylene blue and indigo blue under UV and visible light to define clear research goals.
- Analyze the role of reactive oxygen species (•OH, $O_2{\bullet}^-$, h^+) in photocatalytic degradation processes.
- Determine the kinetic parameters of dye photodegradation using pseudo-first-order, pseudo-second-order, and Langmuir–Hinshelwood models.
- Study the structural stability of the photocatalysts after multiple use cycles to ensure robustness and build trust in the research outcomes.

- Functionalize multi-walled carbon nanotubes (MWCNTs) through solvothermal treatment in an alkaline medium to systematically increase surface area and active sites.
- Dope the functionalized MWCNTs with platinum and palladium nanoparticles to develop efficient electrocatalysts.
- Characterize the electrocatalysts using electrochemical techniques (LSV, CV, EIS, CA) to evaluate their performance in the hydrogen evolution reaction (HER).
- Evaluate the electrochemical stability and durability of the catalysts after multiple operating cycles.
- Analyze the potential of the developed catalysts in the electrodegradation of aqueous pollutants.
- Integrate adsorbent, photocatalytic, and electrocatalytic properties into multifunctional hybrid materials.

Chapter 1. Highly Adsorptive Organic Xerogels for Efficient Removal of Metformin from Aqueous Solutions: Experimental and Theoretical Approach

1.1 Introduction

Emerging contaminants in water effluents pose a global challenge, as even trace concentrations [ppb (μg/L) to ppm (mg/L)] can harm environmental quality and human health, threatening the availability of safe drinking water (Foretz et al., 2014; Hernández et al., 2015). Pharmaceuticals, personal care products, pesticides, dyes, and industrial chemicals are increasingly recognized as major contributors to this form of water pollution (Balakrishnan et al., 2022b).

For these reasons, emerging pollutants have received significant attention in recent years due to their anthropogenic origins and the absence of well-established regulations governing their disposal (Desai et al., 2014; Foretz et al., 2014). It is estimated that globally, approximately 350,000 synthetic compounds have disposal and control processes that remain uncertain (Balakrishnan et al., 2022b). Among these emerging pollutants, pharmaceutical compounds pose a particularly challenging removal process from water due to their complex nature. These accessible sites (i.e., the transfer of reactant molecules on active sites per unit time), even when part of the carbon surface is masked by nanoparticle coverage (Zahra et al., 2020).

4.4 Conclusions

This work demonstrates that alkaline solvothermal functionalization significantly improves the structural and electrochemical properties of MWCNTs for HER. The treatment increased surface area from 109 to 189 $m^2\ g^{-1}$, pore volume from 0.44 to 0.97 $cm^3\ g^{-1}$ and reduced the I_D/I_G ratio from 1.16 to 0.96, evidencing improved graphitic ordering. After Pt–Pd decoration, nanoparticles of 17.7–30.8 nm were uniformly dispersed, leading to a higher exchange current density (1.09×10^{-3} A cm^{-2}) compared with functionalized MWCNTs (5.01×10^{-5} A cm^{-2}). In acidic media, the MWCNT-KOH catalyst exhibited an overpotential of −0.20 V at 10 mA cm^{-2} with a Tafel slope of 84 mV dec^{-1}, while $MWCNT_f$-PdPt further lowered the kinetic barrier and maintained stability over 1000 cycles. The incorporation of Pt and Pd nanoparticles onto the functionalized MWCNTs resulted in well-dispersed metallic clusters that served as highly active catalytic sites, particularly effective in proton-rich acidic media. Among the key findings was the successful introduction of oxygen-containing functional groups via solvothermal alkaline treatment, which enhanced surface wettability, increased the electrochemically active surface area, and reduced the charge-transfer resistance. Although noble metals limit scalability, the results highlight solvothermal functionalization as a versatile, scalable strategy to enhance porosity, surface chemistry, and active-site accessibility, providing a foundation for integrating earth-abundant metals into next-generation HER catalysts.

6. General conclusions

This doctoral work demonstrates the successful development of multifunctional materials with adsorbent, photocatalytic, and electrocatalytic activity, designed for the efficient treatment of emerging contaminants and sustainable environmental applications. Through rational material design, controlled functionalization, and the use of low-cost precursors, the study establishes a coherent strategy to address water pollution with advanced functional materials.

1. Structure–property–performance relationships were systematically established across all material systems. The tuning of surface chemistry, porosity, crystallinity, and electronic structure—via controlled synthesis routes and targeted doping—proved decisive in enhancing adsorption capacity, photocatalytic efficiency, and electrocatalytic activity.
2. Resorcinol–formaldehyde xerogels exhibited outstanding adsorption performance for metformin, achieving a maximum capacity of 325 mg g^{-1}, surpassing reported values in the literature. Adsorption was governed by electrostatic interactions, hydrogen bonding, and ion exchange, strongly influenced by pH, temperature, and competing ions. These findings validate xerogels as highly tunable and robust adsorbents for pharmaceutical contaminants.
3. Agro-industrial and biomass-derived supports (agave bagasse and coffee grounds) were successfully transformed into high-performance catalytic materials, demonstrating that waste-derived carbons can rival conventional supports while improving sustainability and circular economy metrics.
4. CeO_2-doped agave bagasse carbons achieved complete (100%) methylene blue removal, combining adsorption and photocatalysis. The introduction of cerium oxide enhanced visible-light absorption, defect density, and surface reactivity, while UV irradiation ensured superior mineralization efficiency and long-term cyclic stability.
5. BiOCl-based hydrochars doped with CeO_2 and Fe_2O_3 showed exceptional photocatalytic efficiencies (>99%), benefiting from reduced band gaps, improved charge separation, and dopant-dependent reaction mechanisms. The coexistence of photocatalytic and photo-Fenton pathways enabled efficient degradation under diverse pH conditions, highlighting the versatility of these materials for complex effluents.
6. Alkaline solvothermal functionalization of MWCNTs significantly enhanced their electrocatalytic performance for the hydrogen evolution reaction (HER) by increasing surface area, improving graphitic ordering, and

introducing oxygenated functional groups. Subsequent Pt–Pd decoration generated highly active and stable catalytic sites, reducing overpotential and charge-transfer resistance in acidic media.

7. Across all systems, synergistic effects between adsorption, catalytic activity, and material structure were identified, confirming that multifunctionality is a powerful approach for contaminant removal rather than relying on single-function materials.
8. Operational parameters such as pH, temperature, light source, catalyst mass, and reuse cycles were shown to critically affect performance, providing practical design guidelines for scaling and real-world implementation in water treatment and purification technologies.
9. Despite the use of noble metals in some systems, the work demonstrates that surface functionalization and support engineering can maximize catalytic efficiency while minimizing metal loading, offering a pathway toward economically viable and scalable solutions.

Overall, this research provides a comprehensive and integrated framework for designing multifunctional materials capable of addressing emerging contaminants through adsorption, photocatalysis, and electrocatalysis. By combining high performance, reusability, and sustainability—particularly through the valorization of biomass waste—the study contributes meaningful advances toward next-generation materials for environmental remediation, clean energy, and resource-efficient water treatment systems.

7. References

Abbas, A., Ahmad, T., Hussain, S., Noman, M., Shahzad, T., Iftikhar, A., Cheema, Ijaz, M., Tahir, M., Gohari, G., Li, B., Mahmood, F., & Shahid, M. (2022). Immobilized biogenic zinc oxide nanoparticles as photocatalysts for degradation of methylene blue dye and treatment of textile effluents. *International Journal of Environmental Science and Technology*, *19*(11), 11333–11346. https://doi.org/10.1007/s13762-021-03872-4

Adhikari, C., Kaur, M., & Ravichandran. (2020). Sunlight Assisted Degradation of Methylene Blue as a Model Dye using Bismuth Oxychloride Nanoparticles: Ecofriendly and industry efficient photocatalysis for waste chemical treatment. *Asian Journal of Chemistry*, *32*(1), 115–121. https://doi.org/10.14233/ajchem.2020.22367

Adnan, Omer, M., Khan, B., Khan, I., Alamzeb, M., Zada, F. M., Ullah, I., Shah, R., Alqarni, M., & Simal-Gandara, J. (2022). Equilibrium, Kinetic and Thermodynamic Studies for the Adsorption of Metanil Yellow Using Carbonized Pistachio Shell-Magnetic Nanoparticles. *Water*, *14*(24). https://doi.org/10.3390/w14244139

Afza, N., Shivakumar, M. S., Alam, M. W., Kumar, A. N., Bhatt, A. S., Murthy, H. C. A., Ravikumar, C. R., Mylarappa, M., & Selvanandan, S. (2022). Facile hydrothermal synthesis of cerium oxide/rGO nanocomposite for photocatalytic and supercapacitor applications. *Applied Surface Science Advances*, *11*, 100307. https://doi.org/10.1016/j.apsadv.2022.100307

Aguilar-Maruri, S. A., Ramos-Galicia, L., Ocampo-Pérez, R., Forgionny, A., Ruíz-Camacho, B., Serna-Carrizales, J. Carlos., Cabrera-Ruiz, J., López-Ortiz, A., Palestino, G., & Sano, N. (2025). Waste-derived catalytic hydrochars from coffee grounds doped with BiOCl, CeO2, and α-Fe2O3: Structural insights and enhanced photocatalytic performance. *Journal of Environmental Chemical Engineering*, *13*(5), 117799. https://doi.org/10.1016/j.jece.2025.117799

Ahmad, A., Mohd-Setapar, S. H., Chuong, C. S., Khatoon, A., Wani, W. A., Kumar, R., & Rafatullah, M. (2015). Recent advances in new generation dye removal technologies: novel search for approaches to reprocess wastewater. *RSC Advances*, *5*(39), 30801–30818. https://doi.org/10.1039/C4RA16959J

AlAreeqi, S., Bahamon, D., Polychronopoulou, K., & Vega, L. F. (2022). Insights into the thermal stability and conversion of carbon-based materials by using ReaxFF reactive force field: Recent advances and future directions. *Carbon*, *196*, 840–866. https://doi.org/10.1016/j.carbon.2022.05.035

Ali, M. H. H., Abdelkarim, M. S., & Al-Afify, A. D. G. (2024). Characterization and photodegradation of methylene blue dye using bio-synthesized cerium oxide nanoparticles with Spirulina platensis extract. *Discover Applied Sciences*, *6*(3), 94. https://doi.org/10.1007/s42452-024-05736-1

Alinaghi, M., Mokarram, P., Ahmadi, M., & Bozorg-ghalati, F. (2024). Biosynthesis of palladium, platinum, and their bimetallic nanoparticles using rosemary and ginseng herbal plants: evaluation of anticancer activity. *Scientific Reports*, *14*(1), 5798. https://doi.org/10.1038/s41598-024-56275-z

Aljamali, N. M., Khdur, R., & Alfatlawi, I. O. (2021). Physical and chemical adsorption and its applications. *International Journal of Thermodynamics and Chemical Kinetics*, *7*(2), 1–8.

Allen, C. L., Atkinson, B. N., & Williams, J. M. J. (2012). Transamidation of Primary Amides with Amines Using Hydroxylamine Hydrochloride as an Inorganic Catalyst. *Angewandte Chemie International Edition*, *51*(6), 1383–1386. https://doi.org/10.1002/anie.201107348

Al-Muhtaseb, S. A., & Ritter, J. A. (2003). Preparation and Properties of Resorcinol–Formaldehyde Organic and Carbon Gels. *Advanced Materials*, *15*(2), 101–114. https://doi.org/10.1002/adma.200390020

Al-Nuaim, M. A., Alwasiti, A. A., & Shnain, Z. Y. (2023). The photocatalytic process in the treatment of polluted water. *Chemical Papers*, *77*(2), 677–701. https://doi.org/10.1007/s11696-022-02468-7

Alterary, S. S., Alyabes, R. M., Alshahrani, A. A., & Al-Alshaikh, M. A. (2022). Unfunctionalized and Functionalized Multiwalled Carbon Nanotubes/Polyamide Nanocomposites as Selective-Layer Polysulfone Membranes. *Polymers*, *14*(8). https://doi.org/10.3390/polym14081544

Al-Tohamy, R., Ali, S. S., Li, F., Okasha, K. M., Mahmoud, Y. A.-G., Elsamahy, T., Jiao, H., Fu, Y., & Sun, J. (2022). A critical review on the treatment of dye-containing wastewater: Ecotoxicological and health concerns of textile dyes and possible remediation approaches for environmental safety. *Ecotoxicology and Environmental Safety*, *231*, 113160. https://doi.org/10.1016/j.ecoenv.2021.113160

Antonini, G., Ordonez-Loza, J., Mathew, J., Cullen, J., Muller, C., Al-Omari, A., Bell, K., Santoro, D., & Pearce, J. M. (2025). Electrode Materials Comparison for Hydrogen Production from Wastewater Electrolysis of Spiked Secondary Effluent. *Sustainability*, *17*(9). https://doi.org/10.3390/su17093988

Arumugam, A., Karthikeyan, C., Haja Hameed, A. S., Gopinath, K., Gowri, S., & Karthika, V. (2015). Synthesis of cerium oxide nanoparticles using Gloriosa superba L. leaf extract and their structural, optical and antibacterial properties. *Materials Science and Engineering: C*, *49*, 408–415. https://doi.org/10.1016/j.msec.2015.01.042

Asefa, G., Negussa, D., Lemessa, G., & Alemu, T. (2024). The Study of Photocatalytic Degradation Kinetics and Mechanism of Malachite Green Dye on Ni–TiO2 Surface Modified with Polyaniline. *Journal of Nanomaterials*, *2024*(1), 5259089. https://doi.org/10.1155/2024/5259089

Awad, M. E., Farrag, A. M., El-Bindary, A. A., El-Bindary, M. A., & Kiwaan, H. A. (2023). Photocatalytic degradation of Rhodamine B dye using low-cost pyrofabricated titanium dioxide quantum dots-kaolinite nanocomposite. *Applied Organometallic Chemistry*, *37*(7), e7113. https://doi.org/10.1002/aoc.7113

Badran, I., Hassan, A., Manasrah, A. D., & Nassar, N. N. (2019). Experimental and theoretical studies on the thermal decomposition of metformin. *Journal of Thermal Analysis and Calorimetry*, *138*(1), 433–441. https://doi.org/10.1007/s10973-019-08213-9

Bakry, A. M., Alamier, W. M., Salama, R. S., Samy El-Shall, M., & Awad, F. S. (2022). Remediation of water containing phosphate using ceria nanoparticles decorated partially reduced graphene oxide (CeO2-PRGO) composite. *Surfaces and Interfaces*, *31*, 102006. https://doi.org/10.1016/j.surfin.2022.102006

Balaji, D., Arunachalam, P., Duraimurugan, K., Madhavan, J., Theerthagiri, J., Al-Mayouf, A. M., & Choi, M. Y. (2020). Highly efficient Ni0.5Fe0.5Se2/MWCNT electrocatatalyst for hydrogen evolution reaction in acid media. *International Journal of Hydrogen Energy*, *45*(13), 7838–7847. https://doi.org/10.1016/j.ijhydene.2019.09.039

Balakrishnan, A., Sillanpää, M., Jacob, M. M., & Vo, D.-V. N. (2022a). Metformin as an emerging concern in wastewater: Occurrence, analysis and treatment methods. *Environmental Research*, *213*, 113613. https://doi.org/10.1016/j.envres.2022.113613

Balakrishnan, A., Sillanpää, M., Jacob, M. M., & Vo, D.-V. N. (2022b). Metformin as an emerging concern in wastewater: Occurrence, analysis and treatment methods. *Environmental Research*, *213*, 113613. https://doi.org/10.1016/j.envres.2022.113613

Balasubramani, K., Sivarajasekar, N., & Naushad, Mu. (2020). Effective adsorption of antidiabetic pharmaceutical (metformin) from aqueous medium using graphene oxide nanoparticles: Equilibrium and statistical modelling. *Journal of Molecular Liquids*, *301*, 112426. https://doi.org/10.1016/j.molliq.2019.112426

Balint, L.-C., Hulka, I., & Kellenberger, A. (2022). Pencil Graphite Electrodes Decorated with Platinum Nanoparticles as Efficient Electrocatalysts for Hydrogen Evolution Reaction. *Materials*, *15*(1). https://doi.org/10.3390/ma15010073

Balu, S., Ganapathy, D., Arya, S., Atchudan, R., & Sundramoorthy, A. K. (2024). Advanced photocatalytic materials based degradation of micropollutants and their use in hydrogen production – a review. *RSC Adv.*, *14*(20), 14392–14424. https://doi.org/10.1039/D4RA01307G

Bhangare, D., Rajput, N., Jadav, T., Sahu, A. K., Tekade, R. K., & Sengupta, P. (2022). Systematic strategies for degradation kinetic study of pharmaceuticals: an issue of utmost importance concerning current stability analysis practices. *Journal of Analytical Science and Technology*, *13*(1), 7. https://doi.org/10.1186/s40543-022-00317-6

Bhatti, M. A., Dawi, E., Tahira, A., Hulio, A. A., Halepoto, I. A., Chang, S. A., Solangi, A. G., Nafady, A., Tonezzer, M., Haj Ismail, A. A. K., & Ibupoto, Z. H. (2024). UV photodegradation of methylene blue using microstructural carbon materials derived from citrullus colocynthis. *Frontiers in Materials*, *Volume 11-2024*. https://doi.org/10.3389/fmats.2024.1407485

Bi, S., Geng, Z., Yang, L., Zhao, L., Qu, C., Gao, Z., Jin, L., Xue, M., & Zhang, C. (2024). Construction of Efficient Ru@NiMoCu Porous Electrode for High Current Alkaline Water Electrolysis. *Advanced Energy Materials*, *14*(44), 2303623. https://doi.org/10.1002/aenm.202303623

Boehm, H.-P., Diehl, E., Heck, W., & Sappok, R. (1964). Surface Oxides of Carbon. *Angewandte Chemie International Edition in English*, *3*(10), 669–677. https://doi.org/10.1002/anie.196406691

Boita, J., Nicolao, L., Alves, M. C. M., & Morais, J. (2014). Observing Pt nanoparticle formation at the atomic level during polyol synthesis. *Physical*

Chemistry Chemical Physics, *16*(33), 17640–17647. https://doi.org/10.1039/C4CP01925C

Brandon, N. P., & Kurban, Z. (2017). Clean energy and the hydrogen economy. *Philosophical Transactions of the Royal Society A: Mathematical, Physical and Engineering Sciences*, *375*(2098), 20160400. https://doi.org/10.1098/rsta.2016.0400

Bystrzejewski, M., Lange, H., Huczko, A., Elim, H. I., & Ji, W. (2007). Study of the optical limiting properties of carbon-encapsulated magnetic nanoparticles. *Chemical Physics Letters*, *444*(1), 113–117. https://doi.org/10.1016/j.cplett.2007.06.125

Cachet-Vivier, C., Bastide, S., Laurent, M., Zlotea, C., & Latroche, M. (2012). Hydrogen sorption properties of Pd nanoparticles dispersed on graphitic carbon studied with a cavity microelectrode. *Electrochimica Acta*, *83*, 133–139. https://doi.org/10.1016/j.electacta.2012.08.037

Calvache-Muñoz, J., Prado, F. A., Tirado, L., Daza-Gomez, L. C., Cuervo-Ochoa, G., Calambas, H. L., & Rodríguez-Páez, J. E. (2019). Structural and Optical Properties of CeO2 Nanoparticles Synthesized by Modified Polymer Complex Method. *Journal of Inorganic and Organometallic Polymers and Materials*, *29*(3), 813–826. https://doi.org/10.1007/s10904-018-01056-1

Cam, T. S., Omarov, S. O., Chebanenko, M. I., Izotova, S. G., & Popkov, V. I. (2022). Recent progress in the synthesis of CeO2-based nanocatalysts towards efficient oxidation of CO. *Journal of Science: Advanced Materials and Devices*, *7*(1), 100399. https://doi.org/10.1016/j.jsamd.2021.11.001

Carrales-Alvarado, D. H., Rodríguez-Ramos, I., Leyva-Ramos, R., Mendoza-Mendoza, E., & Villela-Martínez, D. E. (2020). Effect of surface area and physical–chemical properties of graphite and graphene-based materials on their adsorption capacity towards metronidazole and trimethoprim antibiotics in aqueous solution. *Chemical Engineering Journal*, *402*, 126155. https://doi.org/10.1016/j.cej.2020.126155

Carrara, N., Badano, J. M., Vailard, S., Vera, C., & Quiroga, M. (2020). Selective Hydrogenation of Diketones on Supported Transition Metal Catalysts. *Catalysis Letters*, *150*(2), 461–470. https://doi.org/10.1007/s10562-019-02983-5

Chatterjee, D., & Dasgupta, S. (2005). Visible light induced photocatalytic degradation of organic pollutants. *Journal of Photochemistry and Photobiology C: Photochemistry Reviews*, *6*(2), 186–205. https://doi.org/10.1016/j.jphotochemrev.2005.09.001

Che Ramli, Z. A., Asim, N., Isahak, W. N. R. W., Emdadi, Z., Ahmad-Ludin, N., Yarmo, M. A., & Sopian, K. (2014). Photocatalytic Degradation of Methylene Blue under UV Light Irradiation on Prepared Carbonaceous TiO2. *The Scientific World Journal*, *2014*(1), 415136. https://doi.org/10.1155/2014/415136

Chen, H., Yu, X., Zhu, Y., Fu, X., & Zhang, Y. (2016). Controlled synthesis of {001} facets-dominated dye-sensitized BiOCl with high photocatalytic efficiency under visible-light irradiation. *Journal of Nanoparticle Research*, *18*(8), 225. https://doi.org/10.1007/s11051-016-3529-4

Chen, M., Jiang, Y., Mei, P., Zhang, Y., Zheng, X., Xiao, W., You, Q., Yan, X., & Tang, H. (2019). Polyacrylamide Microspheres-Derived Fe3C@N-doped Carbon Nanospheres as Efficient Catalyst for Oxygen Reduction Reaction. *Polymers*, *11*(5). https://doi.org/10.3390/polym11050767

Chen, Y., Wang, T., Pan, J., Chen, A., & Chen, Y. (2022). Design and fabrication of carbon spheres-supported cerium oxide heterostructured composites for enhanced photocatalytic activity. *Ceramics International*, *48*(12), 17714–17722. https://doi.org/10.1016/j.ceramint.2022.03.041

Cheng, N., Stambula, S., Wang, D., Banis, M. N., Liu, J., Riese, A., Xiao, B., Li, R., Sham, T.-K., Liu, L.-M., Botton, G. A., & Sun, X. (2016). Platinum single-atom and cluster catalysis of the hydrogen evolution reaction. *Nature Communications*, *7*(1), 13638. https://doi.org/10.1038/ncomms13638

Chiu, Y.-H., Chang, T.-F. M., Chen, C.-Y., Sone, M., & Hsu, Y.-J. (2019). Mechanistic Insights into Photodegradation of Organic Dyes Using Heterostructure Photocatalysts. *Catalysts*, *9*(5). https://doi.org/10.3390/catal9050430

Comí, M., Fernández, M., Santamaría, A., Lligadas, G., Ronda, J. C., Galià, M., & Cádiz, V. (2017). Carboxylic Acid Ionic Modification of Castor-Oil-Based Polyurethanes Bearing Amine Groups: Chemically Tunable Physical Properties and Recyclability. *Macromolecular Chemistry and Physics*, *218*(23), 1700379. https://doi.org/10.1002/macp.201700379

Cusioli, L. F., Nishi, L., Beltran, L. B., Ribeiro, A. C., Bergamasco, R., Bulla, M. K., Facina, R. K., & Mateus, G. A. P. (2023). Synthesis of a Chemically Modified Biosorbent Based on the Invasive Plant Leucaena leucocephala and Its Application in Metformin Removal. *Water*, *15*(14). https://doi.org/10.3390/w15142600

Daskalaki, V. M., Antoniadou, M., Li Puma, G., Kondarides, D. I., & Lianos, P. (2010). Solar Light-Responsive Pt/CdS/TiO2 Photocatalysts for Hydrogen Production and Simultaneous Degradation of Inorganic or Organic Sacrificial Agents in Wastewater. *Environmental Science & Technology*, *44*(19), 7200–7205. https://doi.org/10.1021/es9038962

Dave, P. N., Kamaliya, B., Macwan, P. M., & Trivedi, J. H. (2023). Fabrication and characterization of a gum ghatti-cl-poly(N-isopropyl acrylamide-co-acrylic acid)/CoFe2O4 nanocomposite hydrogel for metformin hydrochloride drug removal from aqueous solution. *Current Research in Green and Sustainable Chemistry*, *6*, 100349. https://doi.org/10.1016/j.crgsc.2022.100349

Daza-Gómez, L.-C., Hernández-Contreras, X.-A., Cruz, L. M., & Díaz, D. (2024). Recent Advances in Plastic Degradation and Conversion by Photocatalysis. In *Plastic Degradation and Conversion by Photocatalysis (Volume 2): From Waste to Wealth* (Vol. 1490, pp. 151–193). American Chemical Society. https://doi.org/10.1021/bk-2024-1490.ch007

De Gisi, S., Lofrano, G., Grassi, M., & Notarnicola, M. (2016). Characteristics and adsorption capacities of low-cost sorbents for wastewater treatment: A review. *Sustainable Materials and Technologies*, *9*, 10–40. https://doi.org/10.1016/j.susmat.2016.06.002

Deng, J., Xu, L., Zhang, L., Peng, J., Guo, S., Liu, J., & Koppala, S. (2019). Recycling of Carbon Fibers from CFRP Waste by Microwave Thermolysis. *Processes*, *7*(4). https://doi.org/10.3390/pr7040207

Desai, D., Wong, B., Huang, Y., Ye, Q., Tang, D., Guo, H., Huang, M., & Timmins, P. (2014). Surfactant-Mediated Dissolution of Metformin Hydrochloride Tablets: Wetting Effects Versus Ion Pairs Diffusivity. *Journal of Pharmaceutical Sciences*, *103*(3), 920–926. https://doi.org/10.1002/jps.23852

Desnelli, D., Department of Chemistry Universitas Sriwijaya Jalan Palembang Prabumulih Km 32 Indralaya Ogan Ilir 30662, F. of M. and N. S., Padilah, I. H., Ulfa, M., Eliza, E., Mara, A., & Fatma, F. (2023). Synthesis of Chitosan−Al2O3 composite using the sol-gel method and its application in photodegradation of methylene blue. *Indonesian Journal of Fundamental and Applied Chemistry*, *8*(1), 40–47. https://doi.org/10.24845/ijfac.v8.i1.40

Devarahosahalli Veeranna, K., Theeta Lakshamaiah, M., & Thimmasandra Narayan, R. (2014). Photocatalytic Degradation of Indigo Carmine Dye Using Calcium Oxide. *International Journal of Photochemistry*, *2014*(1), 530570. https://doi.org/10.1155/2014/530570

Dezfuli, A. S., Ganjali, M. R., Naderi, H. R., & Norouzi, P. (2015). A high performance supercapacitor based on a ceria/graphene nanocomposite synthesized by a facile sonochemical method. *RSC Advances*, *5*(57), 46050–46058. https://doi.org/10.1039/C5RA02957K

Doğdu Okçu, G., Tunacan, T., & Dikmen, E. (2019). Removal of indigo dye by photocatalysis process using Taguchi experimental design. *Environmental Research and Technology*, *2*(2), 63–72. https://doi.org/10.35208/ert.457739

Dujearic-Stephane, K., Gupta, M., Kumar, A., Sharma, V., Pandit, S., Bocchetta, P., & Kumar, Y. (2021). The Effect of Modifications of Activated Carbon Materials on the Capacitive Performance: Surface, Microstructure, and Wettability. *Journal of Composites Science*, *5*(3). https://doi.org/10.3390/jcs5030066

Edwards, H. G. M. (2001). Spectra–Structure Correlations in Raman Spectroscopy. In *Handbook of Vibrational Spectroscopy*. https://doi.org/10.1002/0470027320.s4103

Ejsmont, A., Kadela, K., Grzybek, G., Darvishzad, T., Słowik, G., Lofek, M., Goscianska, J., Kotarba, A., & Stelmachowski, P. (2023). Speciation of Oxygen Functional Groups on the Carbon Support Controls the Electrocatalytic Activity of Cobalt Oxide Nanoparticles in the Oxygen Evolution Reaction. *ACS Applied Materials & Interfaces*, *15*(4), 5148–5160. https://doi.org/10.1021/acsami.2c18403

Elgrishi, N., Rountree, K. J., McCarthy, B. D., Rountree, E. S., Eisenhart, T. T., & Dempsey, J. L. (2018). A Practical Beginner's Guide to Cyclic Voltammetry.

Journal of Chemical Education, *95*(2), 197–206. https://doi.org/10.1021/acs.jchemed.7b00361

El-taweel, R. M., Mohamed, N., Alrefaey, K. A., Husien, S., Abdel-Aziz, A. B., Salim, A. I., Mostafa, N. G., Said, L. A., Fahim, I. S., & Radwan, A. G. (2023). A review of coagulation explaining its definition, mechanism, coagulant types, and optimization models; RSM, and ANN. *Current Research in Green and Sustainable Chemistry*, *6*, 100358. https://doi.org/10.1016/j.crgsc.2023.100358

Esquivel-Castro, T. A., Ceballos, J., Torres-Zanoni, E., Padmasree, K. P., Valadez-Renteria, E., Aldana-Sanchez, I., Quevedo-Lopez, M., Rodriguez-Gonzalez, V., & Oliva, J. (2024). Solar photocatalytic degradation of methylene blue dye and 4-CP herbicide by using a biodegradable fiber support decorated with Ce0.9Bi0.1O2 porous nanoparticles. *Inorganic Chemistry Communications*, *168*, 112946. https://doi.org/10.1016/j.inoche.2024.112946

Farbod, M., Tadavani, S. K., & Kiasat, A. (2011). Surface oxidation and effect of electric field on dispersion and colloids stability of multiwalled carbon nanotubes. *Colloids and Surfaces A: Physicochemical and Engineering Aspects*, *384*(1), 685–690. https://doi.org/10.1016/j.colsurfa.2011.05.041

Feng, Z., Eiubovi, I., Shao, Y., Fan, Z., & Tan, R. (2024). Review of Digital Twin Technology Applications in Hydrogen Energy. *CHAIN*, *1*(1), 54–74. https://doi.org/10.23919/CHAIN.2024.000001

Ficanha, A. M. M., Oro, C. E. D., Franceschi, E., Dallago, R. M., & Mignoni, M. L. (2021). Evaluation of Different Ionic Liquids as Additives in the Immobilization of Lipase CAL B by Sol-Gel Technique. *Applied Biochemistry and Biotechnology*, *193*(7), 2162–2181. https://doi.org/10.1007/s12010-021-03533-9

Figueiredo, J. L., & Pereira, M. F. R. (2008). Carbon as Catalyst. In *Carbon Materials for Catalysis* (pp. 177–217). https://doi.org/10.1002/9780470403709.ch6

Fito, J., Abewaa, M., Mengistu, A., Angassa, K., Ambaye, A. D., Moyo, W., & Nkambule, T. (2023). Adsorption of methylene blue from textile industrial wastewater using activated carbon developed from Rumex abyssinicus plant. *Scientific Reports*, *13*(1), 5427. https://doi.org/10.1038/s41598-023-32341-w

Fleischmann, S., Zhang, Y., Wang, X., Cummings, P. T., Wu, J., Simon, P., Gogotsi, Y., Presser, V., & Augustyn, V. (2022). Continuous transition from double-layer to Faradaic charge storage in confined electrolytes. *Nature Energy*, *7*(3), 222–228. https://doi.org/10.1038/s41560-022-00993-z

Foretz, M., Guigas, B., Bertrand, L., Pollak, M., & Viollet, B. (2014). Metformin: From Mechanisms of Action to Therapies. *Cell Metabolism*, *20*(6), 953–966. https://doi.org/10.1016/j.cmet.2014.09.018

Forgionny, A., Acelas, N. Y., Jimenez-Orozco, C., & Flórez, E. (2020). Toward the design of efficient adsorbents for Hg2+ removal: Molecular and thermodynamic insights. *International Journal of Quantum Chemistry*, *120*(15), e26258. https://doi.org/10.1002/qua.26258

FRISCH, M. J. (n.d.). GAUSSIAN09. *Http://Www.Gaussian.Com/*. https://cir.nii.ac.jp/crid/1571698600718545408

Fu, L., Li, J., Wang, G., Luan, Y., & Dai, W. (2021). Adsorption behavior of organic pollutants on microplastics. *Ecotoxicology and Environmental Safety*, *217*, 112207. https://doi.org/10.1016/j.ecoenv.2021.112207

Gaikwad, M. M., Kakunuri, M., & Sharma, C. S. (2019). Enhanced catalytic graphitization of resorcinol formaldehyde derived carbon xerogel to improve its anodic performance for lithium ion battery. *Materials Today Communications*, *20*, 100569. https://doi.org/10.1016/j.mtcomm.2019.100569

Gao, P., Yin, Z., Feng, L., Liu, Y., Du, Z., Duan, Z., & Zhang, L. (2020). Solvothermal synthesis of multiwall carbon nanotubes/BiOI photocatalysts for the efficient degradation of antipyrine under visible light. *Environmental Research*, *185*, 109468. https://doi.org/10.1016/j.envres.2020.109468

Garg, A., & Chopra, L. (2022). Dye Waste: A significant environmental hazard. *Materials Today: Proceedings*, *48*, 1310–1315. https://doi.org/10.1016/j.matpr.2021.09.003

Ge, J., Zhang, Y., & Park, S.-J. (2019). Recent Advances in Carbonaceous Photocatalysts with Enhanced Photocatalytic Performances: A Mini Review. *Materials*, *12*(12). https://doi.org/10.3390/ma12121916

Ge, S., Wang, S., Mai, W., Zhang, K., Tanveer, M., Wang, L., & Tian, C. (2023). Characteristics and acidic soil amelioration effects of biochar derived from a typical halophyte Salicornia europaea L. (common glasswort). *Environmental Science and Pollution Research*, *30*(24), 66113–66124. https://doi.org/10.1007/s11356-023-27182-z

Ghorai, K., Panda, A., Bhattacharjee, M., Mandal, D., Hossain, A., Bera, P., Seikh, Md. M., & Gayen, A. (2021). Facile synthesis of CuCr2O4/CeO2 nanocomposite: A new Fenton like catalyst with domestic LED light assisted improved photocatalytic activity for the degradation of RhB, MB and MO dyes. *Applied Surface Science*, *536*, 147604. https://doi.org/10.1016/j.apsusc.2020.147604

González García, A. P., Carlos Hernández, S., & Díaz Jiménez, L. (2025). Agave lechuguilla waste can be applied as biochar-adsorbent to remove arsenic from water. *International Journal of Environmental Science and Technology*, *22*(10), 9193–9208. https://doi.org/10.1007/s13762-024-06226-y

Gorman, M. (1957). The evidence from infrared spectroscopy for hydrogen bonding: A case history of the correlation and interpretation of data. *Journal of Chemical Education*, *34*(6), 304. https://doi.org/10.1021/ed034p304

Groeneveld, I., Kanelli, M., Ariese, F., & van Bommel, M. R. (2023). Parameters that affect the photodegradation of dyes and pigments in solution and on substrate – An overview. *Dyes and Pigments*, *210*, 110999. https://doi.org/10.1016/j.dyepig.2022.110999

Guevara-Bernal, D. F., Cáceres Ortíz, M. Y., Gutiérrez Cifuentes, J. A., Bastos-Arrieta, J., Palet, C., & Candela, A. M. (2022). Coffee Husk and Lignin Revalorization: Modification with Ag Nanoparticles for Heavy Metals Removal and Antifungal Assays. *Water*, *14*(11). https://doi.org/10.3390/w14111796

Hassaan, M. A., El-Nemr, M. A., Elkatory, M. R., Ragab, S., Niculescu, V.-C., & El Nemr, A. (2023). Principles of Photocatalysts and Their Different Applications: A Review. *Topics in Current Chemistry*, *381*(6), 31. https://doi.org/10.1007/s41061-023-00444-7

Heidari, B. S., Cheraghchi, V.-S., Motahari, S., Motlagh, G. H., & Davachi, S. M. (2018). Optimized mercapto-modified resorcinol formaldehyde xerogel for adsorption of lead and copper ions from aqueous solutions. *Journal of Sol-*

Gel Science and Technology, *88*(1), 236–248. https://doi.org/10.1007/s10971-018-4782-z

Hembram, K. P. S. S., & Rao, G. M. (2012). Origin of structural defects in multiwall carbon nanotube. *Materials Letters*, *72*, 68–70. https://doi.org/10.1016/j.matlet.2011.12.078

Henderson, J. (1995). The analysis of ancient glasses part I: Materials, properties, and early European glass. *JOM*, *47*(11), 62–64. https://doi.org/10.1007/BF03221315

Hernández, B., Pflüger, F., Kruglik, S. G., Cohen, R., & Ghomi, M. (2015). Protonation–deprotonation and structural dynamics of antidiabetic drug metformin. *Journal of Pharmaceutical and Biomedical Analysis*, *114*, 42–48. https://doi.org/10.1016/j.jpba.2015.04.041

Hernández-Gordillo, A., Rodríguez-González, V., Oros-Ruiz, S., & Gómez, R. (2016). Photodegradation of Indigo Carmine dye by CdS nanostructures under blue-light irradiation emitted by LEDs. *Catalysis Today*, *266*, 27–35. https://doi.org/10.1016/j.cattod.2015.09.001

Hethnawi, A., Alnajjar, M., Manasrah, A. D., Hassan, A., Vitale, G., Jeong, R., & Nassar, N. N. (2020). Metformin Removal from Water Using Fixed-bed Column of Silica-Alumina Composite. *Colloids and Surfaces A: Physicochemical and Engineering Aspects*, *597*, 124814. https://doi.org/10.1016/j.colsurfa.2020.124814

Hossain Bhuiyan, M. M., & Siddique, Z. (2025). Hydrogen as an alternative fuel: A comprehensive review of challenges and opportunities in production, storage, and transportation. *International Journal of Hydrogen Energy*, *102*, 1026–1044. https://doi.org/10.1016/j.ijhydene.2025.01.033

Hossain, N., Nizamuddin, S., Selvakannan, P., Griffin, G., Madapusi, S., & Shah, K. (2022). The effect of KOH activation and Ag nanoparticle incorporation on rice husk-based porous materials for wastewater treatment. *Chemosphere*, *291*, 132760. https://doi.org/10.1016/j.chemosphere.2021.132760

Houas, A., Lachheb, H., Ksibi, M., Elaloui, E., Guillard, C., & Herrmann, J.-M. (2001). Photocatalytic degradation pathway of methylene blue in water. *Applied Catalysis B: Environmental*, *31*(2), 145–157. https://doi.org/10.1016/S0926-3373(00)00276-9

Huang, X., Liu, Y., Liu, S., Li, Z., Tan, X., Ding, Y., Zeng, G., Xu, Y., Zeng, W., & Zheng, B. (2016). Removal of metformin hydrochloride by Alternanthera philoxeroides biomass derived porous carbon materials treated with hydrogen peroxide. *RSC Advances*, *6*(83), 79275–79284. https://doi.org/10.1039/C6RA08365J

Huo, Y., Xiu, S., Meng, L.-Y., & Quan, B. (2023). Solvothermal synthesis and applications of micro/nano carbons: A review. *Chemical Engineering Journal*, *451*, 138572. https://doi.org/10.1016/j.cej.2022.138572

Ibarra Torres, C. E., Serrano Quezada, T. E., Kharissova, O. V, Kharisov, B. I., & Gómez de la Fuente, Ma. I. (2021). Carbon-based aerogels and xerogels: Synthesis, properties, oil sorption capacities, and DFT simulations. *Journal of Environmental Chemical Engineering*, *9*(1), 104886. https://doi.org/10.1016/j.jece.2020.104886

Inozemtseva, A. I., Kataev, E. Yu., Frolov, A. S., Amati, M., Gregoratti, L., Beranová, K., Dieste, V. P., Escudero, C., Fedorov, A., Tarasov, A. V, Usachov, D. Yu., Vyalikh, D. V, Shao-Horn, Y., Itkis, D. M., & Yashina, L. V. (2021). On the catalytic and degradative role of oxygen-containing groups on carbon electrode in non-aqueous ORR. *Carbon*, *176*, 632–641. https://doi.org/10.1016/j.carbon.2020.12.008

Ismail, M., Wu, Z., Zhang, L., Ma, J., Jia, Y., Hu, Y., & Wang, Y. (2019). High-efficient synergy of piezocatalysis and photocatalysis in bismuth oxychloride nanomaterial for dye decomposition. *Chemosphere*, *228*, 212–218. https://doi.org/10.1016/j.chemosphere.2019.04.121

Jaihindh, D. P., Chen, C.-C., & Fu, Y.-P. (2018). Reduced graphene oxide-supported Ag-loaded Fe-doped TiO2 for the degradation mechanism of methylene blue and its electrochemical properties. *RSC Advances*, *8*(12), 6488–6501. https://doi.org/10.1039/C7RA13418E

Jayakumar, G., Irudayaraj, A. A., & Raj, A. D. (2019). Investigation on the synthesis and photocatalytic activity of activated carbon–cerium oxide (AC–CeO2) nanocomposite. *Applied Physics A*, *125*(11), 742. https://doi.org/10.1007/s00339-019-3044-4

Jumah, A. bin. (2024). A comprehensive review of production, applications, and the path to a sustainable energy future with hydrogen. *RSC Advances*, *14*(36), 26400–26423. https://doi.org/10.1039/D4RA04559A

Kalagatur, N. K., Karthick, K., Allen, J. A., Ghosh, O. S. N., Chandranayaka, S., Gupta, V. K., Krishna, K., & Mudili, V. (2017). Application of activated carbon derived from seed shells of Jatropha curcas for decontamination of zearalenone mycotoxin. *Frontiers in Pharmacology*, *8*(OCT). https://doi.org/10.3389/fphar.2017.00760

Kandy, M. M. (2020). Carbon-based photocatalysts for enhanced photocatalytic reduction of CO2 to solar fuels. *Sustainable Energy & Fuels*, *4*(2), 469–484. https://doi.org/10.1039/C9SE00827F

Kant, R. (2012). Textile dyeing industry an environmental hazard. *Natural Science*, *04*. https://doi.org/10.4236/ns.2012.41004

Karmaker, S. C., Chapman, A., Sen, K. K., Hosan, S., & Saha, B. B. (2023). Renewable Energy Pathways toward Accelerating Hydrogen Fuel Production: Evidence from Global Hydrogen Modeling. *Sustainability*, *15*(1). https://doi.org/10.3390/su15010588

Kasbaji, M., Ibrahim, I., Mennani, M., abdelatty abuelalla, O., fekry, S. S., Mohamed, M. M., Salama, T. M., Moneam, I. A., Mbarki, M., Moubarik, A., & Oubenali, M. (2023). Future trends in dye removal by metal oxides and their Nano/Composites: A comprehensive review. *Inorganic Chemistry Communications*, *158*, 111546. https://doi.org/10.1016/j.inoche.2023.111546

Katwal, R., Kothari, R., & Pathania, D. (2021). Chapter 10 - An overview on degradation kinetics of organic dyes by photocatalysis using nanostructured electrocatalyst. In L. Singh & D. M. Mahapatra (Eds.), *Delivering Low-Carbon Biofuels with Bioproduct Recovery* (pp. 195–213). Elsevier. https://doi.org/10.1016/B978-0-12-821841-9.00005-0

Kedara Shivasharma, T., Sahu, R., Rath, M. C., Keny, S. J., & Sankapal, B. R. (2023). “Exploring tin oxide based materials: A critical review on synthesis, characterizations and supercapacitive energy storage.” *Chemical Engineering Journal*, *477*, 147191. https://doi.org/10.1016/j.cej.2023.147191

Khamkure, S., Gamero-Melo, P., Garrido-Hoyos, S. E., Reyes-Rosas, A., Pacheco-Catalán, D.-E., & López-Martínez, A. M. (2023). The Development of Fe3O4-Monolithic Resorcinol-Formaldehyde Carbon Xerogels Using Ultrasonic-Assisted Synthesis for Arsenic Removal of Drinking Water. *Gels*, *9*(8). https://doi.org/10.3390/gels9080618

Kim, J., Oh, J., Baskaran, S., Kim, T. G., Kim, S., Yang, J., Jung, J., & Yoon, S. M. (2024). Rhenium redefined as electrocatalyst: Hydrogen evolution efficiency boost via Pt and Ni doping. *Applied Catalysis B: Environment and Energy*, *347*, 123791. https://doi.org/10.1016/j.apcatb.2024.123791

Kłonkowski, A. M., Grobelna, B., Widernik, T., Jankowska-Frydel, A., & Mozgawa, W. (1999). The Coordination State of Copper(II) Complexes Anchored and Grafted onto the Surface of Organically Modified Silicates. *Langmuir*, *15*(18), 5814–5819. https://doi.org/10.1021/la981256+

Kumari, P., & Kumar, A. (2023). ADVANCED OXIDATION PROCESS: A remediation technique for organic and non-biodegradable pollutant. *Results in Surfaces and Interfaces*, *11*, 100122. https://doi.org/10.1016/j.rsurfi.2023.100122

Kumari, T., Gopal, R., Goyal, A., & Joshi, J. (2019). Sol–Gel Synthesis of Pd@PdO Core–Shell Nanoparticles and Effect of Precursor Chemistry on Their Structural and Optical Properties. *Journal of Inorganic and Organometallic Polymers and Materials*, *29*(2), 316–325. https://doi.org/10.1007/s10904-018-1001-x

Kuspanov, Z., Bakbolat, B., Baimenov, A., Issadykov, A., Yeleuov, M., & Daulbayev, C. (2023). Photocatalysts for a sustainable future: Innovations in large-scale environmental and energy applications. *Science of The Total Environment*, *885*, 163914. https://doi.org/10.1016/j.scitotenv.2023.163914

Kusuma, K. B., Manju, M., Ravikumar, C. R., Raghavendra, N., Amulya, M. A. S., Nagaswarupa, H. P., Murthy, H. C. A., Kumar, M. R. A., & Shashi Shekhar, T. R. (2022). Photocatalytic degradation of Methylene Blue and electrochemical sensing of paracetamol using Cerium oxide nanoparticles synthesized via sonochemical route. *Applied Surface Science Advances*, *11*, 100304. https://doi.org/10.1016/j.apsadv.2022.100304

Kweon, D. H., Okyay, M. S., Kim, S.-J., Jeon, J.-P., Noh, H.-J., Park, N., Mahmood, J., & Baek, J.-B. (2020). Ruthenium anchored on carbon nanotube electrocatalyst for hydrogen production with enhanced Faradaic efficiency. *Nature Communications*, *11*(1), 1278. https://doi.org/10.1038/s41467-020-15069-3

Kyzas, G. Z., Nanaki, S. G., Koltsakidou, A., Papageorgiou, M., Kechagia, M., Bikiaris, D. N., & Lambropoulou, D. A. (2015). Effectively designed molecularly imprinted polymers for selective isolation of the antidiabetic drug metformin and its transformation product guanylurea from aqueous media. *Analytica Chimica Acta*, *866*, 27–40. https://doi.org/10.1016/j.aca.2015.01.045

Lama, G., Meijide, J., Sanromán, A., & Pazos, M. (2022). Heterogeneous Advanced Oxidation Processes: Current Approaches for Wastewater Treatment. *Catalysts*, *12*(3). https://doi.org/10.3390/catal12030344

Lekhak, U. M. (2023). 2 - Ecotoxicity of synthetic dyes. In S. P. Govindwar, M. B. Kurade, B.-H. Jeon, & A. Pandey (Eds.), *Current Developments in Bioengineering and Biotechnology* (pp. 45–67). Elsevier. https://doi.org/10.1016/B978-0-323-91235-8.00021-8

Li, C., & Baek, J.-B. (2020). Recent Advances in Noble Metal (Pt, Ru, and Ir)-Based Electrocatalysts for Efficient Hydrogen Evolution Reaction. *ACS Omega*, *5*(1), 31–40. https://doi.org/10.1021/acsomega.9b03550

Li, Q., Ni, Z., Gong, J., Zhu, D., & Zhu, Z. (2008). Carbon nanotubes coated by carbon nanoparticles of turbostratic stacked graphenes. *Carbon*, *46*(3), 434–439. https://doi.org/10.1016/j.carbon.2007.12.002

Li, S., Liu, J., Yin, Z., Ren, P., Lin, L., Gong, Y., Yang, C., Zheng, X., Cao, R., Yao, S., Deng, Y., Liu, X., Gu, L., Zhou, W., Zhu, J., Wen, X., Xu, B., & Ma, D. (2020). Impact of the Coordination Environment on Atomically Dispersed Pt Catalysts for Oxygen Reduction Reaction. *ACS Catalysis*, *10*(1), 907–913. https://doi.org/10.1021/acscatal.9b04558

Li, T., Cui, Z., Yuan, W., & Li, C. M. (2016). Ionic liquid functionalized carbon nanotubes: metal-free electrocatalyst for hydrogen evolution reaction. *RSC Advances*, *6*(16), 12792–12796. https://doi.org/10.1039/C5RA25460D

Li, X., Shen, X., Jiang, W., Xi, Y., & Li, S. (2024). Comprehensive review of emerging contaminants: Detection technologies, environmental impact, and management strategies. *Ecotoxicology and Environmental Safety*, *278*, 116420. https://doi.org/10.1016/j.ecoenv.2024.116420

Liquete, C., Maes, J., La Notte, A., & Bidoglio, G. (2011). Securing water as a resource for society: an ecosystem services perspective. *Ecohydrology & Hydrobiology*, *11*(3), 247–259. https://doi.org/10.2478/v10104-011-0044-1

Liu, B., Liu, B., Li, Q., Li, Z., Liu, R., Zou, X., Wu, W., Cui, W., Liu, Z., Li, D., Zou, B., Cui, T., & Zou, G. (2010). Solvothermal synthesis of monodisperse selfassembly CeO2 nanospheres and their enhanced blue-shifting in ultraviolet absorption. *Journal of Alloys and Compounds*, *503*(2), 519–524. https://doi.org/10.1016/j.jallcom.2010.05.047

Liu, W., Zuo, H., Wang, J., Xue, Q., Ren, B., & Yang, F. (2021). The production and application of hydrogen in steel industry. *International Journal of Hydrogen Energy*, *46*(17), 10548–10569. https://doi.org/10.1016/j.ijhydene.2020.12.123

Liu, X., Huang, C., Waqas, M., Wang, L., Huang, D., Huang, Q., Yang, Z., Fan, Y., Hou, C., & Chen, W. (2023). Controllable design of N-doped carbon nanotubes with assembled Pt nanoparticles for methanol oxidation reaction. *Molecular Catalysis*, *551*, 113612. https://doi.org/10.1016/j.mcat.2023.113612

Long, D. A. (2004). Infrared and Raman characteristic group frequencies. Tables and charts George Socrates John Wiley and Sons, Ltd, Chichester, Third Edition, 2001. Price £135. *Journal of Raman Spectroscopy*, *35*(10), 905. https://doi.org/https://doi.org/10.1002/jrs.1238

Low, J., Yu, J., Jaroniec, M., Wageh, S., & Al-Ghamdi, A. A. (2017). Heterojunction Photocatalysts. *Advanced Materials*, *29*(20), 1601694. https://doi.org/10.1002/adma.201601694

Lu, J., Zhou, W., Zhang, X., & Xiang, G. (2020). Electronic Structures and Lattice Dynamics of Layered BiOCl Single Crystals. *The Journal of Physical Chemistry Letters*, *11*(3), 1038–1044. https://doi.org/10.1021/acs.jpclett.9b03575

Lu, Y., Liu, X., Wang, W., Cheng, J., Yan, H., Tang, C., Kim, J.-K., & Luo, Y. (2015). Hierarchical, porous CuS microspheres integrated with carbon nanotubes for high-performance supercapacitors. *Scientific Reports*, *5*(1), 16584. https://doi.org/10.1038/srep16584

Luo, N., Li, X., Wang, X., Yan, H., Zhang, C., & Wang, H. (2010). Synthesis and characterization of carbon-encapsulated iron/iron carbide nanoparticles by a detonation method. *Carbon*, *48*(13), 3858–3863. https://doi.org/10.1016/j.carbon.2010.06.051

Lyngsie, G., Krumina, L., Tunlid, A., & Persson, P. (2018). Generation of hydroxyl radicals from reactions between a dimethoxyhydroquinone and iron oxide nanoparticles. *Scientific Reports*, *8*(1), 10834. https://doi.org/10.1038/s41598-018-29075-5

Ma, R., Zhou, Y., Wang, F., Yan, K., Liu, Q., & Wang, J. (2017). Efficient electrocatalysis of hydrogen evolution by ultralow-Pt-loading bamboo-like nitrogen-doped carbon nanotubes. *Materials Today Energy*, *6*, 173–180. https://doi.org/10.1016/j.mtener.2017.10.003

Ma, T.-Y., Lin, C.-H., & Chen, J.-S. (2023). Surface bonding of MN4 macrocyclic metal complexes with pyridine-functionalized multi-walled carbon nanotubes for non-aqueous Li-O2 batteries. *Journal of Colloid and Interface Science*, *635*, 242–253. https://doi.org/10.1016/j.jcis.2022.12.148

Mahzoura, M., Tahri, N., Daramola, M. O., Duplay, J., Schäfer, G., & Amar, R. Ben. (2019). Comparative investigation of indigo blue dye removal efficiency of activated carbon and natural clay in adsorption/ultrafiltration system. *Desalination and Water Treatment*, *164*, 326–338. https://doi.org/10.5004/dwt.2019.24361

Majumdar, A., Tran, K. D., Malhotra, D., Tran, D. T., Kim, N. H., & Lee, J. H. (2024). Heteroatom-Doped Carbon Allotropes in Water-Splitting Application. In *Heteroatom-Doped Carbon Allotropes: Progress in Synthesis, Characterization, and Applications* (Vol. 1491, pp. 177–222). American Chemical Society. https://doi.org/10.1021/bk-2024-1491.ch007

Mao, C., Cheng, X., Xia, M., Tian, J., Zhang, Z., Zhao, Z., Huang, H., Wu, Q., Wang, X., Yang, L., & Hu, Z. (2025). Volmer/Heyrovsky-Dominated Hydrogen Evolution on Pt–N–C Single Sites Triggered by Negatively Charged Adsorbed Hydrogen: A Theoretical Insight. *ACS Catalysis*, *15*(13), 11113–11122. https://doi.org/10.1021/acscatal.5c02724

Martins, F. P., De-León Almaraz, S., Botelho Junior, A. B., Azzaro-Pantel, C., & Parikh, P. (2024). Hydrogen and the sustainable development goals: Synergies and trade-offs. *Renewable and Sustainable Energy Reviews*, *204*, 114796. https://doi.org/10.1016/j.rser.2024.114796

McMichael, S., Fernández-Ibáñez, P., & Byrne, J. A. (2021). A Review of Photoelectrocatalytic Reactors for Water and Wastewater Treatment. *Water*, *13*(9). https://doi.org/10.3390/w13091198

Medina, J. C., Portillo-Vélez, N. S., Bizarro, M., Hernández-Gordillo, A., & Rodil, S. E. (2018). Synergistic effect of supported ZnO/Bi2O3 heterojunctions for photocatalysis under visible light. *Dyes and Pigments*, *153*, 106–116. https://doi.org/https://doi.org/10.1016/j.dyepig.2018.02.006

Mian, M. M., & Liu, G. (2018). Recent progress in biochar-supported photocatalysts: synthesis, role of biochar, and applications. *RSC Advances*, *8*(26), 14237–14248. https://doi.org/10.1039/C8RA02258E

Mohammad, A. H., Radovic, I., Ivanović, M., & Kijevčanin, M. (2022). Adsorption of Metformin on Activated Carbon Produced from the Water Hyacinth Biowaste Using H3PO4 as a Chemical Activator. *Sustainability*, *14*(18). https://doi.org/10.3390/su141811144

Morsy, M., Abdel-Salam, A. I., Gomaa, I., Moustafa, H., Kalil, H., & Helal, A. (2023). Highly Efficient Photocatalysts for Methylene Blue Degradation Based on a Platform of Deposited GO-ZnO Nanoparticles on Polyurethane Foam. *Molecules*, *28*(1). https://doi.org/10.3390/molecules28010108

Mota-Resendiz, K., Sánchez-Silva, J. M., Forgionny, A., Medellín-Castillo, N. A., Labrada-Delgado, G. J., & Ocampo-Pérez, R. (2025). Valorization of waste cigarette butts into high-performance activated carbons for water remediation. *Journal of Water Process Engineering*, *75*, 107998. https://doi.org/10.1016/j.jwpe.2025.107998

Murcia Mesa, J. J., Guarín Romero, J. R., Cely Macías, Á. C., Rojas Sarmiento, H. A., Cubillos Lobo, J. A., Navío Santos, J. A., & Hidalgo López, M. del C. (2017). Methylene blue degradation over M-TiO2 photocatalysts (M= Au or Pt) / Degradación de azul de metileno sobre fotocatalizadores M-TiO2 (M = Au o Pt). *Ciencia En Desarrollo*, *8*(1), 109–117. https://doi.org/10.19053/01217488.v8.n1.2017.5352

Nasiri, S., Rabiei, M., Palevicius, A., Janusas, G., Vilkauskas, A., Nutalapati, V., & Monshi, A. (2023). Modified Scherrer equation to calculate crystal size by XRD with high accuracy, examples Fe2O3, TiO2 and V2O5. *Nano Trends*, *3*, 100015. https://doi.org/10.1016/j.nwnano.2023.100015

Nasrollahpour, A., & Moradi, S. E. (2016). Photochemical degradation of methylene blue by metal oxide-supported activated carbon photocatalyst. *Desalination and Water Treatment*, *57*(19), 8854–8862. https://doi.org/10.1080/19443994.2015.1035675

Němec, T., Šonský, J., Gruber, J., de Prado, E., Kupčík, J., & Klementová, M. (2020). Platinum and platinum oxide nanoparticles generated by unipolar spark discharge. *Journal of Aerosol Science*, *141*, 105502. https://doi.org/10.1016/j.jaerosci.2019.105502

Nichols, F., Lu, J. E., Mercado, R., Dudschus, R., Bridges, F., & Chen, S. (2020). Platinum Oxide Nanoparticles for Electrochemical Hydrogen Evolution: Influence of Platinum Valence State. *Chemistry – A European Journal*, *26*(18), 4136–4142. https://doi.org/10.1002/chem.201904559

Nikolopoulos, I., Kordouli, E., Mourgkogiannis, N., Karapanagioti, H. K., Lycourghiotis, A., & Kordulis, C. (2023). Valorization of Pyrolyzed Biomass Residues for the Transformation of Waste Cooking Oil into Green Diesel. *Catalysts*, *13*(6). https://doi.org/10.3390/catal13061004

Nishmitha, P. S., Akhilghosh, K. A., Aiswriya, V. P., Ramesh, A., Muthuchamy, M., & Muthukumar, A. (2025). Understanding emerging contaminants in water and wastewater: A comprehensive review on detection, impacts, and solutions. *Journal of Hazardous Materials Advances*, *18*, 100755. https://doi.org/10.1016/j.hazadv.2025.100755

Niu, H., Wang, Q., Huang, C., Zhang, M., Yan, Y., Liu, T., & Zhou, W. (2023). Noble Metal-Based Heterogeneous Catalysts for Electrochemical Hydrogen Evolution Reaction. *Applied Sciences*, *13*(4). https://doi.org/10.3390/app13042177

Ocampo-Pérez, R., Leyva-Ramos, R., Sanchez-Polo, M., & Rivera-Utrilla, J. (2013). Role of pore volume and surface diffusion in the adsorption of aromatic compounds on activated carbon. *Adsorption*, *19*(5), 945–957. https://doi.org/10.1007/s10450-013-9502-y

Okab, A. A., Jabbar, Z. H., Graimed, B. H., Alwared, A. I., Ammar, S. H., & Hussein, M. A. (2023). A comprehensive review highlights the photocatalytic heterojunctions and their superiority in the photo-destruction of organic pollutants in industrial wastewater. *Inorganic Chemistry Communications*, *158*, 111503. https://doi.org/10.1016/j.inoche.2023.111503

Oladoye, P. O., Ajiboye, T. O., Omotola, E. O., & Oyewola, O. J. (2022). Methylene blue dye: Toxicity and potential elimination technology from wastewater. *Results in Engineering*, *16*, 100678. https://doi.org/10.1016/j.rineng.2022.100678

Ologunagba, D., & Kattel, S. (2022). Pt- and Pd-modified transition metal nitride catalysts for the hydrogen evolution reaction. *Physical Chemistry Chemical Physics*, *24*(20), 12149–12157. https://doi.org/10.1039/D2CP00792D

Olvera Vargas, H., Roa-Morales, G., Marín, R., Ramírez, M. T., Balderas, P., & Barrera-Díaz, C. E. (2010). Evaluation of a Blue Indigo Dye Degradation with Electrochemical Peroxidation by UV-Vis Spectrophotometry. *ECS Transactions*, *29*(1), 251. https://doi.org/10.1149/1.3532322

Orea-Calderón, B. I., Gracia-Espino, E., Kuzhikandathil, A., Chacón-Torres, J. C., Castillo, C. G., Lopéz-Urías, F., & Muñoz-Sandoval, E. (2025). Electrochemical Properties for Hydrogen Production of Nitrogen-Doped Sponge-Like Carbon Nanotubes as High-Surface Area Catalyst. *Energy Technology*, *n/a*(n/a), e202500964. https://doi.org/10.1002/ente.202500964

Papaderakis, A. A., Ejigu, A., Yang, J., Elgendy, A., Radha, B., Keerthi, A., Juel, A., & Dryfe, R. A. W. (2023a). Anion Intercalation into Graphite Drives Surface Wetting. *Journal of the American Chemical Society*, *145*(14), 8007–8020. https://doi.org/10.1021/jacs.2c13630

Parkash, S., Kotanigawa, T., & Chakrabartty, S. K. (1982). Changes in pore structure of precipitated iron oxide catalysts during pretreatment and hydrocarbon synthesis reaction. *Fuel Processing Technology*, *5*(3), 203–212. https://doi.org/10.1016/0378-3820(82)90015-7

Patel, K., Parangi, T., Solanki, G. K., Mishra, M. K., Patel, K. D., & Pathak, V. M. (2021). Photocatalytic degradation of methylene blue and crystal violet dyes under UV light irradiation by sonochemically synthesized CuSnSe nanocrystals. *The European Physical Journal Plus*, *136*(7), 743. https://doi.org/10.1140/epjp/s13360-021-01725-0

Pekala, R. W. (1989). Organic aerogels from the polycondensation of resorcinol with formaldehyde. *Journal of Materials Science*, *24*(9), 3221–3227. https://doi.org/10.1007/BF01139044

Phuruangrat, A., Wannapop, S., Sakhon, T., Kuntalue, B., Thongtem, T., & Thongtem, S. (2023). Characterization and photocatalytic properties of BiVO4 synthesized by combustion method. *Journal of Molecular Structure*, *1274*, 134420. https://doi.org/10.1016/j.molstruc.2022.134420

Pinedo-Escobar, J. A., Fan, J., Moctezuma, E., Gomez-Solís, C., Carrillo Martinez, C. J., & Gracia-Espino, E. (2021). Nanoparticulate Double-

Heterojunction Photocatalysts Comprising TiO2(Anatase)/WO3/TiO2(Rutile) with Enhanced Photocatalytic Activity toward the Degradation of Methyl Orange under Near-Ultraviolet and Visible Light. *ACS Omega*, *6*(18), 11840–11848. https://doi.org/10.1021/acsomega.0c06054

Puga, F., Navío, J. A., & Hidalgo, M. C. (2024). A critical view about use of scavengers for reactive species in heterogeneous photocatalysis. *Applied Catalysis A: General*, *685*, 119879. https://doi.org/10.1016/j.apcata.2024.119879

Puttaraju, T. D., Shashank, M., Raja Naika, H., Nagaraju, G., & Manjunatha, M. (2022). Synthesis of bismuth oxychloride nanoparticles via co-precipitation method: Evaluation of photocatalytic activity. *Materials Today: Proceedings*, *62*, 5533–5539. https://doi.org/10.1016/j.matpr.2022.04.333

Qadeer, M. A., Zhang, X., Farid, M. A., Tanveer, M., Yan, Y., Du, S., Huang, Z.-F., Tahir, M., & Zou, J.-J. (2024). A review on fundamentals for designing hydrogen evolution electrocatalyst. *Journal of Power Sources*, *613*, 234856. https://doi.org/10.1016/j.jpowsour.2024.234856

Qiu, C., Jiang, L., Gao, Y., & Sheng, L. (2023). Effects of oxygen-containing functional groups on carbon materials in supercapacitors: A review. *Materials & Design*, *230*, 111952. https://doi.org/10.1016/j.matdes.2023.111952

Quinson, J., Inaba, M., Neumann, S., Swane, A. A., Bucher, J., Simonsen, S. B., Theil Kuhn, L., Kirkensgaard, J. J. K., Jensen, K. M. Ø., Oezaslan, M., Kunz, S., & Arenz, M. (2018). Investigating Particle Size Effects in Catalysis by Applying a Size-Controlled and Surfactant-Free Synthesis of Colloidal Nanoparticles in Alkaline Ethylene Glycol: Case Study of the Oxygen Reduction Reaction on Pt. *ACS Catalysis*, *8*(7), 6627–6635. https://doi.org/10.1021/acscatal.8b00694

Qureshi, A. A., Javed, S., Javed, H. M. A., Jamshaid, M., Ali, U., & Akram, M. A. (2022). Systematic Investigation of Structural, Morphological, Thermal, Optoelectronic, and Magnetic Properties of High-Purity Hematite/Magnetite Nanoparticles for Optoelectronics. *Nanomaterials*, *12*(10). https://doi.org/10.3390/nano12101635

Ramírez-Muñiz, K., Song, S., Berber-Mendoza, S., & Tong, S. (2010). Adsorption of the complex ion Au(CN)2- onto sulfur-impregnated activated carbon in aqueous solutions. *Journal of Colloid and Interface Science*, *349*(2), 602–606. https://doi.org/10.1016/j.jcis.2010.05.056

Rawool, S. A., Kar, Y., & Polshettiwar, V. (2022). g-C3N4/dendritic fibrous nanosilica doped with potassium for photocatalytic CO2 reduction. *Materials Advances*, *3*(23), 8449–8459. https://doi.org/10.1039/D2MA00809B

Reichenbächer, M., & Popp, J. (2012). Electronic Absorption Spectroscopy. In M. Reichenbächer & J. Popp (Eds.), *Challenges in Molecular Structure Determination* (pp. 145–214). Springer Berlin Heidelberg. https://doi.org/10.1007/978-3-642-24390-5_3

Reza, K. M., Kurny, A. S. W., & Gulshan, F. (2017). Parameters affecting the photocatalytic degradation of dyes using TiO2: a review. *Applied Water Science*, *7*(4), 1569–1578. https://doi.org/10.1007/s13201-015-0367-y

Robertson, J., & O'Reilly, E. P. (1987). Electronic and atomic structure of amorphous carbon. *Physical Review B*, *35*(6), 2946–2957. https://doi.org/10.1103/PhysRevB.35.2946

Rodriguez-Miguel, S., Ma, Y., Farid, G., Amade, R., Ospina, R., Andujar, J. L., Bertran-Serra, E., & Chaitoglou, S. (2024). Vertical graphene nanowalls supported hybrid W2C/WOx composite material as an efficient non-noble metal electrocatalyst for hydrogen evolution. *Heliyon*, *10*(10). https://doi.org/10.1016/j.heliyon.2024.e31230

Romdhani, M., Aloulou, W., Aloulou, H., Charcosset, C., Mahouche-Chergui, S., Carbonnier, B., & Amar, R. Ben. (2021). Performance studies of indigo dye removal using TiO2 modified clay and zeolite ultrafiltration membrane hybrid system. *Desalination and Water Treatment*, *243*, 262–274. https://doi.org/10.5004/dwt.2021.27887

Rosen, M. A., & Koohi-Fayegh, S. (2016). The prospects for hydrogen as an energy carrier: an overview of hydrogen energy and hydrogen energy systems. *Energy, Ecology and Environment*, *1*(1), 10–29. https://doi.org/10.1007/s40974-016-0005-z

Roy, M., & Saha, R. (2021). 6 - Dyes and their removal technologies from wastewater: A critical review. In S. Bhattacharyya, N. K. Mondal, J. Platos, V. Snášel, & P. Krömer (Eds.), *Intelligent Environmental Data Monitoring for Pollution Management* (pp. 127–160). Academic Press. https://doi.org/10.1016/B978-0-12-819671-7.00006-3

Rubtsov, I. V, Kumar, K., & Hochstrasser, R. M. (2005). Dual-frequency 2D IR photon echo of a hydrogen bond. *Chemical Physics Letters*, *402*(4), 439–443. https://doi.org/10.1016/j.cplett.2004.12.083

Ryabicheva, M., Zhigalenok, Y., Abdimomyn, S., Skakov, M., Miniyazov, A., Zhanbolatova, G., Mukhamedova, N., Ospanova, Z., Djenizian, T., & Malchik, F. (2025). From lab to market: Economic viability of modern hydrogen evolution reaction catalysts. *Fuel*, *395*, 135227. https://doi.org/10.1016/j.fuel.2025.135227

Sahoo, S., Bhuyan, M., Sahu, A. kumar, Alagarsamy, P., & Sahoo, D. (2023). Photodegradation of methylene blue by metal-nanoparticles-modulated-graphene-based composites: An efficient way of sewage water management. *Solid State Sciences*, *142*, 107255. https://doi.org/10.1016/j.solidstatesciences.2023.107255

Salazar-Rabago, J. J., Leyva-Ramos, R., Rivera-Utrilla, J., Ocampo-Perez, R., & Cerino-Cordova, F. J. (2017). Biosorption mechanism of Methylene Blue from aqueous solution onto White Pine (Pinus durangensis) sawdust: Effect of operating conditions. *Sustainable Environment Research*, *27*(1), 32–40. https://doi.org/10.1016/j.serj.2016.11.009

Samuvel Raj, R., Prince Arulraj, G., Anand, N., Kanagaraj, B., Lubloy, E., & Naser, M. Z. (2023). Nanomaterials in geopolymer composites: A review. *Developments in the Built Environment*, *13*, 100114. https://doi.org/10.1016/j.dibe.2022.100114

Sanchez-Silva, J. M., Collins-Martínez, V. H., Padilla-Ortega, E., Aguilar-Aguilar, A., Labrada-Delgado, G. J., Gonzalez-Ortega, O., Palestino-Escobedo, G., & Ocampo-Pérez, R. (2022a). Characterization and transformation of nanche stone (Byrsonima crassifolia) in an activated hydrochar with high adsorption capacity towards metformin in aqueous solution. *Chemical Engineering Research and Design*, *183*, 580–594. https://doi.org/10.1016/j.cherd.2022.05.054

Sánchez-Silva, J. M., Ojeda-Galván, H. J., Villabona-Leal, E. G., Labrada-Delgado, G. J., Aguilar-Maruri, S. A., Fuentes-Ramírez, R., González-Ortega, O., López-Ramón, M. V., & Ocampo-Pérez, R. (2024). Synergistic photocatalysis of a hydrochar/CeO2 composite for dye degradation under visible light. *Environmental Science and Pollution Research*, *31*(11), 16453–16472. https://doi.org/10.1007/s11356-024-32281-6

Sandhu, I. S., Chitkara, M., Dhillon, G., Rana, S., & Kumar, A. (2021). Ecofriendly and enhanced photocatalytic degradation of Indigo dye by graphene oxide nanoparticles. *Optical and Quantum Electronics*, *53*(4), 200. https://doi.org/10.1007/s11082-021-02835-w

Sarigul, N., Korkmaz, F., & Kurultak, İ. (2019). A New Artificial Urine Protocol to Better Imitate Human Urine. *Scientific Reports*, *9*(1), 20159. https://doi.org/10.1038/s41598-019-56693-4

Sarkar, S., & Peter, S. C. (2018). An overview on Pd-based electrocatalysts for the hydrogen evolution reaction. *Inorganic Chemistry Frontiers*, *5*(9), 2060–2080. https://doi.org/10.1039/C8QI00042E

Scholz, M. (2006). Chapter 1 - Water quality standards. In M. Scholz (Ed.), *Wetland Systems to Control Urban Runoff* (pp. 1–5). Elsevier. https://doi.org/10.1016/B978-044452734-9/50004-9

Seddigi, Z. S., Gondal, M. A., Baig, U., Ahmed, S. A., Abdulaziz, M. A., Danish, E. Y., Khaled, M. M., & Lais, A. (2017). Facile synthesis of light harvesting semiconductor bismuth oxychloride nano photo-catalysts for efficient removal of hazardous organic pollutants. *PLOS ONE*, *12*(2), e0172218-. https://doi.org/10.1371/journal.pone.0172218

Seemen, H., Kukli, K., Jõgiaas, T., Ritslaid, P., Link, J., Stern, R., Dueñas, S., Castán, H., & Tamm, A. (2020). Properties of atomic layer deposited iron oxide and bismuth oxide chloride structures. *Journal of Alloys and Compounds*, *846*, 156099. https://doi.org/10.1016/j.jallcom.2020.156099

Sekar, S., Bathula, C., Rabani, I., Lee, J. W., Lee, S. H., Seo, Y.-S., & Lee, S. (2022). Enhanced photocatalytic crystal-violet degradation performances of sonochemically-synthesized AC-CeO2 nanocomposites. *Ultrasonics Sonochemistry*, *90*, 106177. https://doi.org/10.1016/j.ultsonch.2022.106177

Serna-Carrizales, J. C., Zárate Guzmán, A. I., Forgionny, A., Acelas, N., Pérez, S., Muñoz-Saldaña, J., & Ocampo-Perez, R. (2024). Production of activated carbon from agave residues and its synergistic application in a hybrid adsorption-AOPs system for effective removal of sulfamethazine from aqueous solutions. *Environmental Research*, *250*, 118559. https://doi.org/10.1016/j.envres.2024.118559

Serna-Carrizales, J. C., Zárate-Guzmán, A. I., Aguilar-Aguilar, A., Forgionny, A., Bailón-García, E., Flórez, E., Gómez-Durán, C. F. A., & Ocampo-Pérez, R. (2023). Optimization of Binary Adsorption of Metronidazole and Sulfamethoxazole in Aqueous Solution Supported with DFT Calculations. *Processes*, *11*(4). https://doi.org/10.3390/pr11041009

Shinde, S. S., Sami, A., & Lee, J.-H. (2015). Electrocatalytic hydrogen evolution using graphitic carbon nitride coupled with nanoporous graphene co-doped by S and Se. *Journal of Materials Chemistry A*, *3*(24), 12810–12819. https://doi.org/10.1039/C5TA02656C

Shiraishi, S. (2003). Chapter 27 - Electric Double Layer Capacitors. In E. YASUDA, M. INAGAKI, K. KANEKO, M. ENDO, A. OYA, & Y. TANABE (Eds.), *Carbon Alloys* (pp. 447–457). Elsevier Science. https://doi.org/10.1016/B978-008044163-4/50027-9

Singh, Y. P., Pandey, A., Vishwakarma, S., & Modi, G. (2019). A review on iron chelators as potential therapeutic agents for the treatment of Alzheimer's and Parkinson's diseases. *Molecular Diversity*, *23*(2), 509–526. https://doi.org/10.1007/s11030-018-9878-4

Sood, S., Kumar, S., Umar, A., Kaur, A., Mehta, S. K., & Kansal, S. K. (2015). TiO2 quantum dots for the photocatalytic degradation of indigo carmine dye. *Journal of Alloys and Compounds*, *650*, 193–198. https://doi.org/10.1016/j.jallcom.2015.07.164

Spessato, L., Duarte, V. A., Viero, P., Zanella, H., Fonseca, J. M., Arroyo, P. A., & Almeida, V. C. (2021). Optimization of Sibipiruna activated carbon preparation by simplex-centroid mixture design for simultaneous adsorption of rhodamine B and metformin. *Journal of Hazardous Materials*, *411*, 125166. https://doi.org/10.1016/j.jhazmat.2021.125166

Staaf, L. G. H., Lundgren, P., & Enoksson, P. (2014). Present and future supercapacitor carbon electrode materials for improved energy storage used in intelligent wireless sensor systems. *Nano Energy*, *9*, 128–141. https://doi.org/10.1016/j.nanoen.2014.06.028

Stamatin, S. N., Borghei, M., Dhiman, R., Andersen, S. M., Ruiz, V., Kauppinen, E., & Skou, E. M. (2015). Activity and stability studies of platinized multi-walled carbon nanotubes as fuel cell electrocatalysts. *Applied Catalysis B: Environmental*, *162*, 289–299. https://doi.org/10.1016/j.apcatb.2014.07.005

Sudolská, M., Dubecký, M., Sarkar, S., Reckmeier, C. J., Zbořil, R., Rogach, A. L., & Otyepka, M. (2015). Nature of Absorption Bands in Oxygen-Functionalized Graphitic Carbon Dots. *The Journal of Physical Chemistry C*, *119*(23), 13369–13373. https://doi.org/10.1021/acs.jpcc.5b04080

Sun, A., Hou, X., & Hu, X. (2020). Super-performance photothermal conversion of 3D macrostructure graphene-CuFeSe2 aerogel contributes to durable and fast clean-up of highly viscous crude oil in seawater. *Nano Energy*, *70*, 104511. https://doi.org/10.1016/j.nanoen.2020.104511

Sundqvist, B. (2021). Carbon under pressure. *Physics Reports*, *909*, 1–73. https://doi.org/10.1016/j.physrep.2020.12.007

Suresh, R., Ponnuswamy, V., & Mariappan, R. (2013). Effect of annealing temperature on the microstructural, optical and electrical properties of CeO2 nanoparticles by chemical precipitation method. *Applied Surface Science*, *273*, 457–464. https://doi.org/10.1016/j.apsusc.2013.02.062

Szalewicz, K. (2003). Hydrogen Bond. In R. A. Meyers (Ed.), *Encyclopedia of Physical Science and Technology (Third Edition)* (pp. 505–538). Academic Press. https://doi.org/10.1016/B0-12-227410-5/00322-7

Thommes, M., Kaneko, K., Neimark, A. V, Olivier, J. P., Rodriguez-Reinoso, F., Rouquerol, J., & Sing, K. S. W. (2015). *Physisorption of gases, with special reference to the evaluation of surface area and pore size distribution (IUPAC Technical Report)*. *87*(9–10), 1051–1069. https://doi.org/10.1515/pac-2014-1117

Tkaczyk, A., Mitrowska, K., & Posyniak, A. (2020). Synthetic organic dyes as contaminants of the aquatic environment and their implications for ecosystems: A review. *Science of The Total Environment*, *717*, 137222. https://doi.org/10.1016/j.scitotenv.2020.137222

Toghan, A., Abd El-Lateef, H. M., Taha, K. K., & Modwi, A. (2021). Mesoporous TiO2@g-C3N4 composite: construction, characterization, and boosting indigo carmine dye destruction. *Diamond and Related Materials*, *118*, 108491. https://doi.org/10.1016/j.diamond.2021.108491

Tomaz, A. T., Costa, C. R., de Lourdes S. Vasconcellos, M., Pedicini, R., & Ribeiro, J. (2022). Evaluation of Photoelectrocatalysis with Electrode Based on Ti/RuO2-TiO2 Modified with Tin and Tantalum Oxides for the Degradation of Indigo Blue Dye. *Nanomaterials*, *12*(23). https://doi.org/10.3390/nano12234301

Tran, D. P. H., Pham, M.-T., Bui, X.-T., Wang, Y.-F., & You, S.-J. (2022). CeO2 as a photocatalytic material for CO2 conversion: A review. *Solar Energy*, *240*, 443–466. https://doi.org/10.1016/j.solener.2022.04.051

Trivedi, R., & Chakraborty, B. (2025). Heyrovsky-Driven Hydrogen Evolution on Pt-Rh/FePS3: A Theoretical Approach. *ChemistrySelect*, *10*(17), e202500018. https://doi.org/10.1002/slct.202500018

Tsaviv, J. N., Eneji, I. S., Sha'Ato, R., Ahemen, I., Jubu, P. R., & Yusof, Y. (2024). Photodegradation, kinetics and non-linear error functions of methylene blue dye using SrZrO3 perovskite photocatalyst. *Heliyon*, *10*(14), e34517. https://doi.org/10.1016/j.heliyon.2024.e34517

Tsukahara, Y., Yamauchi, T., Kawamoto, T., & Wada, Y. (2008). Functionalization of Multi-Walled Carbon Nanotubes Realized by Microwave-Driven Chemistry Inducing Dispersibility in Liquid Media. *Bulletin of the Chemical Society of Japan*, *81*(3), 387–392. https://doi.org/10.1246/bcsj.81.387

Tuyen, L. T. T., Quang, D. A., Tam Toan, T. T., Tung, T. Q., Hoa, T. T., Mau, T. X., & Khieu, D. Q. (2018). Synthesis of CeO2/TiO2 nanotubes and heterogeneous photocatalytic degradation of methylene blue. *Journal of Environmental Chemical Engineering*, *6*(5), 5999–6011. https://doi.org/10.1016/j.jece.2018.09.022

Ulya, L. H., Fatimah, H., & Alif, N. (2022). Photodegradation of Indigosol Blue Dye Using TiO2/Natural Zeolite Photocatalyst. *Jurnal Kimia Valensi*, *8*(1), 54–59. https://doi.org/10.15408/jkv.v8i1.24558

Valli Nachiyar, C., Rakshi, A. D., Sandhya, S., Britlin Deva Jebasta, N., & Nellore, J. (2023). Developments in treatment technologies of dye-containing effluent: A review. *Case Studies in Chemical and Environmental Engineering*, *7*, 100339. https://doi.org/10.1016/j.cscee.2023.100339

Villabona-Leal, E. G., Escobar-Villanueva, A. G., Pérez-Pérez, E. B., Martínez-Gutiérrez, H., & Ovando-Medina, V. M. (2021). Efficient photothermal supports from carbonized agave flower stalk for solar water evaporation. *International Journal of Energy Research*, *45*(13), 19521–19534. https://doi.org/10.1002/er.7051

Villabona-Leal, E. G., López-Neira, J. P., Pedraza-Avella, J. A., Pérez, E., & Meza, O. (2015). Screening of factors influencing the photocatalytic activity of TiO2:Ln (Ln=La, Ce, Pr, Nd, Sm, Eu and Gd) in the degradation of dyes. *Computational Materials Science*, *107*, 48–53. https://doi.org/10.1016/j.commatsci.2015.05.014

Vinoth, S., Ong, W.-J., & Pandikumar, A. (2021). Sulfur-doped graphitic carbon nitride incorporated bismuth oxychloride/Cobalt based type-II heterojunction as a highly stable material for photoelectrochemical water splitting. *Journal of Colloid and Interface Science*, *591*, 85–95. https://doi.org/10.1016/j.jcis.2021.01.104

Wang, H., & Pilon, L. (2012). Physical interpretation of cyclic voltammetry for measuring electric double layer capacitances. *Electrochimica Acta*, *64*, 130–139. https://doi.org/10.1016/j.electacta.2011.12.118

Wang, H., Shang, J., Xiao, Z., Aprea, P., & Hao, S. (2020). Novel construction of carbon bonds in CeO2@C with efficiently photocatalytic activity. *Dyes and Pigments*, *182*, 108669. https://doi.org/10.1016/j.dyepig.2020.108669

Wang, R., Zhang, L., Wang, N., Zhang, X., Huang, L., Zhang, Q., Lin, H., Chen, J., Jiao, Y., & Xu, Y. (2024). Transforming electrochemical hydrogen Production: Tannic Acid-Boosted CoNi alloy integration with Multi-Walled carbon nanotubes for advanced bifunctional catalysis. *Journal of Colloid and Interface Science*, *661*, 113–122. https://doi.org/10.1016/j.jcis.2024.01.109

Wang, S., Lu, A., & Zhong, C.-J. (2021). Hydrogen production from water electrolysis: role of catalysts. *Nano Convergence*, *8*(1), 4. https://doi.org/10.1186/s40580-021-00254-x

Wang, S., Ning, X., Liu, X., Shakouri, M., Hu, Y., Yuan, H., Liu, P., Lu, X., Guo, Y., & Wang, Y. (2024). Ruthenium co-anchored by nitrogen and oxygen on lignin derived carbon for high-efficient hydrogen evolution. *Carbon*, *217*, 118611. https://doi.org/10.1016/j.carbon.2023.118611

Wang, Y., Du, K., Xu, R., Cui, D., Shi, Y., Hao, W., & Du, Y. (2023). Bismuth-based semiconductor heterostructures for photocatalytic pollution gases removal. *Current Opinion in Green and Sustainable Chemistry*, *41*, 100824. https://doi.org/10.1016/j.cogsc.2023.100824

Weldekirstos, H. D., Habtewold, B., & Kabtamu, D. M. (2022). Surfactant-Assisted Synthesis of NiO-ZnO and NiO-CuO Nanocomposites for

Enhanced Photocatalytic Degradation of Methylene Blue Under UV Light Irradiation. *Frontiers in Materials*, *Volume 9-2022*. https://doi.org/10.3389/fmats.2022.832439

Wu, K.-R., Hung, C.-H., Yeh, C.-W., Wang, C.-C., & Wu, J.-K. (2012). Effect of N,C-ITO on Composite N,C-TiO2/N,C-ITO/ITO Electrode Used for Photoelectrochemical Degradation of Aqueous Pollutant with Simultaneous Hydrogen Production. *International Journal of Photoenergy*, *2012*(1), 829327. https://doi.org/10.1155/2012/829327

Wu, T.-S., Syu, L.-Y., Lin, C.-N., Lin, B.-H., Liao, Y.-H., Weng, S.-C., Huang, Y.-J., Jeng, H.-T., Lu, S.-Y., Chang, S.-L., & Soo, Y.-L. (2019). Enhancement of catalytic activity by UV-light irradiation in CeO2 nanocrystals. *Scientific Reports*, *9*(1), 8018. https://doi.org/10.1038/s41598-019-44543-2

Xu, L., Zhang, J., Ding, J., Liu, T., Shi, G., Li, X., Dang, W., Cheng, Y., & Guo, R. (2020). Pore Structure and Fractal Characteristics of Different Shale Lithofacies in the Dalong Formation in the Western Area of the Lower Yangtze Platform. *Minerals*, *10*(1). https://doi.org/10.3390/min10010072

Xu, X., Shao, Z., & Jiang, S. P. (2022). High-Entropy Materials for Water Electrolysis. *Energy Technology*, *10*(11), 2200573. https://doi.org/10.1002/ente.202200573

Yadav, N., & Nagarajan, R. (2023). Optical bandgap variation and photo-Fenton property evolution in Fe-doped Bi2YO4Cl. *Solid State Sciences*, *139*, 107154. https://doi.org/10.1016/j.solidstatesciences.2023.107154

Yaman, E., Gökmen, F., Temel, S., Özbay, N., & Özsin, G. (2021). Değerli Metal Katalizörlerde Katalizör Destek Malzemesi Olarak Biyotabanlı Malzemelerin Üretilmesi ve Karakterizasyonu. *Avrupa Bilim ve Teknoloji Dergisi*, *23*, 181–188. https://doi.org/10.31590/ejosat.858676

Yang, X., Sun, S., Cui, J., Yang, M., Luo, Y., & Liang, S. (2021). Synthesis, Functional Modifications, and Diversified Applications of Hybrid BiOCl-Based Heterogeneous Photocatalysts: A Review. *Crystal Growth & Design*, *21*(11), 6576–6618. https://doi.org/10.1021/acs.cgd.1c00866

Yayapao, O., Thongtem, T., Phuruangrat, A., & Thongtem, S. (2015). Synthesis and characterization of highly efficient Gd doped ZnO photocatalyst irradiated with ultraviolet and visible radiations. *Materials Science in*

Semiconductor Processing, *39*, 786–792. https://doi.org/10.1016/j.mssp.2015.06.039

Yu, M., Budiyanto, E., & Tüysüz, H. (2022). Principles of Water Electrolysis and Recent Progress in Cobalt-, Nickel-, and Iron-Based Oxides for the Oxygen Evolution Reaction. *Angewandte Chemie International Edition*, *61*(1), e202103824. https://doi.org/10.1002/anie.202103824

Zahra, R., Pervaiz, E., Yang, M., Rabi, O., Saleem, Z., Ali, M., & Farrukh, S. (2020). A review on nickel cobalt sulphide and their hybrids: Earth abundant, pH stable electro-catalyst for hydrogen evolution reaction. *International Journal of Hydrogen Energy*, *45*(46), 24518–24543. https://doi.org/10.1016/j.ijhydene.2020.06.236

Zamiri, R., Abbastabar Ahangar, H., Kaushal, A., Zakaria, A., Zamiri, G., Tobaldi, D., & Ferreira, J. M. F. (2015). Dielectrical Properties of CeO2 Nanoparticles at Different Temperatures. *PLOS ONE*, *10*(4), e0122989-. https://doi.org/10.1371/journal.pone.0122989

Zhan, D., Velmurugan, J., & Mirkin, M. V. (2009). Adsorption/Desorption of Hydrogen on Pt Nanoelectrodes: Evidence of Surface Diffusion and Spillover. *Journal of the American Chemical Society*, *131*(41), 14756–14760. https://doi.org/10.1021/ja902876v

Zhang, J., Abudoureheman, M., Ma, X., Kong, W., Xuan, X., & Pan, S. (2020). Controllable synthesis and spontaneous phase transition of photonic coordination polymer to produce a strong second-harmonic generation response. *Science China Materials*, *63*(7), 1272–1278. https://doi.org/10.1007/s40843-020-1281-y

Zhang, J., Wang, T., Liu, P., Liao, Z., Liu, S., Zhuang, X., Chen, M., Zschech, E., & Feng, X. (2017). Efficient hydrogen production on MoNi4 electrocatalysts with fast water dissociation kinetics. *Nature Communications*, *8*(1), 15437. https://doi.org/10.1038/ncomms15437

Zhang, P., Qiao, Z.-A., & Dai, S. (2015). Recent advances in carbon nanospheres: synthetic routes and applications. *Chemical Communications*, *51*(45), 9246–9256. https://doi.org/10.1039/C5CC01759A

Zhang, S., & Wang, D. (2015). Preparation of novel BiOBr/CeO2 heterostructured photocatalysts and their enhanced photocatalytic activity. *RSC Advances*, *5*(113), 93032–93040. https://doi.org/10.1039/C5RA13581H

Zhang, Y., Shao, Q., Jiang, H., Liu, L., Wu, M., Lin, J., Zhang, J., Wu, S., Dong, M., & Guo, Z. (2020). One-step co-precipitation synthesis of novel BiOCl/CeO2 composites with enhanced photodegradation of rhodamine B. *Inorganic Chemistry Frontiers*, *7*(6), 1345–1361. https://doi.org/10.1039/C9QI01524H

Zhao, K., Zhang, J., Li, H., Zhang, X., Hua, Y., & Di, L. (2024). Boosting HER performance by using plasma prepared N-doped CNTs to support Pt nanoparticles. *International Journal of Hydrogen Energy*, *90*, 1271–1278. https://doi.org/10.1016/j.ijhydene.2024.10.103

Zhao, M., Cao, Y., Liu, X., Deng, J., Li, D., & Gu, H. (2014). Effect of nitrogen atomic percentage on N+-bombarded MWCNTs in cytocompatibility and hemocompatibility. *Nanoscale Research Letters*, *9*(1), 142. https://doi.org/10.1186/1556-276X-9-142

Zhao, Q., Liu, X., Sun, M., Du, C., & Liu, Z. (2015). Natural kaolin derived stable SBA-15 as a support for Fe/BiOCl: a novel and efficient Fenton-like catalyst for the degradation of 2-nitrophenol. *RSC Advances*, *5*(46), 36948–36956. https://doi.org/10.1039/C5RA01804H

Zhong, W., Tu, W., Wang, Z., Lin, Z., Xu, A., Ye, X., Chen, D., & Xiao, B. (2020). Ultralow-temperature assisted synthesis of single platinum atoms anchored on carbon nanotubes for efficiently electrocatalytic acidic hydrogen evolution. *Journal of Energy Chemistry*, *51*, 280–284. https://doi.org/10.1016/j.jechem.2020.04.035

Zhou, J., Liu, Y., Li, B., Li, H., Chen, G., & Qiu, R. (2023). Coagulation of trace arsenic and cadmium from drinking water using titanium potassium oxalate. *Npj Clean Water*, *6*(1), 9. https://doi.org/10.1038/s41545-023-00227-z

Zhu, S., Liu, Y., Liu, S., Zeng, G., Jiang, L., Tan, X., Zhou, L., Zeng, W., Li, T., & Yang, C. (2017). Adsorption of emerging contaminant metformin using graphene oxide. *Chemosphere*, *179*, 20–28. https://doi.org/10.1016/j.chemosphere.2017.03.071

Zou, C., Ji, W., Shen, Z., Tang, Q., & Fan, M. (2018). NH3 molecule adsorption on spinel-type ZnFe2O4 surface: A DFT and experimental comparison study. *Applied Surface Science*, *442*, 778–786. https://doi.org/10.1016/j.apsusc.2018.02.037

Zulkiflee, A., Khan, M. M., Khan, A., Khan, M. Y., Dafalla, H. D. M., & Harunsani, M. H. (2023). Sn-doped BiOCl for photoelectrochemical activities and photocatalytic dye degradation under visible light. *Heliyon*, *9*(11), e21270. https://doi.org/10.1016/j.heliyon.2023.e21270

8. Appendix

8.1 Published articles

Article 1

DOI: 10.3390/pr12071431

processes

MDPI

Article

Highly Adsorptive Organic Xerogels for Efficient Removal of Metformin from Aqueous Solutions: Experimental and Theoretical Approach

S. A. Aguilar-Maruri [1,*], D. Perera-Triana [1], Elizabeth Flórez [2], Angélica Forgionny [2], Gabriela Palestino [1], C. F. A. Gómez-Durán [1] and Raúl Ocampo-Pérez [1]

[1] Centro de Investigación y Estudios de Posgrado, Facultad de Ciencias Químicas, Universidad Autónoma de San Luis Potosí, San Luis Potosí 78260, Mexico; a324928@alumnos.uaslp.mx (D.P.-T.); palestinogabriela@uaslp.mx (G.P.); azael.gomez@uaslp.mx (C.F.A.G.-D.); raul.ocampo@uaslp.mx (R.O.-P.)

[2] Grupo de Investigación de Materiales con Impacto (MAT&MPAC), Facultad de Ciencias Básicas, Universidad de Medellín, Medellín 050026, Colombia; mforgionny@udemedellin.edu.co (A.F.)

* Correspondence: a348454@alumnos.uaslp.mx

Abstract: Metformin, widely prescribed to treat type 2 diabetes for its effectiveness and low cost, has raised concerns about its presence in aqueous effluents and its potential environmental and public health impacts. To address this issue, xerogels were synthesized from resorcinol and formaldehyde, with molar ratios ranging from 0.05 to 0.40. These xerogels were thoroughly characterized using FT-IR, SEM, TGA, and TEM analyses. Batch adsorption experiments were performed with standard metformin solutions at concentrations of 50 and 500 mg/L, varying pH, and temperature to determine the adsorption isotherms of the synthesized xerogels. The adsorption data revealed a maximum adsorption capacity of 325 mg/g at pH 11 and 25 °C. Quantum chemical calculations revealed that electrostatic interactions govern metformin adsorption onto xerogels. The xerogels' adsorption capacity was evaluated in competitive systems with $CaCl_2$, NaCl, $MgCl_2$, and synthetic urines. Reuse cycles demonstrated that xerogels could be reused for up to three cycles without any loss in adsorptive efficiency. The adsorption mechanisms of metformin in the adsorption process highlight the strong electrostatic interactions and hydrogen bonds between the adsorbate and the adsorbent material. Xerogels synthesized show promise as efficient adsorbents to remove metformin from aqueous solutions, helping to mitigate its environmental impact.

Keywords: metformin; xerogels; adsorption

Citation: Aguilar-Maruri, S.A.; Perera-Triana, D.; Flórez, E.; Forgionny, A.; Palestino, G.; Gómez-Durán, C.F.A.; Ocampo-Pérez, R. Highly Adsorptive Organic Xerogels for Efficient Removal of Metformin from Aqueous Solutions: Experimental and Theoretical Approach. *Processes* **2024**, *12*, 1431. https://doi.org/10.3390/pr12071431

Academic Editors: Jan Derco, Andreja Žgajnar Gotvajn and Angelika Kassai

Received: 5 June 2024
Revised: 29 June 2024
Accepted: 4 July 2024
Published: 9 July 2024

1. Introduction

The regulation of discharge concentrations of emerging contaminants in water effluents is currently a global concern. Even at concentrations as low as ppb (µg/L) to ppm (mg/L), these pollutants can degrade environment quality and have a direct impact on human health, leading to deficiencies in ensuring the availability of safe drinking water [1,2]. Furthermore, emerging contaminants like pharmaceuticals, personal care products, pesticides, herbicides, dyes, and industrial chemicals such as hydrocarbons are increasingly being recognized as significant contributors to water pollution [3].

For these reasons, emerging pollutants have received significant attention in recent years due to their anthropogenic origins and the absence of well-established regulations governing their disposal [1,4]. It is estimated that globally, there are approximately 350,000 synthetic compounds for which the disposal and control processes remain uncertain [3]. Among these emerging pollutants, pharmaceutical compounds pose a particularly challenging removal process from water due to their complex nature. These compounds exhibit high solubility in water because of their polar properties, and their ionization degree varies depending on pH levels. In addition, pharmaceutical compounds have a slow

Article 2
DOI: 10.1016/j.envres.2025.122977

Environmental Research 286 (2025) 122977

Contents lists available at ScienceDirect

Environmental Research

journal homepage: www.elsevier.com/locate/envres

Photodegradation of methylene blue using carbonized bagasse doped with cerium oxide nanoparticles

Saul A. Aguilar-Maruri[a,*], Raúl Ocampo-Pérez[a,**], Lourdes Ramos-Galicia[b], Virginia Collins-Martínez[c], Gabriela Palestino[a], Noriaki Sano[d]

[a] Centro de Investigación y Estudios de Posgrado, Facultad de Ciencias Químicas, Universidad Autónoma de San Luis Potosí, San Luis Potosí 78260, Mexico
[b] Centro de Investigación en Materiales Avanzados S.C., Unidad Monterrey, Alianza Norte 202, Parque PIIT, 66628, Apodaca, Mexico
[c] Centro de Investigación en Materiales Avanzados, Departamento de Ingeniería y Química de Materiales, S.C., Miguel de Cervantes 120, Chihuahua 31136, Mexico
[d] Department of Chemical Engineering, Graduate School of Engineering, Kyoto University, Nishikyo-ku, Kyoto, 615-8510, Japan

ARTICLE INFO

Keywords:
Agave bagasse
Cerium oxide nanoparticles
Photocatalytic degradation
Methylene blue

ABSTRACT

The increasing need for sustainable and effective materials for environmental remediation drives the development of new catalytic supports for photocatalytic processes. Despite numerous advances, a gap remains in utilizing biomass-based materials for efficient photocatalysis, particularly in degrading organic pollutants. This research explored the potential of agave bagasse, a waste product from tequila production in Mexico, as a sustainable catalytic support doped with cerium oxide nanoparticles (CeONP) to degrade methylene blue (MB). The hybrid structures were synthesized through ultrasonic coupling and pyrolysis, where agave bagasse was doped with 0.5 wt% CeONPs. The resulting materials were characterized using Raman spectroscopy, XRD, XPS, SEM, and nitrogen physisorption. The degradation of MB was evaluated under both LED and UV light using a heterogeneous photocatalysis process. Under UV light, the photocatalytic performance remained high, achieving over 99.5 % degradation across multiple reuse cycles. In contrast, the efficiency under LED light was lower due to the reduced photon energy. Post-cycle analysis reveals structural fragmentation and changes in the distribution of cerium nanoparticles, impacting material effectiveness. Scavenger experiments revealed that by $\bullet O_2^-$, h^+, and $\bullet OH$ radicals, the degradation of MB by our composite is primarily driven. This study highlights the revalorization of agave bagasse as an effective and durable photocatalyst, providing a solution for waste management and the demand for efficient photocatalytic materials in environmental applications.

1. Introduction

The contamination of water bodies by synthetic dyes is an escalating environmental issue due to their profound impact on aquatic ecosystems and human health (Tkaczyk et al., 2020). Among the wide range of dyes utilized in various industries, methylene blue (MB) is of particular concern. Its extensive use in both industrial and medical contexts, combined with its chemical stability and resistance to degradation, contributes to its persistence in aquatic environments and poses significant ecological risks (Al-Tohamy et al., 2022). MB is recognized for its toxicity, as well as its carcinogenic and mutagenic potential. When released into wastewater, it can lead to eutrophication, aesthetic degradation, and serious harm to aquatic organisms (Fito et al., 2023).

Water remediation is essential for environmental protection, as it directly impacts ecosystems, public health, and overall well-being (Liquete et al., 2011). It addresses a broad range of pollutants, from conventional to emerging contaminants, while promoting sustainable water use and conservation (Kumari and Kumar, 2023). The choice of remediation method depends on the type of pollutant, the extent of contamination, and the target water quality standards (Scholz, 2006). Available techniques include physical processes like filtration, chemical methods such as coagulation and precipitation, and biological treatments like microbial degradation (El-taweel et al., 2023). Advanced technologies, including membrane filtration, electrochemical treatment, and photocatalysis, are increasingly favored for their efficiency and adaptability (Okab et al., 2023).

This article is part of a special issue entitled: WWEM-GEET-GC-2024 published in Environmental Research.
* Corresponding author.
** Corresponding author.
E-mail addresses: a348454@alumnos.uaslp.mx (S.A. Aguilar-Maruri), raul.ocampo@uaslp.mx (R. Ocampo-Pérez).

https://doi.org/10.1016/j.envres.2025.122977
Received 25 February 2025; Received in revised form 30 April 2025; Accepted 28 September 2025
Available online 2 October 2025
0013-9351/

Article 3
DOI: 10.1016/j.jece.2025.117799

Journal of Environmental Chemical Engineering 13 (2025) 117799

Contents lists available at ScienceDirect

Journal of Environmental Chemical Engineering

journal homepage: www.elsevier.com/locate/jece

Waste-derived catalytic hydrochars from coffee grounds doped with BiOCl, CeO_2, and α-Fe_2O_3: Structural insights and enhanced photocatalytic performance

Saul A. Aguilar-Maruri [a,b,*], Lourdes Ramos-Galicia [c], Raúl Ocampo-Pérez [a,**], Angélica Forgionny [d], Beatriz Ruíz-Camacho [e], Juan Carlos. Serna-Carrizales [a], Julián Cabrera-Ruiz [e], Alejandro López-Ortiz [f], Gabriela Palestino [a], Noriaki Sano [b]

[a] Center for Research and Graduate Studies, Faculty of Chemical Sciences, Autonomous University of San Luis Potosí, San Luis Potosí 78260, Mexico
[b] Department of Chemical Engineering, Graduate School of Engineering, Kyoto University, Nishikyo-ku, Kyoto 615-8510, Japan
[c] Center for Research in Advanced Materials S.C., Monterrey Unit, Alianza Norte 202, Parque PIIT, Apodaca C.P 66628, Mexico
[d] Grupo de investigación Materiales con Impacto (Mat&mpac), Facultad de Ciencias Básicas, Universidad de Medellín, Carrera 87 No. 30-65, Medellín 050026, Colombia
[e] Department of Chemical Engineering, Division of Natural and Exact Sciences, University of Guanajuato, Noria Alta S/n, Guanajuato 36050, Mexico
[f] Centro de Investigación en Materiales Avanzados (CIMAV), S.C. Miguel de Cervantes 120, Complejo Industrial Chihuahua, Chihuahua, Chihuahua 31136, Mexico

ARTICLE INFO

Keywords:
Waste-derived
Hydrochar
Coffee grounds
BiOCl
Indigo blue
Photodegradation

ABSTRACT

In this study, hydrochars were synthesized from coffee grounds via a solvothermal process and doped with metallic oxides, resulting in hydrochars being denoted as H, H-Bi (BiOCl), H-Bi/Ce (BiOCl-CeO_2), and H-Bi/Fe (BiOCl-Fe_2O_3). The photocatalytic degradation of indigo blue dye was evaluated under UV light, with varying parameters such as pH (3, 7, and 11), initial hydrochar mass (0.1, 0.2, and 0.3 g/L), and dye concentration (25–75 mg/L). H is directly degraded by electron transfer and UV light, with limited reactive oxygen species (ROS) generation. H-Bi generates abundant •OH and $O_2•^-$, with h^+ predominating under alkaline conditions. H-Bi/Ce combines h^+ and •OH due to oxygen defects in CeO_2. H-Bi/Fe utilizes Fenton and photo-Fenton reactions at acidic pH, with •OH being the primary mechanism. The highest degradation efficiency (100 %) was achieved with H, H-Bi, and H-Bi/Fe, using 0.1 g/L of hydrochar at pH 3. Under the same conditions, the hydrochars maintained their carbon-oxygen spherical structure and uniform dopant dispersion after four use cycles. Meanwhile, DRS, XPS, and TEM confirmed the presence of heterojunctions, which supported their photocatalytic activity. XPS and energy-EDS indicated the presence of BiOCl, CeO_2, and Fe_2O_3 after four cycles. The higher photocurrent density at 1.23 V vs. RHE was obtained for H-Bi/Fe, demonstrating excellent electrochemical stability under light and a higher electron transfer resistance in basic electrolytes compared to an acid medium. These results demonstrate the effectiveness of these doped hydrochars, offering insights into the transformative potential of biomass-based composites for sustainable industrial applications.

1. Introduction

Synthetic dyes used in the textile industry pose a significant environmental hazard, mainly through water pollution [1,2]. The pollutants increase water turbidity, impede photosynthesis, and interfere with oxygen transfer mechanisms, disrupting marine ecosystems and water self-purification processes [2]. Moreover, these contaminants can render drinking water unsafe for human consumption and reduce soil productivity [2]. The toxicity of synthetic dyes is further complicated by their potential to undergo chemical transformations in the environment, resulting in more harmful byproducts [3]. Current techniques for treating water contaminated with dyes include physical, chemical, and biological methods. Adsorption is widely recognized as one of the most effective and reliable techniques due to its simplicity, accessibility, and

* Corresponding author at: Center for Research and Graduate Studies, Faculty of Chemical Sciences, Autonomous University of San Luis Potosí, San Luis Potosí 78260, Mexico.
** Corresponding author.
E-mail addresses: a348454@alumnos.uaslp.mx (S.A. Aguilar-Maruri), raul.ocampo@uaslp.mx (R. Ocampo-Pérez).

https://doi.org/10.1016/j.jece.2025.117799
Received 30 March 2025; Received in revised form 3 June 2025; Accepted 28 June 2025
Available online 29 June 2025

Article 4
DOI: 10.1016/j.ijhydene.2025.152166

International Journal of Hydrogen Energy 189 (2025) 152166

Contents lists available at ScienceDirect

International Journal of Hydrogen Energy

journal homepage: www.elsevier.com/locate/he

Solvothermal alkaline functionalization of carbon nanotubes for enhanced electrocatalysis in hydrogen production

Saul A. Aguilar-Maruri [a,b,*], Beatriz Ruiz-Camacho [c], Rosalba Fuentes-Ramirez [c], Julian Cabrera-Ruiz [c], Raúl Ocampo-Pérez [a,**], Noriaki Sano [b], Gabriela Palestino [a]

[a] *Centro de Investigación y Estudios de Posgrado, Facultad de Ciencias Químicas, Universidad Autónoma de San Luis Potosí, San Luis Potosí, 78260, Mexico*
[b] *Department of Chemical Engineering, Graduate School of Engineering, Kyoto University, Nishikyo-ku, Kyoto, 615-8510, Japan*
[c] *Department of Chemical Engineering, Division of Natural and Exact Sciences, University of Guanajuato, Noria Alta S/n, Guanajuato, 36050, Mexico*

ARTICLE INFO

Keywords:
HER
Solvothermal functionalization
Electrocatalysist
MWCNT-Funtionalized

ABSTRACT

Hydrogen is a clean, energy-dense fuel that requires efficient electrocatalysts to drive the hydrogen evolution reaction (HER). In this study, multi-walled carbon nanotubes (MWCNTs) were functionalized via an alkaline solvothermal process (KOH, 200 °C, 2 h) and subsequently doped with Pt–Pd nanoparticles. The solvothermal KOH treatment increased the MWCNT surface area from 109 to 189 $m^2\ g^{-1}$ and reduced the crystallite size from 2.9 to 3.1 nm, while Pt–Pd loading further expanded it to 11.4 nm, indicating strong structural modification. The I_D/I_G ratio decreased from 1.16 to 0.96, indicating improved graphitic order. TEM and XRD confirmed the doping of Pt and Pd nanoparticles. These changes translated into enhanced HER performance metrics, including a reduced overpotential of −0.20 V at 10 mA cm^{-2}, a lower Tafel slope of 84 mV dec^{-1}, and a high exchange current density of 1.09×10^{-3} A cm^{-2}, demonstrating improved electrochemical efficiency. The synergistic Pt/Pd sites, oxygenated defects, and Pt–O–C interfaces act as active centers for HER (accelerate Volmer–Heyrovsky HER steps). Both catalysts retained their stability after 1000 cycles, demonstrating that alkaline solvothermal functionalization is a scalable strategy for designing HER catalysts.

1. Introduction

Hydrogen plays a vital role as an energy carrier, addressing key energy challenges and contributing to a sustainable future [1]. With the depletion of fossil fuel resources and increasing environmental concerns, hydrogen emerges as a crucial chemical energy carrier that may complement electricity in a future "hydrogen economy" [2]. In this envisioned scenario, hydrogen produced from non-fossil sources has the potential to extend the lifespan of existing fossil fuel reserves while facilitating the development of infrastructure for hydrogen-based energy systems [3]. Hydrogen is versatile and sustainable, making it a critical element in the transition to a low-carbon economy [4,5]. Transitioning to green hydrogen (produced from renewable resources) requires overcoming challenges like high production costs and the lack of infrastructure, but advancing technologies such as electrolysis and fuel cells can help overcome these obstacles [6,7].

The Hydrogen Evolution Reaction (HER) plays a central role in the production of green hydrogen via water electrolysis [8]. This process involves splitting water molecules into hydrogen and oxygen gas, with the HER occurring as the cathode half-reaction, in which protons are reduced to form hydrogen gas [9]. Achieving this step efficiently is essential for enabling the sustainable and large-scale production of green hydrogen. In the HER process, catalysts provide active sites that lower the energy barrier for proton or water adsorption, accelerate intermediate formation (Volmer step), and facilitate hydrogen desorption (Heyrovsky/Tafel steps), thereby enabling the reaction to proceed at practical rates [10]. As the demand for clean energy alternatives grows, the efficient execution of the HER becomes increasingly critical in supporting the transition toward carbon-neutral energy systems [11,12]. Efficient, stable, and economically viable catalysts are essential for the HER due to the inherently sluggish kinetics of the reaction, particularly under alkaline conditions [13]. The HER requires catalysts that lower energy barriers and enhance reaction rates, but the high cost of noble metals like platinum has driven research toward developing efficient,

* Corresponding author. Centro de Investigación y Estudios de Posgrado, Facultad de Ciencias Químicas, Universidad Autónoma de San Luis Potosí, San Luis Potosí, 78260, Mexico.
** Corresponding author.
E-mail addresses: a348454@alumnos.uaslp.mx (S.A. Aguilar-Maruri), raul.ocampo@uaslp.mx (R. Ocampo-Pérez).

https://doi.org/10.1016/j.ijhydene.2025.152166
Received 25 July 2025; Received in revised form 15 October 2025; Accepted 21 October 2025
Available online 24 October 2025

8.2 Scientific Dissemination and Outreach Activities

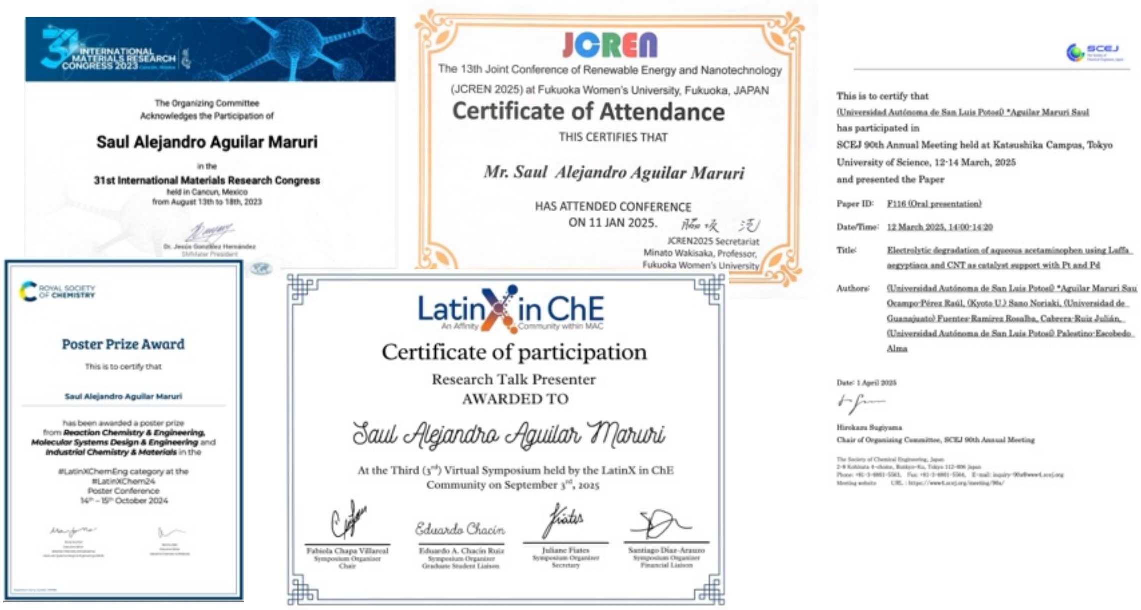

8.3 Appendix tables

Table A1. Cartesian coordinates of the different geometries for metformin-xerogel complex on gas phase.

Xer-Met^{2+}_m1 Center Number	Atomic Number	Atomic Type	Coordinates (Angstroms) X	Y	Z	Xer-Met^{2+}_m2 Center Number	Atomic Number	Atomic Type	Coordinates (Angstroms) X	Y	Z
1	6	0	7.439734	0.081368	-0.892415	1	6	0	-8.061647	-2.592002	-0.310050
2	6	0	6.433287	-0.194589	0.044858	2	6	0	-7.394840	-1.370171	-0.483454
3	6	0	5.437190	-1.156783	-0.187300	3	6	0	-6.185671	-1.270682	-1.190515
4	6	0	5.464960	-1.837265	-1.417914	4	6	0	-5.639935	-2.456146	-1.715000
5	6	0	6.444370	-1.569852	-2.369103	5	6	0	-6.275402	-3.681726	-1.542816
6	6	0	7.414773	-0.613193	-2.097911	6	6	0	-7.472982	-3.735851	-0.840466
7	1	0	6.426211	-2.115804	-3.303609	7	1	0	-5.818422	-4.569149	-1.961557
8	1	0	8.175576	-0.401819	-2.842052	8	1	0	-7.965680	-4.692656	-0.702556
9	6	0	4.368174	-1.447300	0.856011	9	6	0	-5.494095	0.071842	-1.377720
10	6	0	3.146309	-0.540113	0.796458	10	6	0	-4.567348	0.483252	-0.241336
11	6	0	2.996154	0.531637	1.679912	11	6	0	-4.974530	1.402464	0.728684
12	6	0	2.140253	-0.728371	-0.152632	12	6	0	-3.285857	-0.054382	-0.110595
13	6	0	1.881852	1.383613	1.641115	13	6	0	-4.140266	1.793084	1.787200
14	6	0	1.005896	0.073153	-0.231834	14	6	0	-2.408060	0.303680	0.907610
15	1	0	2.250348	-1.531123	-0.875120	15	1	0	-2.958243	-0.798827	-0.829616
16	6	0	0.883906	1.133898	0.678229	16	6	0	-2.847383	1.237364	1.858140
17	1	0	4.029634	-2.486157	0.770320	17	1	0	-4.916952	0.072400	-2.309429
18	1	0	4.810715	-1.399163	1.852815	18	1	0	-6.244896	0.848349	-1.536186
19	8	0	6.500744	0.520518	1.216166	19	8	0	-8.015522	-0.272542	0.062308
20	8	0	4.531023	-2.787201	-1.756039	20	8	0	-4.454655	-2.477226	-2.410425
21	8	0	4.025344	0.715537	2.588598	21	8	0	-6.262532	1.893986	0.593714
22	8	0	-0.205995	1.933769	0.575012	22	8	0	-2.001706	1.557177	2.868526
23	1	0	5.676133	0.475416	1.724455	23	1	0	-7.423427	0.492764	0.126371
24	1	0	3.868300	1.494768	3.130134	24	1	0	-6.480930	2.485085	1.320369
25	1	0	-0.318716	2.422753	1.408398	25	1	0	-2.292024	2.394314	3.270101
26	1	0	4.036090	-3.050888	-0.975067	26	1	0	-4.205057	-1.582149	-2.657296
27	6	0	-0.090880	-0.194615	-1.236774	27	6	0	-1.006626	-0.257016	0.985880
28	8	0	-1.241934	-0.824259	-0.669707	28	8	0	-0.001689	0.656734	0.540792
29	6	0	-1.046553	-2.198044	-0.338292	29	6	0	0.024635	0.845275	-0.873087
30	6	0	-2.332244	-2.774595	0.201437	30	6	0	1.149479	1.783173	-1.236122
31	6	0	-2.428712	-3.081920	1.558344	31	6	0	0.851376	3.073632	-1.672930
32	6	0	-3.448267	-3.001581	-0.626293	32	6	0	2.499419	1.396423	-1.134868

33	6	0	-3.597454	-3.608240	2.101346	33	6	0	1.856776	3.975068	-2.011174
34	1	0	-1.576504	-2.892807	2.203600	34	1	0	-0.187530	3.381883	-1.736432
35	6	0	-4.608174	-3.544173	-0.077041	35	6	0	3.498394	2.299954	-1.491448
36	6	0	-4.698105	-3.850437	1.282327	36	6	0	3.193251	3.590438	-1.928833
37	1	0	-3.650097	-3.823351	3.164254	37	1	0	1.596434	4.978775	-2.333060
38	1	0	-5.462481	-3.725146	-0.714821	38	1	0	4.534826	1.999740	-1.420474
39	1	0	-0.460617	0.742600	-1.651686	39	1	0	-0.745126	-0.478329	2.020225
40	1	0	0.308034	-0.807587	-2.057383	40	1	0	-0.953361	-1.188265	0.404328
41	1	0	-0.716187	-2.745740	-1.235828	41	1	0	0.151361	-0.131110	-1.368362
42	1	0	-0.256628	-2.301960	0.415474	42	1	0	-0.926477	1.265899	-1.221516
43	6	0	-3.395410	-2.677112	-2.111360	43	6	0	2.876549	0.002304	-0.657687
44	8	0	-4.658286	-2.722081	-2.762248	44	8	0	4.259105	-0.160309	-0.370239
45	1	0	-5.205785	-2.025824	-2.384185	45	1	0	4.471351	0.413194	0.373741
46	1	0	-2.913277	-1.703963	-2.249221	46	1	0	2.258715	-0.260486	0.207009
47	1	0	-2.780277	-3.421922	-2.627621	47	1	0	2.660271	-0.726123	-1.446530
48	6	0	-5.950533	-4.475734	1.849461	48	6	0	4.289719	4.540320	-2.349183
49	8	0	-7.083433	-4.065384	1.089855	49	8	0	5.485382	4.247298	-1.632676
50	1	0	-7.813788	-4.651903	1.304212	50	1	0	6.215062	4.684099	-2.080048
51	6	0	8.504255	1.108586	-0.574659	51	6	0	-9.377085	-2.633283	0.436455
52	8	0	7.986243	2.407956	-0.298921	52	8	0	-9.296171	-2.143036	1.772809
53	1	0	7.414550	2.296656	0.468873	53	1	0	-9.007138	-1.227325	1.691187
54	6	0	1.736460	2.598639	2.527494	54	6	0	-4.585770	2.718759	2.895238
55	8	0	0.422764	2.716496	3.102425	55	8	0	-3.607100	3.725723	3.209026
56	1	0	0.245801	1.918045	3.614415	56	1	0	-3.434102	4.236623	2.409009
57	1	0	2.481616	2.631807	3.333132	57	1	0	-5.545040	3.208892	2.683150
58	1	0	1.861276	3.517499	1.948422	58	1	0	-4.716292	2.168198	3.830681
59	1	0	9.115602	0.756672	0.269256	59	1	0	-10.138410	-2.074549	-0.127442
60	1	0	9.166299	1.220092	-1.435376	60	1	0	-9.717363	-3.667815	0.510776
61	1	0	-5.845850	-5.571001	1.821665	61	1	0	4.455689	4.435862	-3.432180
62	1	0	-6.054971	-4.183643	2.903794	62	1	0	3.962770	5.573534	-2.166387
63	1	0	-6.406230	5.737253	-1.802312	63	1	0	12.210704	-2.277484	1.190472
64	1	0	-4.978407	3.481392	-3.218512	64	1	0	10.240827	-4.096961	-0.203214
65	1	0	-6.660304	5.026816	0.649913	65	1	0	11.227107	0.090115	1.091946
66	7	0	-4.478907	2.924283	-2.530333	66	7	0	9.327658	-3.650264	-0.209897
67	6	0	-4.802812	3.092194	-1.330836	67	6	0	9.301451	-2.423664	0.048303
68	7	0	-4.225428	2.357179	-0.282664	68	7	0	8.114485	-1.673299	0.030244
69	6	0	-5.424344	6.135447	-1.537039	69	6	0	11.636233	-2.428092	2.107174
70	6	0	-5.680883	5.481408	0.814945	70	6	0	10.718686	-0.152749	2.027730
71	1	0	-4.547234	2.602778	0.642009	71	1	0	8.216970	-0.701615	0.283677
72	1	0	-3.240803	1.519491	-2.388162	72	1	0	7.528269	-3.979552	-0.634513
73	6	0	-3.365302	1.309332	-0.396231	73	6	0	6.886597	-2.095787	-0.375356
74	7	0	-2.896830	0.976698	-1.585757	74	7	0	6.704321	-3.366906	-0.685345
75	7	0	-4.882223	5.376066	-0.408084	75	7	0	10.436287	-1.589125	2.070563
76	7	0	-3.009700	0.642972	0.711340	76	7	0	5.887186	-1.204854	-0.443321
77	1	0	-4.761017	6.038412	-2.398003	77	1	0	11.348669	-3.478608	2.173587
78	1	0	-2.301860	0.172514	-1.714420	78	1	0	5.823098	-3.703648	-1.042157
79	1	0	-5.537589	7.202162	-1.305726	79	1	0	12.283982	-2.191834	2.960885
80	1	0	-5.836262	6.522055	1.128378	80	1	0	11.357136	0.176091	2.858140
81	1	0	-3.406717	0.860601	1.611590	81	1	0	6.036444	-0.225459	-0.259106
82	1	0	-5.183212	4.956981	1.634714	82	1	0	9.786062	0.414965	2.079055
83	1	0	-2.357857	-0.125506	0.672519	83	1	0	4.957425	-1.482112	-0.718356
84	1	0	-3.921045	5.653202	-0.231715	84	1	0	9.832443	-1.810910	2.856669

Xer-1Met+_m1						Xer-1Met+_m2					
Center	Atomic	Atomic	Coordinates (Angstroms)			Center	Atomic	Atomic	Coordinates (Angstroms)		
Number	Number	Type	X	Y	Z	Number	Number	Type	X	Y	Z
1	6	0	6.264453	-0.385530	0.154844	1	6	0	3.226105	3.986494	0.121743
2	6	0	5.185434	-0.931577	-0.555873	2	6	0	2.325405	3.240756	-0.652973
3	6	0	3.947002	-0.277278	-0.656383	3	6	0	0.935302	3.418473	-0.563795
4	6	0	3.808385	0.956846	0.003889	4	6	0	0.459365	4.370551	0.355591
5	6	0	4.859635	1.510952	0.727320	5	6	0	1.332791	5.111336	1.145450
6	6	0	6.070388	0.833078	0.797954	6	6	0	2.701756	4.907987	1.022946
7	1	0	4.707952	2.461884	1.221703	7	1	0	0.922567	5.831770	1.841429
8	1	0	6.888358	1.263546	1.366169	8	1	0	3.382178	5.482741	1.642567
9	6	0	2.799796	-0.886006	-1.449518	9	6	0	-0.016878	2.607079	-1.430217
10	6	0	1.929671	-1.866695	-0.674521	10	6	0	-0.411110	1.251404	-0.859065
11	6	0	2.089582	-3.247071	-0.818319	11	6	0	0.191304	0.073485	-1.307718
12	6	0	0.954661	-1.429022	0.223343	12	6	0	-1.371569	1.131983	0.146729
13	6	0	1.303202	-4.169663	-0.111589	13	6	0	-0.151962	-1.186123	-0.793333
14	6	0	0.134988	-2.293812	0.941503	14	6	0	-1.764308	-0.088796	0.686112
15	1	0	0.835085	-0.361744	0.381899	15	1	0	-1.828327	2.035029	0.539666
16	6	0	0.317063	-3.673539	0.764078	16	6	0	-1.145117	-1.251758	0.204032
17	1	0	2.154760	-0.094613	-1.848016	17	1	0	-0.932115	3.178548	-1.622415
18	1	0	3.194412	-1.374464	-2.342526	18	1	0	0.419242	2.472863	-2.421964

19	8	0	5.427646	-2.137200	-1.168816	19	8	0	2.893640	2.342429	-1.523610
20	8	0	2.637022	1.675516	-0.015373	20	8	0	-0.881004	4.615299	0.535743
21	8	0	3.086780	-3.653166	-1.689779	21	8	0	1.164670	0.224578	-2.281622
22	8	0	-0.460013	-4.512925	1.492032	22	8	0	-1.505617	-2.436054	0.757036
23	1	0	4.611094	-2.583337	-1.441908	23	1	0	2.252383	1.696908	-1.858972
24	1	0	3.161716	-4.612012	-1.700853	24	1	0	1.559150	-0.623614	-2.505404
25	1	0	-0.446309	-5.393610	1.079055	25	1	0	-1.239166	-3.156980	0.160702
26	1	0	2.053162	1.329907	-0.696600	26	1	0	-1.384030	4.223156	-0.183698
27	6	0	-0.948854	-1.783619	1.863191	27	6	0	-2.848431	-0.185162	1.734878
28	8	0	-2.261569	-1.876865	1.305495	28	8	0	-4.104366	-0.629339	1.216924
29	6	0	-2.522754	-0.924124	0.276240	29	6	0	-4.785371	0.347801	0.431605
30	6	0	-3.945287	-1.076616	-0.203204	30	6	0	-6.115135	-0.204684	-0.019179
31	6	0	-4.188300	-1.613405	-1.467227	31	6	0	-6.299064	-0.538113	-1.360801
32	6	0	-5.041661	-0.702376	0.596844	32	6	0	-7.178186	-0.406378	0.881603
33	6	0	-5.484244	-1.779508	-1.947604	33	6	0	-7.506066	-1.057882	-1.819942
34	1	0	-3.346652	-1.919078	-2.080881	34	1	0	-5.476697	-0.400191	-2.055831
35	6	0	-6.334609	-0.856925	0.100993	35	6	0	-8.388019	-0.911529	0.409805
36	6	0	-6.571188	-1.394361	-1.165877	36	6	0	-8.566032	-1.242714	-0.934961
37	1	0	-5.644789	-2.214833	-2.929202	37	1	0	-7.616311	-1.323695	-2.866845
38	1	0	-7.175982	-0.562395	0.713119	38	1	0	-9.206513	-1.059249	1.100892
39	1	0	-0.987249	-2.384979	2.771003	39	1	0	-2.579993	-0.923961	2.489430
40	1	0	-0.730804	-0.742848	2.141610	40	1	0	-2.967614	0.790495	2.226969
41	1	0	-2.346022	0.091296	0.666587	41	1	0	-4.922203	1.263995	1.028721
42	1	0	-1.836909	-1.072673	-0.566666	42	1	0	-4.187166	0.618292	-0.446989
43	6	0	-4.829431	-0.118120	1.985044	43	6	0	-7.025451	-0.064434	2.355796
44	8	0	-6.014785	-0.022437	2.763703	44	8	0	-8.079351	-0.548389	3.177753
45	1	0	-6.329634	-0.917944	2.926181	45	1	0	-8.051347	-1.510653	3.150815
46	1	0	-4.059956	-0.698013	2.504763	46	1	0	-6.052466	-0.421631	2.708197
47	1	0	-4.460194	0.909355	1.897777	47	1	0	-7.039194	1.023345	2.483098
48	6	0	-7.978653	-1.515455	-1.700285	48	6	0	-9.898445	-1.750523	-1.432978
49	8	0	-8.892853	-1.689378	-0.621933	49	8	0	-10.574466	-2.442523	-0.387519
50	1	0	-9.778877	-1.518841	-0.952464	50	1	0	-11.496416	-2.537641	-0.641154
51	6	0	7.584813	-1.122813	0.203987	51	6	0	4.715262	3.771904	-0.038609
52	8	0	7.492177	-2.432997	0.758575	52	8	0	5.134892	2.433692	0.217964
53	1	0	6.884106	-2.910694	0.183437	53	1	0	4.665809	1.891669	-0.426164
54	6	0	1.512678	-5.664295	-0.184336	54	6	0	0.543389	-2.464635	-1.199524
55	8	0	0.281087	-6.394559	-0.326222	55	8	0	-0.374569	-3.542824	-1.454663
56	1	0	-0.159038	-6.088951	-1.128636	56	1	0	-0.977899	-3.264905	-2.154469
57	1	0	2.197201	-5.961414	-0.989667	57	1	0	1.194967	-2.337745	-2.074027
58	1	0	1.944021	-6.040586	0.747090	58	1	0	1.176742	-2.835212	-0.389127
59	1	0	8.019525	-1.167687	-0.805365	59	1	0	5.025337	4.080086	-1.047895
60	1	0	8.282357	-0.571686	0.837438	60	1	0	5.249401	4.401632	0.675330
61	1	0	-8.223562	-0.605095	-2.268268	61	1	0	-10.499024	-0.895357	-1.778426
62	1	0	-8.028067	-2.361176	-2.400396	62	1	0	-9.734465	-2.406502	-2.299376
63	1	0	0.909316	6.341905	1.979088	63	1	0	9.151437	-0.920819	-0.959148
64	1	0	0.398205	9.164136	0.250830	64	1	0	10.597354	-3.600190	0.434906
65	7	0	0.968926	6.901122	1.132249	65	7	0	9.352053	-1.523500	-0.165454
66	6	0	0.055453	6.631095	0.279464	66	6	0	8.401380	-2.332151	0.111843
67	1	0	-1.765900	5.531093	0.288377	67	1	0	6.616315	-2.978428	-0.849027
68	6	0	0.315678	8.787884	-0.765951	68	6	0	9.919954	-3.812540	1.258454
69	7	0	-0.762315	5.422105	0.358151	69	7	0	7.049885	-2.170508	-0.420997
70	1	0	-0.327632	9.441994	-1.355181	70	1	0	9.932520	-4.878611	1.487025
71	7	0	-0.284733	7.447904	-0.746256	71	7	0	8.551717	-3.439663	0.877228
72	1	0	-2.110333	3.269570	0.551268	72	1	0	4.714643	-1.785889	-1.362588
73	6	0	-0.269026	4.182160	0.510503	73	6	0	6.348575	-1.025978	-0.373792
74	7	0	-1.110798	3.143655	0.587771	74	7	0	5.121670	-0.983143	-0.908500
75	1	0	1.315319	8.767810	-1.210993	75	1	0	10.253822	-3.250819	2.136386
76	7	0	1.046356	3.979668	0.565951	76	7	0	6.857082	0.055000	0.215460
77	1	0	-0.774817	2.206763	0.750112	77	1	0	4.589044	-0.127118	-0.931961
78	1	0	1.679082	4.770800	0.541346	78	1	0	7.798762	0.028946	0.588840
79	1	0	-1.614071	7.636197	-2.361204	79	1	0	7.512392	-5.099690	1.635332
80	6	0	-0.802155	6.983044	-2.036214	80	6	0	7.497453	-4.011516	1.719430
81	1	0	1.434188	3.050856	0.626146	81	1	0	6.323127	0.905459	0.306703
82	1	0	-1.177445	5.963948	-1.972473	82	1	0	6.513282	-3.651723	1.427184
83	1	0	-0.011918	7.009020	-2.793981	83	1	0	7.661601	-3.742609	2.768297

Xer-2Met+_m1						Xer-2Met+_m2					
Center	Atomic	Atomic	Coordinates (Angstroms)			Center	Atomic	Atomic	Coordinates (Angstroms)		
Number	Number	Type	X	Y	Z	Number	Number	Type	X	Y	Z
1	6	0	-6.055142	-1.232775	0.074545	1	6	0	-8.307217	-2.147460	-0.063668
2	6	0	-5.188638	-0.289711	-0.502377	2	6	0	-7.349479	-1.307514	-0.662449
3	6	0	-4.016271	-0.662379	-1.185152	3	6	0	-5.988324	-1.661818	-0.711712
4	6	0	-3.772143	-2.036387	-1.305553	4	6	0	-5.610100	-2.883150	-0.123343
5	6	0	-4.609515	-2.994955	-0.750314	5	6	0	-6.554210	-3.730207	0.471413

6	6	0	-5.744388	-2.580720	-0.057808	6	6	0	-7.888748	-3.353551	0.494973
7	1	0	-4.375278	-4.049162	-0.851393	7	1	0	-6.238340	-4.680427	0.916733
8	1	0	-6.400034	-3.322150	0.385094	8	1	0	-8.626798	-4.014137	0.965647
9	6	0	-3.088998	0.374164	-1.802133	9	6	0	-4.976727	-0.792648	-1.394759
10	6	0	-2.363839	1.279119	-0.811073	10	6	0	-4.363236	0.212530	-0.466547
11	6	0	-2.720350	2.622855	-0.648691	11	6	0	-4.862380	1.516755	-0.323395
12	6	0	-1.314123	0.806067	-0.024382	12	6	0	-3.245479	-0.157464	0.282880
13	6	0	-2.047725	3.481091	0.234184	13	6	0	-4.256446	2.441077	0.547219
14	6	0	-0.605652	1.606754	0.868125	14	6	0	-2.624582	0.718131	1.165423
15	1	0	-1.045299	-0.243474	-0.097910	15	1	0	-2.854326	-1.182972	0.172320
16	6	0	-0.977065	2.955651	0.984192	16	6	0	-3.140067	2.023719	1.298500
17	1	0	-2.346485	-0.153836	-2.400378	17	1	0	-4.168343	-1.432696	-1.815454
18	1	0	-3.649925	0.991895	-2.508031	18	1	0	-5.434121	-0.292284	-2.273725
19	8	0	-5.567108	1.014382	-0.356967	19	8	0	-7.829049	-0.150138	-1.216195
20	8	0	-2.624734	-2.455382	-2.009438	20	8	0	-4.320290	-3.337137	-0.100123
21	8	0	-3.820808	3.036288	-1.378472	21	8	0	-5.950301	1.846034	-1.093692
22	8	0	-0.296725	3.716424	1.875276	22	8	0	-2.512594	2.837192	2.188807
23	1	0	-5.019994	1.638219	-0.858948	23	1	0	-7.089332	0.446449	-1.356699
24	1	0	-4.026608	3.962739	-1.217237	24	1	0	-6.307642	2.665930	-0.760054
25	1	0	-0.455209	4.658701	1.688795	25	1	0	-2.976698	3.670097	2.214295
26	1	0	-2.885025	-3.186746	-2.581279	26	1	0	-3.760053	-2.640825	-0.442393
27	6	0	0.507263	1.047420	1.721381	27	6	0	-1.433568	0.247169	1.958087
28	8	0	1.836272	1.357605	1.275134	28	8	0	-0.194920	0.649351	1.414382
29	6	0	2.185009	0.770240	0.029511	29	6	0	0.172903	-0.040615	0.223933
30	6	0	3.655897	0.976729	-0.247021	30	6	0	1.456123	0.566077	-0.267462
31	6	0	4.043419	1.782170	-1.320256	31	6	0	1.404570	1.776387	-0.962866
32	6	0	4.660901	0.382392	0.539572	32	6	0	2.692498	-0.054904	-0.060407
33	6	0	5.385918	1.987481	-1.627821	33	6	0	2.562665	2.361793	-1.454706
34	1	0	3.280417	2.258858	-1.926771	34	1	0	0.438119	2.271274	-1.113254
35	6	0	6.005494	0.613914	0.235882	35	6	0	3.851799	0.530862	-0.573627
36	6	0	6.385806	1.406030	-0.847996	36	6	0	3.796269	1.734925	-1.268833
37	1	0	5.651774	2.613039	-2.474089	37	1	0	2.505783	3.317467	-1.988308
38	1	0	6.784226	0.176935	0.851456	38	1	0	4.818175	0.026538	-0.418327
39	1	0	0.458109	1.461247	2.727895	39	1	0	-1.392655	0.710679	2.959626
40	1	0	0.392458	-0.044561	1.785366	40	1	0	-1.470945	-0.853162	2.090684
41	1	0	1.944160	-0.304644	0.057561	41	1	0	0.299167	-1.125615	0.441263
42	1	0	1.594887	1.208850	-0.783766	42	1	0	-0.625868	0.055074	-0.538850
43	6	0	4.341972	-0.523626	1.701266	43	6	0	2.807590	-1.330987	0.730804
44	8	0	4.316300	-1.939236	1.313079	44	8	0	3.757531	-2.239784	0.243917
45	1	0	5.187772	-2.168933	0.967669	45	1	0	4.552502	-1.745361	0.062100
46	1	0	5.082817	-0.403603	2.495333	46	1	0	3.029732	-1.084031	1.788272
47	1	0	3.358480	-0.318403	2.115762	47	1	0	1.862524	-1.911831	0.709513
48	6	0	7.842539	1.668755	-1.148905	48	6	0	5.036513	2.355544	-1.845737
49	8	0	8.640747	0.656293	-0.543576	49	8	0	6.076933	2.270256	-0.897673
50	1	0	9.567272	0.906213	-0.609300	50	1	0	6.818623	2.720758	-1.277686
51	6	0	-7.294987	-0.766315	0.805188	51	6	0	-9.769470	-1.791844	-0.032543
52	8	0	-7.008740	0.037230	1.948048	52	8	0	-10.036951	-0.436509	0.202075
53	1	0	-6.622765	0.860410	1.628269	53	1	0	-9.464155	0.062102	-0.380241
54	6	0	-2.477463	4.910893	0.485647	54	6	0	-4.786677	3.842152	0.685623
55	8	0	-1.369432	5.824430	0.541145	55	8	0	-4.095359	4.781221	-0.095402
56	1	0	-0.963645	5.890529	-0.331407	56	1	0	-4.022439	4.433562	-0.975447
57	1	0	-3.204252	5.274681	-0.250418	57	1	0	-5.873693	3.884198	0.453430
58	1	0	-2.953550	5.001890	1.465719	58	1	0	-4.649633	4.231215	1.714885
59	1	0	-7.951771	-0.223558	0.113589	59	1	0	-10.240599	-2.109883	-0.984641
60	1	0	-7.845737	-1.631584	1.176388	60	1	0	-10.296896	-2.302489	0.793101
61	1	0	7.991625	1.688266	-2.235978	61	1	0	5.319440	1.816214	-2.772582
62	1	0	8.116920	2.658776	-0.758930	62	1	0	4.857102	3.414542	-2.120604
63	1	0	0.389676	-3.286434	-3.260572	63	1	0	9.832120	1.527995	-0.912248
64	7	0	0.101639	-3.711327	2.305113	64	6	0	9.679946	1.556528	0.165243
65	6	0	0.709398	-2.396414	-2.708513	65	1	0	10.503652	1.059708	0.672103
66	1	0	1.320084	-1.778385	-3.365886	66	1	0	9.592064	2.585097	0.512663
67	1	0	3.314338	-3.794418	-1.139289	67	7	0	9.020562	-3.182028	-1.188433
68	7	0	-0.380962	-3.031931	-0.187951	68	1	0	9.161034	-4.156128	-1.411181
69	1	0	-0.689417	-3.257210	0.773143	69	1	0	8.231120	-2.702125	-1.595368
70	6	0	0.931806	-2.985474	-0.345195	70	6	0	9.510818	-2.796915	0.016040
71	6	0	1.338879	-3.494182	2.056213	71	7	0	7.503163	-0.803584	-1.094173
72	7	0	1.746379	-3.149519	0.742819	72	6	0	8.312170	-0.564784	-0.161749
73	1	0	2.703387	-2.803482	0.668138	73	7	0	9.211984	-1.416752	0.385638
74	1	0	-0.079332	-3.970367	3.269544	74	7	0	10.235569	-3.537552	0.747272
75	7	0	1.511801	-2.758278	-1.536449	75	1	0	6.924322	-0.045454	-1.438298
76	1	0	-1.048998	-2.945825	-0.950877	76	7	0	8.390699	0.834789	0.488687
77	7	0	2.402687	-3.584170	2.907151	77	1	0	7.638354	1.348994	0.025768
78	1	0	2.208764	-3.677788	3.891198	78	1	0	9.678063	-1.144457	1.236754
79	6	0	2.944380	-2.987207	-1.770830	79	1	0	10.594204	-3.106369	1.593090
80	1	0	-0.166290	-1.817590	-2.422289	80	6	0	8.066994	0.845142	1.964629
81	1	0	3.286856	-3.158646	2.650654	81	1	0	8.894553	0.412276	2.522903

82	1	0	3.072379	-3.295724	-2.807847	82	1	0	7.927613	1.879985	2.274792
83	1	0	3.531937	-2.081918	-1.597692	83	1	0	7.155527	0.272503	2.127932
Xer⁻-1Met⁺						**Xer⁻-2Met⁺**					
Center	**Atomic**	**Atomic**	**Coordinates (Angstroms)**			**Center**	**Atomic**	**Atomic**	**Coordinates (Angstroms)**		
Number	**Number**	**Type**	**X**	**Y**	**Z**	**Number**	**Number**	**Type**	**X**	**Y**	**Z**
1	6	0	5.873175	-2.131530	-0.495424	1	6	0	6.181721	-0.560488	-0.164539
2	6	0	4.588370	-2.501831	-0.951268	2	6	0	4.985015	-1.014995	-0.762000
3	6	0	3.528490	-1.625002	-1.027907	3	6	0	3.792191	-0.329568	-0.688445
4	6	0	3.682720	-0.234667	-0.615187	4	6	0	3.701551	0.927962	0.044738
5	6	0	5.000840	0.120645	-0.142966	5	6	0	4.933423	1.369623	0.656381
6	6	0	6.031439	-0.793765	-0.088965	6	6	0	6.104105	0.648865	0.550521
7	1	0	5.142762	1.146486	0.182153	7	1	0	4.893986	2.297128	1.218851
8	1	0	7.010189	-0.478558	0.271692	8	1	0	7.009918	1.023605	1.026393
9	6	0	2.164209	-2.048270	-1.523443	9	6	0	2.526737	-0.838222	-1.341035
10	6	0	1.211766	-2.517288	-0.435645	10	6	0	1.654069	-1.701906	-0.444972
11	6	0	1.131401	-3.865820	-0.049230	11	6	0	1.799861	-3.098284	-0.388535
12	6	0	0.388459	-1.605085	0.224079	12	6	0	0.678627	-1.120037	0.364428
13	6	0	0.204599	-4.286084	0.923397	13	6	0	0.945650	-3.883616	0.408437
14	6	0	-0.547099	-1.979642	1.193032	14	6	0	-0.191960	-1.862156	1.168025
15	1	0	0.517428	-0.556604	-0.028677	15	1	0	0.630153	-0.034935	0.370390
16	6	0	-0.638927	-3.337495	1.523267	16	6	0	-0.055133	-3.255903	1.167128
17	1	0	1.721950	-1.165051	-1.990719	17	1	0	1.946466	0.047037	-1.612358
18	1	0	2.255536	-2.824283	-2.289955	18	1	0	2.759160	-1.383205	-2.261388
19	8	0	4.378865	-3.836182	-1.345087	19	8	0	5.011396	-2.232430	-1.466722
20	8	0	2.721136	0.579922	-0.662752	20	8	0	2.615809	1.562839	0.137248
21	8	0	1.930725	-4.826736	-0.592942	21	8	0	2.758460	-3.758398	-1.097930
22	8	0	-1.541269	-3.719203	2.481779	22	8	0	-0.891637	-3.996974	1.960691
23	1	0	5.078976	-4.365162	-0.921388	23	1	0	5.785860	-2.726229	-1.141355
24	1	0	2.752024	-4.431767	-0.959220	24	1	0	3.505079	-3.159265	-1.317680
25	1	0	-1.688203	-4.674830	2.377843	25	1	0	-0.872020	-4.910906	1.629088
26	6	0	-1.447578	-0.967505	1.849278	26	6	0	-1.260437	-1.196330	1.993237
27	8	0	-2.785374	-0.915664	1.308567	27	8	0	-2.580252	-1.235043	1.408992
28	6	0	-2.841687	-0.401110	-0.015079	28	6	0	-2.706136	-0.435432	0.240765
29	6	0	-4.278513	-0.379477	-0.483829	29	6	0	-4.119312	-0.536352	-0.285933
30	6	0	-4.684835	-1.254794	-1.489930	30	6	0	-4.357114	-1.200083	-1.488609
31	6	0	-5.231439	0.496447	0.073422	31	6	0	-5.214926	0.014189	0.408598
32	6	0	-5.998935	-1.271219	-1.952664	32	6	0	-5.642961	-1.318923	-2.011798
33	1	0	-3.959730	-1.945828	-1.907029	33	1	0	-3.519341	-1.644134	-2.016088
34	6	0	-6.539508	0.483922	-0.406056	34	6	0	-6.495276	-0.095937	-0.129619
35	6	0	-6.937909	-0.393110	-1.418011	35	6	0	-6.724904	-0.758625	-1.337956
36	1	0	-6.290082	-1.975257	-2.726625	36	1	0	-5.799552	-1.855403	-2.942991
37	1	0	-7.266045	1.159768	0.025759	37	1	0	-7.332061	0.329825	0.408531
38	1	0	-1.600109	-1.209685	2.900917	38	1	0	-1.383211	-1.704167	2.949737
39	1	0	-0.990562	0.028967	1.775569	39	1	0	-0.979180	-0.150453	2.178409
40	1	0	-2.410491	0.613617	-0.040069	40	1	0	-2.454072	0.612087	0.476122
41	1	0	-2.243191	-1.017184	-0.694975	41	1	0	-2.002443	-0.765533	-0.531150
42	6	0	-4.841871	1.465512	1.177919	42	6	0	-5.010915	0.741443	1.727781
43	8	0	-5.954851	2.033262	1.867403	43	8	0	-6.213388	0.939349	2.470308
44	1	0	-6.415560	1.308605	2.303314	44	1	0	-6.549407	0.066579	2.700012
45	1	0	-4.161838	0.962905	1.871143	45	1	0	-4.264269	0.205250	2.319926
46	1	0	-4.304847	2.318168	0.749611	46	1	0	-4.621642	1.747344	1.539377
47	6	0	-8.346832	-0.352533	-1.956087	47	6	0	-8.112911	-0.820313	-1.926063
48	8	0	-9.272711	-0.124327	-0.891181	48	8	0	-9.078047	-1.006724	-0.888220
49	1	0	-10.097296	0.177376	-1.281442	49	1	0	-9.936818	-0.758730	-1.240756
50	6	0	7.000365	-3.102911	-0.553312	50	6	0	7.458758	-1.293360	-0.387174
51	8	0	6.691300	-4.364438	0.134283	51	8	0	7.360427	-2.715563	-0.030206
52	1	0	6.308094	-4.097165	0.979874	52	1	0	6.926177	-2.723961	0.832732
53	6	0	0.155136	-5.718861	1.380583	53	6	0	1.135332	-5.372526	0.515592
54	8	0	-1.204837	-6.238068	1.434960	54	8	0	-0.116730	-6.103675	0.374807
55	1	0	-1.579439	-6.107978	0.555909	55	1	0	-0.496460	-5.830070	-0.468358
56	1	0	0.774852	-6.345080	0.739269	56	1	0	1.861156	-5.718104	-0.220095
57	1	0	0.511693	-5.821287	2.410245	57	1	0	1.490587	-5.658554	1.510483
58	1	0	7.236448	-3.440476	-1.570262	58	1	0	7.762295	-1.335242	-1.440732
59	1	0	7.909965	-2.662190	-0.128433	59	1	0	8.274185	-0.825040	0.176638
60	1	0	-8.425505	0.453200	-2.701996	60	1	0	-8.318082	0.116428	-2.466614
61	1	0	-8.566939	-1.298394	-2.470514	61	1	0	-8.161664	-1.638744	-2.657862
62	1	0	-0.014454	6.551752	-1.269003	62	1	0	-0.817545	6.432577	1.263332
63	7	0	0.322482	7.181319	-0.545445	63	1	0	-2.439193	3.348816	-0.034099
64	1	0	1.189067	9.499723	-0.232613	64	1	0	-2.450703	6.218287	0.656250
65	6	0	1.537847	6.967440	-0.211162	65	1	0	2.925733	6.794806	1.224996
66	6	0	1.754351	9.209023	0.649512	66	6	0	-1.404096	6.250185	0.361730
67	7	0	2.248597	5.741372	-0.569199	67	1	0	-0.178566	2.568372	-0.738044
68	1	0	3.161605	5.837492	-0.994766	68	7	0	0.523824	3.285377	-0.658023

69	6	0	1.772245	4.502222	-0.365195	69	6	0	0.212893	4.521441	-0.296153
70	7	0	2.305201	7.861399	0.457425	70	6	0	2.611673	5.106056	0.079432
71	7	0	0.594146	4.319856	0.229051	71	7	0	-1.052173	4.954082	-0.237539
72	1	0	0.030447	5.121683	0.486254	72	7	0	3.036968	3.971919	-0.316701
73	1	0	2.584530	9.898579	0.805126	73	7	0	3.327315	6.187811	0.524523
74	7	0	2.500674	3.445696	-0.747523	74	6	0	-2.140183	4.112390	-0.758597
75	1	0	3.393884	3.555936	-1.201699	75	1	0	4.032063	3.828611	-0.175337
76	1	0	1.087553	9.244787	1.516613	76	7	0	1.220964	5.396807	0.016652
77	1	0	0.246864	3.396525	0.437800	77	1	0	1.535345	3.075704	-0.707598
78	1	0	2.150595	2.504746	-0.652215	78	1	0	4.328019	6.076888	0.595960
79	6	0	3.384963	7.497476	1.379097	79	1	0	0.984944	6.377473	0.000765
80	1	0	4.237726	8.160738	1.223176	80	1	0	-2.998048	4.747526	-0.967352
81	1	0	3.709175	6.469951	1.229027	81	1	0	-1.842121	3.641083	-1.696576
82	1	0	3.049933	7.601630	2.416543	82	1	0	-1.273381	7.073638	-0.347873

Xer^{-}-Met^{+}_m1						Xer^{-}-Met^{+}_m2					
Center	Atomic	Atomic	Coordinates (Angstroms)			Center	Atomic	Atomic	Coordinates (Angstroms)		
Number	Number	Type	X	Y	Z	Number	Number	Type	X	Y	Z
1	6	0	5.716385	-1.618168	-0.279645	1	6	0	6.298326	-0.161664	-0.258873
2	6	0	4.451088	-1.932628	-0.823501	2	6	0	5.163603	-0.767251	-0.843089
3	6	0	3.393762	-1.049657	-0.845220	3	6	0	3.898989	-0.223702	-0.785170
4	6	0	3.529560	0.286646	-0.276881	4	6	0	3.661432	1.032753	-0.083713
5	6	0	4.827522	0.584318	0.282908	5	6	0	4.832555	1.630035	0.514957
6	6	0	5.856538	-0.333444	0.276873	6	6	0	6.079342	1.048018	0.425660
7	1	0	4.955011	1.567955	0.723815	7	1	0	4.684537	2.560484	1.053982
8	1	0	6.819850	-0.062444	0.708114	8	1	0	6.934626	1.537490	0.890727
9	6	0	2.050693	-1.412189	-1.437429	9	6	0	2.702375	-0.892439	-1.423042
10	6	0	1.056814	-1.994838	-0.445887	10	6	0	1.934761	-1.829041	-0.504361
11	6	0	0.963269	-3.377352	-0.213039	11	6	0	2.242013	-3.197094	-0.413033
12	6	0	0.206806	-1.158056	0.276931	12	6	0	0.896946	-1.344517	0.291479
13	6	0	-0.000523	-3.898996	0.670467	13	6	0	1.483766	-4.056243	0.404594
14	6	0	-0.765657	-1.633840	1.161452	14	6	0	0.117394	-2.162501	1.114664
15	1	0	0.344092	-0.088568	0.145864	15	1	0	0.722484	-0.272630	0.270223
16	6	0	-0.868429	-3.019431	1.337030	16	6	0	0.415525	-3.530425	1.148623
17	1	0	1.625893	-0.481835	-1.822135	17	1	0	2.023432	-0.087844	-1.715748
18	1	0	2.173298	-2.099812	-2.280175	18	1	0	2.998105	-1.429618	-2.329718
19	8	0	4.259230	-3.215198	-1.369106	19	8	0	5.332626	-1.990662	-1.517015
20	8	0	2.569399	1.104286	-0.272677	20	8	0	2.509026	1.539053	-0.005717
21	8	0	1.784813	-4.275195	-0.826915	21	8	0	3.272050	-3.758753	-1.106909
22	8	0	-1.807280	-3.501274	2.211703	22	8	0	-0.330281	-4.343653	1.961704
23	1	0	4.942878	-3.789410	-0.978719	23	1	0	6.158790	-2.382620	-1.180389
24	1	0	2.619325	-3.844823	-1.115116	24	1	0	3.944199	-3.082496	-1.342669
25	1	0	-1.948597	-4.439338	1.997973	25	1	0	-0.203892	-5.257131	1.653159
26	6	0	-1.692787	-0.697123	1.888731	26	6	0	-1.022622	-1.605050	1.924328
27	8	0	-3.008311	-0.582535	1.304761	27	8	0	-2.328036	-1.811800	1.343035
28	6	0	-3.013175	0.074094	0.044289	28	6	0	-2.544298	-1.061890	0.155246
29	6	0	-4.430443	0.151056	-0.475415	29	6	0	-3.935289	-1.339826	-0.366825
30	6	0	-4.795512	-0.607603	-1.586577	30	6	0	-4.092320	-2.056738	-1.552109
31	6	0	-5.405878	0.963375	0.136553	31	6	0	-5.088632	-0.903283	0.315134
32	6	0	-6.090331	-0.569480	-2.099649	32	6	0	-5.354766	-2.337557	-2.070395
33	1	0	-4.053516	-1.250849	-2.048046	33	1	0	-3.207724	-2.413365	-2.069395
34	6	0	-6.694015	1.007191	-0.392486	34	6	0	-6.346610	-1.175188	-0.218402
35	6	0	-7.050936	0.247446	-1.509337	35	6	0	-6.495635	-1.890254	-1.409382
36	1	0	-6.349714	-1.183653	-2.956949	36	1	0	-5.446378	-2.911848	-2.987591
37	1	0	-7.437999	1.633733	0.081879	37	1	0	-7.228113	-0.836337	0.310010
38	1	0	-1.886286	-1.052623	2.900680	38	1	0	-1.086956	-2.099528	2.893459
39	1	0	-1.234689	0.300116	1.942696	39	1	0	-0.865310	-0.529223	2.082762
40	1	0	-2.582824	1.084216	0.147627	40	1	0	-2.416252	0.013431	0.363849
41	1	0	-2.387445	-0.465491	-0.674955	41	1	0	-1.805749	-1.327128	-0.609081
42	6	0	-5.061565	1.804484	1.355055	42	6	0	-4.972740	-0.124305	1.615336
43	8	0	-6.201687	2.296456	2.058291	43	8	0	-6.191245	-0.049121	2.354287
44	1	0	-6.678149	1.529723	2.393706	44	1	0	-6.423750	-0.949021	2.606319
45	1	0	-4.408639	1.227015	2.015233	45	1	0	-4.169692	-0.554890	2.219759
46	1	0	-4.509336	2.697395	1.044219	46	1	0	-4.702904	0.915015	1.401171
47	6	0	-8.437619	0.350754	-2.094723	47	6	0	-7.866097	-2.127851	-1.993864
48	8	0	-9.405079	0.463561	-1.048468	48	8	0	-8.804609	-2.399200	-0.950351
49	1	0	-10.214088	0.808559	-1.435445	49	1	0	-9.685852	-2.261794	-1.307842
50	6	0	6.846409	-2.580576	-0.399252	50	6	0	7.652338	-0.746264	-0.464749
51	8	0	6.512345	-3.908952	0.133267	51	8	0	7.719659	-2.160822	-0.072002
52	1	0	6.095721	-3.734834	0.987323	52	1	0	7.287979	-2.198024	0.791464
53	6	0	-0.065854	-5.373088	0.965588	53	6	0	1.845300	-5.509785	0.548892
54	8	0	-1.426148	-5.891241	0.909208	54	8	0	0.687079	-6.385014	0.428237
55	1	0	-1.766009	-5.664559	0.035657	55	1	0	0.279411	-6.178747	-0.421023
56	1	0	0.579575	-5.927045	0.284387	56	1	0	2.607574	-5.786904	-0.178861

57	**1**	**0**	**0.250000**	**-5.588722**	**1.991047**	**57**	**1**	**0**	**2.229866**	**-5.727424**	**1.550176**
58	**1**	**0**	**7.122881**	**-2.805367**	**-1.436992**	**58**	**1**	**0**	**7.960348**	**-0.778991**	**-1.517332**
59	**1**	**0**	**7.737909**	**-2.191655**	**0.106809**	**59**	**1**	**0**	**8.406820**	**-0.172190**	**0.086001**
60	**1**	**0**	**-8.488022**	**1.233577**	**-2.750357**	**60**	**1**	**0**	**-8.178058**	**-1.235243**	**-2.557517**
61	**1**	**0**	**-8.635889**	**-0.532423**	**-2.717960**	**61**	**1**	**0**	**-7.818099**	**-2.964523**	**-2.704788**
62	**1**	**0**	**4.671313**	**4.731223**	**-2.269232**	**62**	**1**	**0**	**-1.144557**	**8.214367**	**-2.160885**
63	**6**	**0**	**5.108080**	**4.886108**	**-1.284749**	**63**	**6**	**0**	**-1.692662**	**8.343514**	**-1.229837**
64	**1**	**0**	**5.839384**	**5.696402**	**-1.334135**	**64**	**1**	**0**	**-2.753332**	**8.488090**	**-1.448654**
65	**7**	**0**	**2.899458**	**3.341338**	**-0.997490**	**65**	**7**	**0**	**0.769469**	**7.378169**	**-0.635805**
66	**7**	**0**	**4.062908**	**5.270542**	**-0.337758**	**66**	**7**	**0**	**-1.554997**	**7.142928**	**-0.407272**
67	**6**	**0**	**2.923037**	**4.440240**	**-0.363846**	**67**	**6**	**0**	**-0.227732**	**6.687919**	**-0.263246**
68	**1**	**0**	**1.973304**	**2.918017**	**-0.941520**	**68**	**1**	**0**	**1.634734**	**6.855775**	**-0.499686**
69	**1**	**0**	**5.616361**	**3.957946**	**-0.991732**	**69**	**1**	**0**	**-1.301412**	**9.239453**	**-0.729919**
70	**7**	**0**	**1.850731**	**5.039686**	**0.339339**	**70**	**7**	**0**	**-0.202829**	**5.378290**	**0.273316**
71	**1**	**0**	**-0.172311**	**6.385188**	**0.905136**	**71**	**1**	**0**	**-0.194186**	**2.893645**	**0.496107**
72	**1**	**0**	**1.984228**	**6.010195**	**0.573679**	**72**	**1**	**0**	**-1.092517**	**4.906198**	**0.286899**
73	**6**	**0**	**0.597557**	**4.499416**	**0.583092**	**73**	**6**	**0**	**0.912919**	**4.629429**	**0.614002**
74	**7**	**0**	**0.327898**	**3.277909**	**0.312923**	**74**	**7**	**0**	**2.087510**	**5.137458**	**0.619631**
75	**7**	**0**	**-0.260637**	**5.421106**	**1.198195**	**75**	**7**	**0**	**0.572510**	**3.324534**	**0.995739**
76	**1**	**0**	**-0.636600**	**3.046210**	**0.534659**	**76**	**1**	**0**	**2.793972**	**4.452397**	**0.874006**
77	**6**	**0**	**4.611597**	**5.596888**	**0.983059**	**77**	**6**	**0**	**-2.362894**	**7.218962**	**0.814888**
78	**1**	**0**	**-1.225270**	**5.125312**	**1.232008**	**78**	**1**	**0**	**1.362645**	**2.702020**	**1.081269**
79	**1**	**0**	**5.294540**	**6.444020**	**0.889145**	**79**	**1**	**0**	**-3.416982**	**7.309688**	**0.543753**
80	**1**	**0**	**3.824505**	**5.870931**	**1.685180**	**80**	**1**	**0**	**-2.245010**	**6.325115**	**1.427036**
81	**1**	**0**	**5.166202**	**4.749080**	**1.413333**	**81**	**1**	**0**	**-2.086285**	**8.087896**	**1.431282**
Xer$^-$-Met$^+$_m3						**Xer^{2-}-Met_m1**					
Center	**Atomic**	**Atomic**	**Coordinates (Angstroms)**			**Center**	**Atomic**	**Atomic**	**Coordinates (Angstroms)**		
Number	**Number**	**Type**	**X**	**Y**	**Z**	**Number**	**Number**	**Type**	**X**	**Y**	**Z**
1	**6**	**0**	**5.218679**	**-2.986187**	**-0.556648**	**1**	**6**	**0**	**-9.116072**	**-2.223575**	**-0.429960**
2	**6**	**0**	**3.884509**	**-3.122840**	**-1.000449**	**2**	**6**	**0**	**-7.963552**	**-1.604620**	**-0.969105**
3	**6**	**0**	**3.003305**	**-2.067755**	**-1.091678**	**3**	**6**	**0**	**-6.675994**	**-1.966589**	**-0.639488**
4	**6**	**0**	**3.413335**	**-0.721623**	**-0.708325**	**4**	**6**	**0**	**-6.436996**	**-3.052205**	**0.309844**
5	**6**	**0**	**4.777612**	**-0.605504**	**-0.247952**	**5**	**6**	**0**	**-7.628664**	**-3.659907**	**0.862478**
6	**6**	**0**	**5.622968**	**-1.692584**	**-0.178481**	**6**	**6**	**0**	**-8.895223**	**-3.254285**	**0.502583**
7	**1**	**0**	**5.107939**	**0.382957**	**0.055400**	**7**	**1**	**0**	**-7.476461**	**-4.455817**	**1.585084**
8	**1**	**0**	**6.645504**	**-1.555675**	**0.172313**	**8**	**1**	**0**	**-9.763748**	**-3.747675**	**0.939485**
9	**6**	**0**	**1.581000**	**-2.242629**	**-1.573802**	**9**	**6**	**0**	**-5.459779**	**-1.293326**	**-1.241883**
10	**6**	**0**	**0.566311**	**-2.506967**	**-0.473365**	**10**	**6**	**0**	**-4.884382**	**-0.128604**	**-0.446371**
11	**6**	**0**	**0.242225**	**-3.809839**	**-0.058869**	**11**	**6**	**0**	**-5.363483**	**1.182137**	**-0.600877**
12	**6**	**0**	**-0.070642**	**-1.446097**	**0.170087**	**12**	**6**	**0**	**-3.834040**	**-0.330202**	**0.452852**
13	**6**	**0**	**-0.739117**	**-4.033250**	**0.925329**	**13**	**6**	**0**	**-4.790746**	**2.250176**	**0.114325**
14	**6**	**0**	**-1.052217**	**-1.623051**	**1.149695**	**14**	**6**	**0**	**-3.225239**	**0.701504**	**1.170976**
15	**1**	**0**	**0.247022**	**-0.444402**	**-0.104734**	**15**	**1**	**0**	**-3.497613**	**-1.351717**	**0.599368**
16	**6**	**0**	**-1.389680**	**-2.934084**	**1.508254**	**16**	**6**	**0**	**-3.723679**	**1.997743**	**0.991298**
17	**1**	**0**	**1.305291**	**-1.302539**	**-2.057773**	**17**	**1**	**0**	**-4.685571**	**-2.061764**	**-1.300220**
18	**1**	**0**	**1.522731**	**-3.037168**	**-2.324396**	**18**	**1**	**0**	**-5.676983**	**-0.962049**	**-2.263270**
19	**8**	**0**	**3.430569**	**-4.403418**	**-1.365878**	**19**	**8**	**0**	**-8.148228**	**-0.561805**	**-1.895453**
20	**8**	**0**	**2.617517**	**0.254794**	**-0.769527**	**20**	**8**	**0**	**-5.274216**	**-3.416921**	**0.619965**
21	**8**	**0**	**0.847474**	**-4.911884**	**-0.585246**	**21**	**8**	**0**	**-6.389732**	**1.493927**	**-1.446944**
22	**8**	**0**	**-2.339993**	**-3.124380**	**2.477460**	**22**	**8**	**0**	**-3.177463**	**3.018036**	**1.723696**
23	**1**	**0**	**4.024525**	**-5.043653**	**-0.933662**	**23**	**1**	**0**	**-9.043495**	**-0.210267**	**-1.745977**
24	**1**	**0**	**1.724755**	**-4.681973**	**-0.962352**	**24**	**1**	**0**	**-6.917952**	**0.699777**	**-1.670208**
25	**1**	**0**	**-2.660777**	**-4.038554**	**2.393807**	**25**	**1**	**0**	**-3.365471**	**3.847798**	**1.255016**
26	**6**	**0**	**-1.746685**	**-0.449849**	**1.787858**	**26**	**6**	**0**	**-2.057579**	**0.452137**	**2.100017**
27	**8**	**0**	**-3.055963**	**-0.163571**	**1.250653**	**27**	**8**	**0**	**-0.801169**	**0.948955**	**1.634353**
28	**6**	**0**	**-3.026124**	**0.326356**	**-0.083160**	**28**	**6**	**0**	**-0.238701**	**0.194397**	**0.553515**
29	**6**	**0**	**-4.437784**	**0.602577**	**-0.547466**	**29**	**6**	**0**	**1.109530**	**0.748500**	**0.164871**
30	**6**	**0**	**-5.005161**	**-0.202770**	**-1.533883**	**30**	**6**	**0**	**1.238233**	**1.472017**	**-1.027409**
31	**6**	**0**	**-5.209538**	**1.649607**	**-0.005282**	**31**	**6**	**0**	**2.259182**	**0.560569**	**0.958916**
32	**6**	**0**	**-6.303140**	**0.013601**	**-1.991796**	**32**	**6**	**0**	**2.462217**	**2.000231**	**-1.430543**
33	**1**	**0**	**-4.422371**	**-1.023443**	**-1.939012**	**33**	**1**	**0**	**0.351967**	**1.622839**	**-1.640527**
34	**6**	**0**	**-6.500991**	**1.868371**	**-0.480036**	**34**	**6**	**0**	**3.480761**	**1.082258**	**0.529250**
35	**6**	**0**	**-7.060938**	**1.059767**	**-1.472297**	**35**	**6**	**0**	**3.604849**	**1.814112**	**-0.652329**
36	**1**	**0**	**-6.724184**	**-0.640021**	**-2.750051**	**36**	**1**	**0**	**2.532008**	**2.565491**	**-2.359622**
37	**1**	**0**	**-7.087875**	**2.674672**	**-0.059876**	**37**	**1**	**0**	**4.421337**	**0.960494**	**1.064093**
38	**1**	**0**	**-1.933675**	**-0.639063**	**2.844785**	**38**	**1**	**0**	**-2.216332**	**0.966508**	**3.050258**
39	**1**	**0**	**-1.114859**	**0.443944**	**1.692027**	**39**	**1**	**0**	**-1.985225**	**-0.627866**	**2.298159**
40	**1**	**0**	**-2.415979**	**1.243799**	**-0.130574**	**40**	**1**	**0**	**-0.161481**	**-0.861318**	**0.864213**
41	**1**	**0**	**-2.555869**	**-0.402552**	**-0.752156**	**41**	**1**	**0**	**-0.911413**	**0.225083**	**-0.312263**
42	**6**	**0**	**-4.640706**	**2.552105**	**1.077626**	**42**	**6**	**0**	**2.160659**	**-0.190751**	**2.276137**
43	**8**	**0**	**-5.625482**	**3.328317**	**1.758923**	**43**	**8**	**0**	**3.329275**	**-0.108019**	**3.092715**
44	**1**	**0**	**-6.208421**	**2.709472**	**2.211266**	**44**	**1**	**0**	**3.725958**	**0.752083**	**2.915753**
45	**1**	**0**	**-4.059731**	**1.946794**	**1.778829**	**45**	**1**	**0**	**1.284650**	**0.172869**	**2.826637**

46	1	0	-3.959177	3.282858	0.629982	46	1	0	2.003212	-1.261525	2.091080
47	6	0	-8.442181	1.348107	-2.006398	47	6	0	5.016074	2.363209	-1.009024
48	8	0	-9.302790	1.763630	-0.943362	48	8	0	5.971191	2.102676	-0.145305
49	1	0	-10.060627	2.204059	-1.337030	49	6	0	-10.468518	-1.857608	-0.929002
50	6	0	6.147716	-4.149224	-0.598184	50	8	0	-10.743163	-0.416129	-0.815858
51	8	0	5.616953	-5.318598	0.116388	51	1	0	-10.424056	-0.177421	0.064512
52	1	0	5.295389	-4.968793	0.957541	52	6	0	-5.338832	3.645821	-0.000100
53	6	0	-1.047808	-5.423200	1.412220	53	8	0	-4.295320	4.639201	-0.213190
54	8	0	-2.479616	-5.682305	1.481859	54	1	0	-3.772193	4.325926	-0.960776
55	1	0	-2.830144	-5.502914	0.601558	55	1	0	-6.080255	3.698920	-0.797399
56	1	0	-0.558286	-6.165219	0.781937	56	1	0	-5.811977	3.966154	0.934103
57	1	0	-0.708866	-5.569116	2.442586	57	1	0	-10.605955	-2.038317	-2.003128
58	1	0	6.310537	-4.544433	-1.608714	58	1	0	-11.240485	-2.423618	-0.393223
59	1	0	7.125803	-3.874984	-0.185548	59	1	0	5.170198	1.970274	-2.076833
60	1	0	-8.376719	2.139697	-2.768550	60	1	0	4.800430	3.471928	-1.213392
61	1	0	-8.836001	0.448889	-2.500411	61	1	0	7.806809	1.496329	-0.713024
62	1	0	5.099254	7.325026	-1.651325	62	7	0	8.775582	1.213045	-0.720286
63	6	0	4.928393	7.708431	-0.647447	63	7	0	8.229279	-1.040009	-0.148097
64	1	0	4.577827	8.741570	-0.706920	64	1	0	7.250277	-0.779306	-0.214009
65	7	0	5.180010	5.014040	-0.493149	65	6	0	9.039786	-0.106810	-0.458350
66	7	0	3.895899	6.912591	0.014037	66	1	0	11.031512	0.438638	-0.391622
67	6	0	4.095996	5.518881	-0.069258	67	7	0	10.436958	-0.370354	-0.490115
68	1	0	5.108517	3.997380	-0.530415	68	1	0	9.287450	-2.477490	0.009344
69	1	0	5.885087	7.681846	-0.109183	69	1	0	13.396746	0.183596	-0.175157
70	7	0	2.925353	4.821217	0.313501	70	1	0	12.662186	-3.357214	0.745684
71	1	0	0.715635	3.664670	0.261388	71	1	0	9.349079	1.711774	-1.385674
72	1	0	2.097396	5.389332	0.393248	72	7	0	10.298918	-2.658248	-0.108269
73	6	0	2.760347	3.448925	0.419973	73	6	0	11.044481	-1.593141	-0.363535
74	7	0	3.750270	2.643384	0.325371	74	7	0	12.375004	-1.663308	-0.489206
75	7	0	1.431859	3.100231	0.699077	75	6	0	13.078042	-2.912735	-0.159993
76	1	0	3.457164	1.673651	0.407924	76	1	0	10.675290	-3.590246	-0.168019
77	6	0	3.548045	7.451717	1.333308	77	6	0	13.171315	-0.527123	-0.976883
78	1	0	1.238842	2.113250	0.611008	78	1	0	14.121949	-2.679630	0.037096
79	1	0	3.154600	8.463741	1.215562	79	1	0	12.661827	-0.020471	-1.797802
80	1	0	2.786405	6.845738	1.823497	80	1	0	14.112100	-0.910288	-1.365813
81	1	0	4.423888	7.494266	1.998572	81	1	0	13.030213	-3.629713	-0.985212

Xer^{2-}-Met_m2

Center Atomic Atomic Coordinates (Angstroms)

Number	Number	Type	X	Y	Z
1	6	0	6.458822	-0.701333	-0.243891
2	6	0	5.244551	-1.155204	-0.811017
3	6	0	4.042680	-0.496449	-0.673085
4	6	0	3.970078	0.750861	0.085769
5	6	0	5.219081	1.188171	0.671885
6	6	0	6.393461	0.486609	0.507970
7	1	0	5.186284	2.102234	1.256873
8	1	0	7.311972	0.859536	0.961749
9	6	0	2.759523	-1.000120	-1.301704
10	6	0	1.891361	-1.886421	-0.417811
11	6	0	2.090446	-3.273990	-0.337375
12	6	0	0.843806	-1.340238	0.328360
13	6	0	1.251480	-4.079978	0.454312
14	6	0	-0.022772	-2.103437	1.114063
15	1	0	0.722700	-0.262100	0.295289
16	6	0	0.200124	-3.484805	1.169752
17	1	0	2.173357	-0.111771	-1.547762
18	1	0	2.976968	-1.524887	-2.238449
19	8	0	5.271630	-2.346664	-1.558931
20	8	0	2.891809	1.384322	0.217343
21	8	0	3.087082	-3.913559	-1.018474
22	8	0	-0.604122	-4.247191	1.974558
23	1	0	6.057716	-2.841570	-1.268135
24	1	0	3.787532	-3.286012	-1.292501
25	1	0	-0.562654	-5.161090	1.648087
26	6	0	-1.176673	-1.482962	1.870539
27	8	0	-2.471633	-1.786408	1.347819
28	6	0	-2.777981	-1.114942	0.119315
29	6	0	-4.180357	-1.443339	-0.329350
30	6	0	-4.370653	-2.305449	-1.416607
31	6	0	-5.319701	-0.907162	0.304631
32	6	0	-5.645390	-2.635864	-1.869968
33	1	0	-3.493526	-2.724694	-1.905493
34	6	0	-6.588720	-1.235929	-0.175504

35	6	0	-6.777097	-2.105335	-1.250578
36	1	0	-5.764277	-3.315154	-2.713773
37	1	0	-7.519089	-0.846303	0.234585
38	1	0	-1.202681	-1.862239	2.894361
39	1	0	-1.031927	-0.392763	1.908169
40	1	0	-2.651571	-0.029513	0.270626
41	1	0	-2.064401	-1.415265	-0.657642
42	6	0	-5.162231	0.007558	1.507856
43	8	0	-6.379390	0.289297	2.199559
44	1	0	-6.935805	-0.491375	2.102588
45	1	0	-4.427483	-0.431954	2.193157
46	1	0	-4.766913	0.982587	1.193797
47	6	0	-8.242163	-2.411293	-1.675154
48	8	0	-9.181744	-1.832696	-0.962028
49	6	0	7.735729	-1.403608	-0.541218
50	8	0	7.687762	-2.834652	-0.200767
51	1	0	7.260180	-2.863069	0.665390
52	6	0	1.496684	-5.557095	0.593301
53	8	0	0.284454	-6.343408	0.410710
54	1	0	-0.102503	-6.054020	-0.424279
55	1	0	2.267304	-5.881995	-0.105840
56	1	0	1.819483	-5.813916	1.607726
57	1	0	7.988474	-1.425621	-1.609360
58	1	0	8.568247	-0.925604	-0.010382
59	1	0	-8.228718	-2.168927	-2.797404
60	1	0	-8.252971	-3.558815	-1.699749
61	1	0	2.355698	3.373184	0.347818
62	7	0	1.472824	3.839157	0.198741
63	7	0	2.442145	5.999522	0.507512
64	1	0	3.345258	5.541809	0.582489
65	6	0	1.476993	5.209638	0.245590
66	1	0	-0.584488	5.089713	0.175927
67	7	0	0.174410	5.738066	0.029724
68	1	0	1.705720	7.625590	0.351023
69	1	0	-2.850520	5.842062	0.103093
70	1	0	-1.449589	9.265344	0.596479
71	1	0	0.857680	3.366229	-0.448026
72	7	0	0.767661	7.983514	0.102987
73	6	0	-0.166436	7.061779	-0.079615
74	7	0	-1.438257	7.375086	-0.354069
75	6	0	-1.881628	8.775541	-0.277704
76	1	0	0.604016	8.950513	-0.124999
77	6	0	-2.419544	6.358064	-0.761023
78	1	0	-2.962971	8.789292	-0.161900
79	1	0	-1.969716	5.637024	-1.445093
80	1	0	-3.225320	6.854872	-1.296818
81	1	0	-1.620567	9.329309	-1.184637

Table A2. Cartesian coordinates of the different geometries for metformin-xerogel complex on aqueous solution.

Xer					
Center Number	Atomic Number	Atomic Type	Coordinates (Angstroms) X	Y	Z
1	6	0	-6.189545	-1.315003	-0.027316
2	6	0	-5.122907	-0.644340	-0.642770
3	6	0	-3.886928	-1.264809	-0.892304
4	6	0	-3.748395	-2.607588	-0.495891
5	6	0	-4.788176	-3.291749	0.126725
6	6	0	-5.992201	-2.638313	0.357421
7	1	0	-4.635663	-4.323236	0.417600
8	1	0	-6.800997	-3.170391	0.847152
9	6	0	-2.752190	-0.510853	-1.572351
10	6	0	-1.894998	0.346835	-0.649042
11	6	0	-2.059169	1.732817	-0.581828
12	6	0	-0.918204	-0.217477	0.173373
13	6	0	-1.284797	2.540226	0.265769
14	6	0	-0.104262	0.530948	1.018622

Xer^-					
Center Number	Atomic Number	Atomic Type	Coordinates (Angstroms) X	Y	Z
1	6	0	-6.229109	-1.233785	-0.314336
2	6	0	-5.037777	-0.725802	-0.875378
3	6	0	-3.805239	-1.327108	-0.723005
4	6	0	-3.673289	-2.546359	0.062985
5	6	0	-4.897747	-3.045681	0.639431
6	6	0	-6.106901	-2.406841	0.454028
7	1	0	-4.829977	-3.947193	1.239653
8	1	0	-7.007087	-2.823817	0.903596
9	6	0	-2.549812	-0.759404	-1.349465
10	6	0	-1.756922	0.182556	-0.456814
11	6	0	-1.986611	1.568835	-0.439773
12	6	0	-0.764960	-0.316520	0.386741
13	6	0	-1.203671	2.426946	0.355999
14	6	0	0.038499	0.497964	1.190378

15	1	0	-0.786058	-1.295210	0.161878
16	6	0	-0.299315	1.919524	1.058114
17	1	0	-2.092169	-1.212989	-2.093920
18	1	0	-3.156270	0.108478	-2.375680
19	8	0	-5.373118	0.660823	-0.992028
20	8	0	-2.587639	-3.319704	-0.685871
21	8	0	-3.056538	2.261443	-1.386782
22	8	0	0.471568	2.641860	1.911429
23	1	0	-4.571589	1.147033	-1.240385
24	1	0	-3.139329	3.211627	-1.260396
25	1	0	0.471855	3.574790	1.639220
26	1	0	-1.991945	-2.838859	-1.267805
27	6	0	0.978257	-0.113839	1.853854
28	8	0	2.289974	0.024885	1.299273
29	6	0	2.527975	-0.788740	0.150530
30	6	0	3.954233	-0.610831	-0.308717
31	6	0	4.208609	0.099795	-1.480452
32	6	0	5.041162	-1.140177	0.416917
33	6	0	5.509138	0.292934	-1.943860
34	1	0	3.375168	0.520327	-2.034288
35	6	0	6.335319	-0.954074	-0.062682
36	6	0	6.585251	-0.239354	-1.239078
37	1	0	5.680528	0.864228	-2.850552
38	1	0	7.168118	-1.368560	0.491049
39	1	0	1.036505	0.361132	2.832641
40	1	0	0.744645	-1.178169	1.995459
41	1	0	2.322967	-1.841216	0.403632
42	1	0	1.847151	-0.509433	-0.662537
43	6	0	4.804842	-1.925188	1.698235
44	8	0	5.982494	-2.177626	2.456424
45	1	0	6.320047	-1.336809	2.783487
46	1	0	4.055162	-1.410344	2.306500
47	1	0	4.405659	-2.915368	1.455073
48	6	0	7.995582	-0.086271	-1.751392
49	8	0	8.857250	0.292840	-0.673652
50	1	0	9.769733	0.196621	-0.962656
51	6	0	-7.505355	-0.604918	0.191034
52	8	0	-7.410518	0.544605	1.036326
53	1	0	-6.807675	1.154570	0.595734
54	6	0	-1.499870	4.028080	0.418584
55	8	0	-0.274100	4.779969	0.355688
56	1	0	0.137120	4.639619	-0.505753
57	1	0	-2.207664	4.437413	-0.313013
58	1	0	-1.907016	4.259367	1.406558
59	1	0	-7.941069	-0.318333	-0.775662
60	1	0	-8.206334	-1.281184	0.682719
61	1	0	8.333150	-1.039811	-2.181870
62	1	0	8.016645	0.666150	-2.549609

15	1	0	-0.643113	-1.395488	0.418394
16	6	0	-0.187822	1.879301	1.154602
17	1	0	-1.905584	-1.611186	-1.580157
18	1	0	-2.786047	-0.258399	-2.293457
19	8	0	-5.101713	0.463369	-1.624510
20	8	0	-2.551164	-3.107383	0.229480
21	8	0	-2.967669	2.151557	-1.187889
22	8	0	0.584265	2.687102	1.951029
23	1	0	-5.923306	0.920679	-1.375240
24	1	0	-3.664220	1.502211	-1.426571
25	1	0	0.534983	3.592141	1.601179
26	6	0	1.110321	-0.085639	2.068110
27	8	0	2.447493	-0.024719	1.505514
28	6	0	2.634729	-0.875291	0.372010
29	6	0	4.054040	-0.766728	-0.131993
30	6	0	4.283884	-0.300785	-1.427722
31	6	0	5.160103	-1.138786	0.659913
32	6	0	5.569653	-0.214684	-1.958849
33	1	0	3.436422	-0.001856	-2.036031
34	6	0	6.442607	-1.031914	0.121452
35	6	0	6.665940	-0.584792	-1.183239
36	1	0	5.725608	0.151849	-2.965553
37	1	0	7.291303	-1.302266	0.744937
38	1	0	1.194346	0.467737	3.002913
39	1	0	0.873119	-1.132861	2.293474
40	1	0	2.402528	-1.913212	0.658470
41	1	0	1.939034	-0.594891	-0.424258
42	6	0	4.990128	-1.603029	2.092573
43	8	0	4.761847	-0.531659	3.003173
44	1	0	3.938987	-0.106703	2.703400
45	1	0	4.176510	-2.339066	2.155132
46	1	0	5.904708	-2.097671	2.427609
47	6	0	8.072570	-0.556810	-1.731080
48	8	0	8.167696	0.379420	-2.807401
49	1	0	9.008549	0.245388	-3.253102
50	6	0	-7.543860	-0.603189	-0.617554
51	8	0	-7.582832	0.828106	-0.285317
52	1	0	-7.237245	0.901682	0.613646
53	6	0	-1.485249	3.904702	0.414679
54	8	0	-0.280259	4.708163	0.257673
55	1	0	0.102304	4.487212	-0.599433
56	1	0	-2.225103	4.184486	-0.334153
57	1	0	-1.864659	4.198145	1.398178
58	1	0	-7.790784	-0.602759	-1.686170
59	1	0	-8.348913	-1.125773	-0.089178
60	1	0	8.771254	-0.291136	-0.926795
61	1	0	8.344056	-1.561843	-2.086643

Xer^{2-}

Center Number	Atomic Number	Atomic Type	Coordinates (Angstroms) X	Y	Z
1	6	0	-6.442427	-1.021242	-0.397467
2	6	0	-5.201907	-0.560807	-0.896133
3	6	0	-4.009200	-1.235319	-0.735167
4	6	0	-3.985762	-2.512364	-0.026495
5	6	0	-5.258112	-2.959072	0.494255
6	6	0	-6.418654	-2.237230	0.312228
7	1	0	-5.262607	-3.895407	1.043204
8	1	0	-7.357424	-2.618111	0.713653
9	6	0	-2.698485	-0.721373	-1.300457
10	6	0	-1.837642	0.109631	-0.355685
11	6	0	-2.031673	1.489981	-0.188906
12	6	0	-0.792497	-0.483152	0.358544
13	6	0	-1.204490	2.242465	0.665916
14	6	0	0.068790	0.226097	1.199395
15	1	0	-0.661867	-1.555321	0.249936
16	6	0	-0.162430	1.598472	1.351356
17	1	0	-2.116058	-1.603536	-1.575670
18	1	0	-2.882650	-0.152025	-2.217955
19	8	0	-5.181114	0.660946	-1.593789
20	8	0	-2.918419	-3.167939	0.120875
21	8	0	-3.017988	2.177771	-0.841827
22	8	0	0.633441	2.304218	2.218145

Xer- Met^{2+}_m1

Center Number	Atomic Number	Atomic Type	Coordinates (Angstroms) X	Y	Z
1	6	0	7.832265	-0.709994	-0.788966
2	6	0	6.869747	-0.167337	0.077465
3	6	0	5.870665	-0.951780	0.671375
4	6	0	5.847674	-2.318683	0.356216
5	6	0	6.787700	-2.884661	-0.496153
6	6	0	7.769958	-2.072220	-1.058442
7	1	0	6.752731	-3.944908	-0.724829
8	1	0	8.500742	-2.511056	-1.728777
9	6	0	4.858583	-0.377403	1.650053
10	6	0	3.629476	0.227024	0.986336
11	6	0	3.473711	1.611418	0.833318
12	6	0	2.637329	-0.589528	0.453120
13	6	0	2.339376	2.174904	0.219826
14	6	0	1.499402	-0.088261	-0.184246
15	1	0	2.781230	-1.663716	0.512603
16	6	0	1.350062	1.300489	-0.260784
17	1	0	4.529947	-1.184543	2.305697
18	1	0	5.334418	0.362965	2.295594
19	8	0	6.975423	1.179727	0.313777
20	8	0	4.840203	-3.075239	0.925635
21	8	0	4.508716	2.380031	1.308031
22	8	0	0.203777	1.807948	-0.854947

23	1	0	-5.975317	1.158143	-1.336822
24	1	0	-3.708555	1.575952	-1.188156
25	1	0	0.614941	3.238039	1.955913
26	6	0	1.215126	-0.447869	1.921470
27	8	0	2.515391	-0.142217	1.407293
28	6	0	2.819191	-0.780425	0.158872
29	6	0	4.215970	-0.421254	-0.284833
30	6	0	4.393138	0.475788	-1.346753
31	6	0	5.365305	-0.961701	0.322445
32	6	0	5.663380	0.815363	-1.807692
33	1	0	3.513167	0.907376	-1.818144
34	6	0	6.634857	-0.600702	-0.149601
35	6	0	6.811092	0.277827	-1.218597
36	1	0	5.767822	1.510374	-2.639965
37	1	0	7.550344	-0.986587	0.295529
38	1	0	1.250523	-0.118152	2.961806
39	1	0	1.055083	-1.535573	1.907943
40	1	0	2.711274	-1.868439	0.280966
41	1	0	2.099612	-0.462392	-0.605356
42	6	0	5.280691	-1.976432	1.436913
43	8	0	5.305556	-3.339841	0.947383
44	1	0	5.952699	-3.356789	0.233414
45	1	0	6.122564	-1.829471	2.125261
46	1	0	4.356336	-1.881821	2.004920
47	6	0	8.245490	0.617257	-1.695133
48	8	0	9.235752	-0.004548	-1.058389
49	6	0	-7.704900	-0.297800	-0.705674
50	8	0	-7.687060	1.107285	-0.265806
51	1	0	-7.321611	1.094127	0.628514
52	6	0	-1.453364	3.707451	0.897824
53	8	0	-0.249315	4.512643	0.737498
54	1	0	0.111034	4.315210	-0.135243
55	1	0	-2.238797	4.071624	0.236424
56	1	0	-1.755421	3.900688	1.932175
57	1	0	-7.906100	-0.203380	-1.780355
58	1	0	-8.558134	-0.812694	-0.249351
59	1	0	8.200985	0.429193	-2.813908
60	1	0	8.279295	1.750892	-1.643563

23	1	0	6.232252	1.519674	0.829776
24	1	0	4.406607	3.313219	1.097718
25	1	0	0.196405	2.774530	-0.691373
26	1	0	5.041570	-4.009043	0.801234
27	6	0	0.556941	-1.022089	-0.890849
28	8	0	-0.813180	-1.003770	-0.401363
29	6	0	-0.988649	-1.617425	0.892857
30	6	0	-2.313128	-1.145976	1.452114
31	6	0	-2.321433	-0.001708	2.256389
32	6	0	-3.539992	-1.759392	1.129942
33	6	0	-3.511377	0.597598	2.660371
34	1	0	-1.375036	0.441511	2.547306
35	6	0	-4.726301	-1.169846	1.569919
36	6	0	-4.731520	0.030906	2.284613
37	1	0	-3.487795	1.496127	3.268412
38	1	0	-5.661292	-1.667539	1.341778
39	1	0	0.465140	-0.747582	-1.944840
40	1	0	0.942106	-2.045134	-0.844055
41	1	0	-0.933503	-2.706413	0.790125
42	1	0	-0.176675	-1.302842	1.553988
43	6	0	-3.606185	-3.049514	0.339448
44	8	0	-4.903891	-3.179488	-0.259148
45	1	0	-5.029482	-4.101046	-0.510358
46	1	0	-2.834814	-3.061130	-0.436178
47	1	0	-3.417698	-3.895667	1.011604
48	6	0	-6.031089	0.718247	2.575773
49	8	0	-6.476863	1.413878	1.336036
50	1	0	-7.059310	2.140026	1.596872
51	6	0	8.892569	0.179593	-1.398996
52	8	0	8.356330	1.216436	-2.222316
53	1	0	7.891247	1.824573	-1.637756
54	6	0	2.217878	3.662775	-0.045777
55	8	0	0.877090	4.160963	0.163306
56	1	0	0.727116	4.276996	1.108609
57	1	0	2.909030	4.259442	0.555709
58	1	0	2.434507	3.886664	-1.093646
59	1	0	9.520592	0.611764	-0.609882
60	1	0	9.537843	-0.415515	-2.046103
61	1	0	-6.816232	0.015611	2.861157
62	1	0	-5.921972	1.471740	3.355866
63	1	0	-8.140331	0.954871	-2.870506
64	1	0	-6.308276	-1.216263	-3.152407
65	1	0	-8.198837	-1.376297	-1.995229
66	7	0	-5.539397	-0.652324	-2.805252
67	6	0	-5.763250	0.087166	-1.820580
68	7	0	-4.807874	0.889309	-1.217882
69	6	0	-7.944398	1.291777	-1.854378
70	6	0	-7.830504	-1.068138	-1.018326
71	1	0	-5.100729	1.427906	-0.406260
72	1	0	-3.556210	-0.769916	-2.699649
73	6	0	-3.432336	0.715159	-1.344013
74	7	0	-2.928189	-0.217875	-2.123810
75	7	0	-7.102548	0.249136	-1.147452
76	7	0	-2.650678	1.521166	-0.647657
77	1	0	-7.404259	2.237138	-1.870640
78	1	0	-1.994320	-0.554181	-1.878302
79	1	0	-8.879315	1.398943	-1.306533
80	1	0	-8.677232	-0.910484	-0.351982
81	1	0	-3.027825	2.121413	0.069323
82	1	0	-7.144937	-1.810116	-0.610946
83	1	0	-1.625173	1.413274	-0.684257
84	1	0	-6.931313	0.596613	-0.172319

Xer-1Met^{+}_m1

Center Atomic Atomic Coordinates (Angstroms)

Number	Number	Type	X	Y	Z
1	6	0	-4.939985	-3.302188	0.416138
2	6	0	-4.691949	-2.177412	-0.386868
3	6	0	-3.410091	-1.876459	-0.878999
4	6	0	-2.377958	-2.764384	-0.544337
5	6	0	-2.587360	-3.883570	0.245632
6	6	0	-3.870628	-4.134783	0.725809
7	1	0	-1.763684	-4.549495	0.471725
8	1	0	-4.043260	-5.004983	1.349220

Xer^{-}-1Met^{+}

Center Atomic Atomic Coordinates (Angstroms)

Number	Number	Type	X	Y	Z
1	6	0	5.485539	-2.855870	-1.145451
2	6	0	4.105217	-3.112610	-1.073604
3	6	0	3.142805	-2.156899	-1.401127
4	6	0	3.592164	-0.883338	-1.799884
5	6	0	4.961248	-0.593799	-1.856483
6	6	0	5.887071	-1.576930	-1.529582
7	1	0	5.284690	0.395696	-2.155080
8	1	0	6.947415	-1.350227	-1.585459

9	6	0	-3.189250	-0.628594	-1.716557
10	6	0	-3.157776	0.671341	-0.921874
11	6	0	-4.160347	1.638108	-1.056118
12	6	0	-2.132969	0.938894	-0.019622
13	6	0	-4.105843	2.865258	-0.379413
14	6	0	-2.020671	2.134800	0.684439
15	1	0	-1.389083	0.167791	0.151253
16	6	0	-3.008833	3.110267	0.474639
17	1	0	-2.253678	-0.697161	-2.284185
18	1	0	-3.955300	-0.566993	-2.492103
19	8	0	-5.776319	-1.387354	-0.646532
20	8	0	-1.058505	-2.539517	-0.975730
21	8	0	-5.225691	1.276979	-1.858084
22	8	0	-2.899532	4.273504	1.159841
23	1	0	-5.571102	-0.603326	-1.177169
24	1	0	-5.902362	1.961258	-1.880453
25	1	0	-3.472846	4.947647	0.752381
26	1	0	-1.078114	-1.982466	-1.763015
27	6	0	-0.897456	2.359881	1.671957
28	8	0	0.343264	2.820897	1.111660
29	6	0	0.952906	1.896861	0.220885
30	6	0	2.420002	2.204636	0.040509
31	6	0	2.861186	2.756153	-1.161103
32	6	0	3.370851	1.921508	1.043388
33	6	0	4.213215	3.014984	-1.387061
34	1	0	2.137391	2.985991	-1.935776
35	6	0	4.718178	2.192586	0.808090
36	6	0	5.158661	2.733628	-0.404045
37	1	0	4.527205	3.439093	-2.335007
38	1	0	5.448851	1.974856	1.580145
39	1	0	-1.175986	3.124575	2.393294
40	1	0	-0.708870	1.419793	2.211998
41	1	0	0.834210	0.880899	0.622615
42	1	0	0.453414	1.916376	-0.754871
43	6	0	2.969876	1.358821	2.380465
44	8	0	2.854179	-0.107398	2.306897
45	1	0	2.826505	-0.438090	3.213716
46	1	0	3.731217	1.598682	3.125034
47	1	0	2.012915	1.767047	2.707909
48	6	0	6.623430	3.020849	-0.619585
49	8	0	7.376572	1.845312	-0.290806
50	1	0	8.310834	2.076678	-0.260314
51	6	0	-6.339614	-3.574118	0.922290
52	8	0	-6.827393	-2.562314	1.800677
53	1	0	-6.954000	-1.764001	1.276144
54	6	0	-5.207458	3.901038	-0.461278
55	8	0	-4.702768	5.237181	-0.617120
56	1	0	-4.292111	5.327927	-1.485311
57	1	0	-5.926730	3.693443	-1.262284
58	1	0	-5.776518	3.932366	0.471719
59	1	0	-7.023516	-3.704845	0.074410
60	1	0	-6.343664	-4.500311	1.498281
61	1	0	6.795382	3.313879	-1.661226
62	1	0	6.934613	3.856162	0.020988
63	1	0	3.919800	-4.849959	0.571383
64	1	0	7.092580	-3.943024	0.007024
65	7	0	4.667721	-4.465182	0.000391
66	6	0	4.650028	-3.182943	-0.028391
67	1	0	3.694392	-1.580744	1.013213
68	6	0	6.960881	-3.140586	-0.715048
69	7	0	3.526215	-2.398302	0.428287
70	1	0	7.780167	-2.425148	-0.633957
71	7	0	5.706762	-2.435980	-0.442995
72	1	0	1.562554	-1.129132	1.275327
73	6	0	2.241921	-2.632253	0.095141
74	7	0	1.290140	-1.879657	0.643299
75	1	0	6.964693	-3.578384	-1.719283
76	7	0	1.909101	-3.588589	-0.777065
77	1	0	0.331962	-1.985961	0.321714
78	1	0	2.620089	-4.189068	-1.170777
79	1	0	6.370727	-0.465856	-0.771708
80	6	0	5.575045	-1.133908	-1.103946
81	1	0	0.935841	-3.722082	-1.018759
82	1	0	4.621335	-0.666401	-0.871714
83	1	0	5.646151	-1.251882	-2.192246

9	6	0	1.656613	-2.471837	-1.355367
10	6	0	0.915664	-1.962828	-0.126267
11	6	0	1.021077	-2.590119	1.126935
12	6	0	0.071604	-0.854602	-0.219762
13	6	0	0.319716	-2.105121	2.245092
14	6	0	-0.662252	-0.350645	0.853931
15	1	0	-0.020574	-0.368327	-1.186257
16	6	0	-0.517038	-0.987686	2.096419
17	1	0	1.191178	-2.019295	-2.232760
18	1	0	1.520485	-3.551969	-1.455658
19	8	0	3.649526	-4.348973	-0.656221
20	8	0	2.649280	0.032742	-2.116767
21	8	0	1.801096	-3.688282	1.339715
22	8	0	-1.198306	-0.476298	3.159169
23	1	0	4.387736	-4.812755	-0.215910
24	1	0	2.313132	-3.946721	0.552198
25	1	0	-1.251511	-1.159077	3.851466
26	6	0	-1.613447	0.809832	0.688923
27	8	0	-2.990976	0.430988	0.562369
28	6	0	-3.305563	-0.222017	-0.665508
29	6	0	-4.792170	-0.474947	-0.735151
30	6	0	-5.268900	-1.778027	-0.605016
31	6	0	-5.717081	0.572502	-0.924750
32	6	0	-6.633216	-2.060294	-0.660444
33	1	0	-4.560901	-2.584689	-0.444124
34	6	0	-7.076673	0.278148	-0.992788
35	6	0	-7.549777	-1.031815	-0.860723
36	1	0	-6.978914	-3.082021	-0.539903
37	1	0	-7.783968	1.083491	-1.146203
38	1	0	-1.590296	1.454120	1.567748
39	1	0	-1.318786	1.402453	-0.189457
40	1	0	-2.974804	0.406704	-1.508268
41	1	0	-2.767635	-1.173964	-0.741078
42	6	0	-5.236269	2.007280	-1.077226
43	8	0	-6.267779	2.984687	-0.976345
44	1	0	-6.620668	2.959786	-0.080352
45	1	0	-4.444343	2.204012	-0.348779
46	1	0	-4.808060	2.148934	-2.074987
47	6	0	-9.025044	-1.322905	-0.974170
48	8	0	-9.759863	-0.399216	-0.163259
49	1	0	-10.692351	-0.470223	-0.388734
50	6	0	6.479749	-3.955942	-0.884764
51	8	0	6.179620	-4.712049	0.314446
52	1	0	6.256472	-4.122010	1.073733
53	6	0	0.500760	-2.738977	3.603941
54	8	0	-0.751363	-2.905754	4.313480
55	1	0	-1.282160	-3.558550	3.842796
56	1	0	1.018213	-3.693474	3.516901
57	1	0	1.091542	-2.092951	4.260012
58	1	0	6.459699	-4.709865	-1.676956
59	1	0	7.495520	-3.552343	-0.836545
60	1	0	-9.337768	-1.227068	-2.023775
61	1	0	-9.220402	-2.355866	-0.660340
62	1	0	0.666223	4.609811	-0.049932
63	7	0	1.164608	5.238208	0.574558
64	1	0	1.651864	7.640605	1.106397
65	6	0	2.408040	5.309331	0.285949
66	6	0	2.556249	7.322054	1.619665
67	7	0	3.096674	4.498051	-0.653027
68	1	0	3.828298	4.954943	-1.175961
69	6	0	2.828188	3.186905	-1.033337
70	7	0	3.224381	6.284001	0.838285
71	7	0	1.966718	2.483905	-0.245141
72	1	0	1.798135	2.775667	0.704383
73	1	0	3.239146	8.168057	1.723594
74	7	0	3.355632	2.631366	-2.077477
75	1	0	3.885756	3.278273	-2.651554
76	1	0	2.272108	6.966186	2.617952
77	1	0	1.869708	1.498493	-0.453346
78	1	0	3.035596	0.944711	-2.265938
79	6	0	4.559281	5.944903	1.333383
80	1	0	5.209164	6.820094	1.260441
81	1	0	4.999959	5.136296	0.753919
82	1	0	4.523785	5.629115	2.385689

Xer^{-}-Met^{+}_m1

Center Number	Atomic Number	Atomic Type	Coordinates (Angstroms) X	Y	Z
1	6	0	-5.131163	-2.261484	0.147569
2	6	0	-3.848473	-2.403058	0.707883
3	6	0	-2.892265	-1.388465	0.671978
4	6	0	-3.240924	-0.173852	0.043605
5	6	0	-4.506045	-0.018345	-0.545503
6	6	0	-5.427387	-1.058475	-0.492291
7	1	0	-4.741887	0.906263	-1.057019
8	1	0	-6.402118	-0.931384	-0.954154
9	6	0	-1.518005	-1.566233	1.295183
10	6	0	-0.434883	-2.074058	0.350670
11	6	0	-0.166491	-3.442405	0.181460
12	6	0	0.354434	-1.169232	-0.363095
13	6	0	0.874461	-3.881702	-0.655132
14	6	0	1.400657	-1.556889	-1.197641
15	1	0	0.135279	-0.112004	-0.255355
16	6	0	1.653600	-2.930646	-1.332783
17	1	0	-1.199100	-0.594870	1.675587
18	1	0	-1.599060	-2.229726	2.159860
19	8	0	-3.499982	-3.583914	1.334858
20	8	0	-2.316533	0.804054	0.033578
21	8	0	-0.884590	-4.415580	0.818069
22	8	0	2.658736	-3.317097	-2.167716
23	1	0	-4.117456	-4.280005	1.038523
24	1	0	-1.746662	-4.078328	1.120893
25	1	0	2.910455	-4.231063	-1.946552
26	6	0	2.250348	-0.541715	-1.921758
27	8	0	3.509630	-0.260181	-1.292423
28	6	0	3.399221	0.454930	-0.064926
29	6	0	4.778799	0.798812	0.443325
30	6	0	5.278519	0.136817	1.563079
31	6	0	5.581652	1.772829	-0.186084
32	6	0	6.547352	0.420495	2.067561
33	1	0	4.669187	-0.623581	2.040823
34	6	0	6.840813	2.059225	0.334767
35	6	0	7.338506	1.390319	1.458576
36	1	0	6.919366	-0.121752	2.930935
37	1	0	7.450436	2.814395	-0.145872
38	1	0	2.518750	-0.905533	-2.913290
39	1	0	1.683846	0.394260	-2.031625
40	1	0	2.802575	1.367689	-0.225724
41	1	0	2.871890	-0.147532	0.683516
42	6	0	5.070611	2.521652	-1.407020
43	8	0	6.075626	3.244594	-2.113292
44	1	0	6.702275	2.610383	-2.478162
45	1	0	4.557283	1.821892	-2.072551
46	1	0	4.341244	3.277896	-1.098557
47	6	0	8.696079	1.742878	2.010802
48	8	0	9.668593	1.684307	0.959597
49	1	0	10.486653	2.076788	1.279718
50	6	0	-6.153397	-3.356169	0.296374
51	8	0	-5.620675	-4.667484	-0.012324
52	1	0	-5.370647	-4.683128	-0.944000
53	6	0	1.117317	-5.354031	-0.883909
54	8	0	2.524466	-5.699805	-0.833983
55	1	0	2.840272	-5.546701	0.063969
56	1	0	0.552984	-5.953790	-0.171067
57	1	0	0.810292	-5.647934	-1.891989
58	1	0	-6.491289	-3.453674	1.332325
59	1	0	-7.032464	-3.146951	-0.320763
60	1	0	8.669106	2.756309	2.435585
61	1	0	8.956423	1.047747	2.818587
62	1	0	-6.025438	6.602071	-0.838902
63	1	0	-3.951283	4.603962	-3.091459
64	1	0	-4.390375	6.984973	-0.252171
65	1	0	-5.365525	1.384616	1.818804
66	6	0	-5.136148	6.187450	-0.356258
67	1	0	-2.529410	3.711425	-1.623446
68	7	0	-3.113781	3.231309	-0.946577
69	6	0	-4.114282	3.939011	-0.551482
70	6	0	-4.357316	3.152068	1.784582
71	7	0	-4.599252	5.081309	-1.153387

Xer^{2-}-Met_m1

Center Number	Atomic Number	Atomic Type	Coordinates (Angstroms) X	Y	Z
1	6	0	-6.005752	-2.541395	0.027614
2	6	0	-5.230407	-1.577269	-0.647258
3	6	0	-3.847984	-1.563259	-0.629176
4	6	0	-3.121131	-2.568264	0.118046
5	6	0	-3.921453	-3.536249	0.810854
6	6	0	-5.302668	-3.509047	0.763342
7	1	0	-3.401277	-4.295133	1.385945
8	1	0	-5.871524	-4.266269	1.299739
9	6	0	-3.058054	-0.514223	-1.381683
10	6	0	-2.786145	0.775890	-0.621916
11	6	0	-3.574525	1.926800	-0.787548
12	6	0	-1.710761	0.855603	0.261307
13	6	0	-3.233708	3.137581	-0.157862
14	6	0	-1.331499	2.035880	0.907391
15	1	0	-1.153541	-0.059124	0.439671
16	6	0	-2.096212	3.183804	0.664899
17	1	0	-2.091872	-0.965580	-1.617387
18	1	0	-3.547126	-0.280780	-2.332094
19	8	0	-5.886367	-0.575828	-1.377495
20	8	0	-1.842455	-2.572526	0.161518
21	8	0	-4.698547	1.924084	-1.564233
22	8	0	-1.736462	4.352637	1.284995
23	1	0	-6.794663	-0.509625	-1.034706
24	1	0	-5.071595	1.018816	-1.606971
25	1	0	-2.145083	5.089620	0.800559
26	6	0	-0.137851	2.073105	1.825504
27	8	0	1.127344	2.344394	1.173088
28	6	0	1.539391	1.301842	0.283622
29	6	0	2.976278	1.459349	-0.148277
30	6	0	3.261228	1.588297	-1.508135
31	6	0	4.048904	1.377133	0.766418
32	6	0	4.574315	1.575854	-1.977592
33	1	0	2.439896	1.671492	-2.213341
34	6	0	5.353911	1.371899	0.277753
35	6	0	5.639734	1.439869	-1.090086
36	1	0	4.767124	1.644326	-3.044082
37	1	0	6.176576	1.279852	0.980757
38	1	0	-0.239784	2.871452	2.558521
39	1	0	-0.050897	1.114134	2.353015
40	1	0	1.413742	0.333721	0.792552
41	1	0	0.891309	1.290429	-0.597743
42	6	0	3.808626	1.297807	2.259870
43	8	0	3.404008	2.542022	2.830591
44	1	0	2.572373	2.776982	2.385940
45	1	0	3.068368	0.516382	2.481260
46	1	0	4.734858	1.017468	2.764276
47	6	0	7.062909	1.291446	-1.588042
48	8	0	7.605439	-0.000632	-1.347153
49	6	0	-7.491057	-2.562601	-0.118838
50	8	0	-8.113525	-1.277755	0.209699
51	1	0	-7.779217	-1.026103	1.079863
52	6	0	-4.101088	4.360294	-0.300875
53	8	0	-3.332860	5.550959	-0.634147
54	1	0	-2.895742	5.387438	-1.477961
55	1	0	-4.881310	4.193622	-1.042524
56	1	0	-4.579641	4.618946	0.648375
57	1	0	-7.817391	-2.729612	-1.151639
58	1	0	-7.925452	-3.354622	0.500692
59	1	0	7.095583	1.536693	-2.660014
60	1	0	7.722245	1.997441	-1.073049
61	1	0	6.968047	-0.683314	-1.670141
62	7	0	5.670626	-1.989407	-1.858074
63	7	0	6.002444	-2.549131	0.358111
64	1	0	6.881081	-2.056291	0.310071
65	6	0	5.200606	-2.410907	-0.723916
66	1	0	3.311235	-2.661220	-1.397722
67	7	0	3.856985	-2.784806	-0.562436
68	1	0	5.527466	-2.703916	1.249606
69	1	0	1.368333	-3.833703	-1.472213
70	1	0	1.103315	-4.266972	2.018724
71	1	0	4.952012	-1.923343	-2.572501

72	7	0	-3.362686	3.805942	2.237088	72	7	0	3.756918	-3.076568	1.748997
73	7	0	-5.117160	2.168917	2.410844	73	6	0	3.125819	-2.961814	0.624503
74	6	0	-4.047632	5.475361	-2.442167	74	7	0	1.764957	-2.993366	0.450417
75	1	0	-3.012151	3.406626	3.105445	75	6	0	0.921166	-3.262244	1.614513
76	7	0	-4.886121	3.462910	0.516063	76	1	0	3.121953	-3.192173	2.528325
77	1	0	-2.657198	1.665203	-0.347332	77	6	0	1.123716	-2.950786	-0.866281
78	1	0	-4.780117	1.884913	3.319638	78	1	0	-0.125565	-3.174298	1.317393
79	1	0	-5.887757	3.568754	0.455848	79	1	0	1.407750	-2.047428	-1.419281
80	1	0	-4.732605	6.180729	-2.916027	80	1	0	0.042437	-2.910426	-0.722853
81	1	0	-3.066830	5.962576	-2.349085	81	1	0	1.112012	-2.531106	2.408020
82	1	0	-5.395865	5.844098	0.641737						